

# Realistic Runtime Analysis for Quantum Simplex Computation\*

Sabrina Ammann<sup>†</sup>    Sándor P. Fekete<sup>‡</sup>    Paulina L. A. Goedicke<sup>§</sup>    David Gross<sup>‡</sup>  
 Maximilian Hess<sup>¶</sup>    Andreea Lefterovici<sup>||</sup>    Tobias J. Osborne<sup>¶</sup>    Michael Perk<sup>‡</sup>  
 Debora Ramacciotti<sup>¶</sup>    Antonio Rotundo<sup>¶</sup>    S. E. Skelton<sup>¶</sup>    Sebastian Stiller\*  
 Timo de Wolff\*

## Abstract

In recent years, strong expectations have been raised for the possible power of quantum computing for solving difficult optimization problems, based on theoretical, asymptotic worst-case bounds. Can we expect this to have consequences for Linear and Integer Programming when solving instances of practically relevant size, a fundamental goal of Mathematical Programming, Operations Research and Algorithm Engineering? Answering this question faces a crucial impediment: The lack of sufficiently large quantum platforms prevents performing real-world tests for comparison with classical methods.

In this paper, we present a quantum analog for classical runtime analysis when solving real-world instances of important optimization problems. To this end, we measure the *expected practical performance* of quantum computers by analyzing the expected *gate complexity* of a quantum algorithm. The lack of practical quantum platforms for experimental comparison is addressed by *hybrid* benchmarking, in which the algorithm is performed on a classical system, logging the expected cost of the various subroutines that are employed by the quantum versions. In particular, we provide an analysis of quantum methods for Linear Programming, for which recent work has provided asymptotic speedup through quantum subroutines for the Simplex method. We show that a practical quantum advantage for realistic problem sizes would require quantum gate operation times that are considerably below current physical limitations.

**Keywords:** Linear Programming, Simplex algorithm, quantum computing, expected runtime, benchmarking.

\*This work was supported by the German Federal Ministry of Education and Research (BMBF), project QuBRA, and the German Federal Ministry for Economic Affairs and Climate Action (BMWK), project ProvideQ. DG and PG are also supported by Germany's Excellence Strategy – Cluster of Excellence Matter and Light for Quantum Computing (ML4Q) EXC 2004/1 (390534769).

<sup>†</sup>Department of Mathematics, TU Braunschweig, Germany. {s.ammann,sebastian.stiller,t.de-wolff}@tu-bs.de

<sup>‡</sup>Department of Computer Science, TU Braunschweig, Germany. {s.fekete,m.perk}@tu-bs.de

<sup>§</sup>Institute for Theoretical Physics, Universität zu Köln, Germany. {paulina.goedicke,david.gross}@thp.uni-koeln.de

<sup>¶</sup>Supply Chain Innovation, Infineon Technologies AG, Germany. Maximilian.Hess@infineon.com

<sup>||</sup>Department of Physics, Leibniz Universität Hannover, Germany.

{andreea.lefterovici,tobias.osborne,debora.ramacciotti,antonio.rotundo,shawn.skelton}@itp.uni-hannover.de

## 1 Introduction

Measuring the performance of computational methods is at the heart of quantitative science. On the one hand, analyzing and improving the asymptotic worst-case complexity has been leading the way for *theoretical* research; on the other, measuring the computational performance for a set of well-chosen benchmark instances has been a driving force for progress on the *practical* side. These two approaches often complement each other, but do not necessarily lead to the same conclusions, as illustrated by the classical problem of Linear Programming: While the ground-breaking ellipsoid method by Khachiyan [34] was the first algorithm with polynomial-time worst-case complexity (proving that such algorithms do exist), it is of little practical use. On the other hand, the Simplex method by Dantzig [21] may have an exponential worst-case runtime, but is the method of choice for many practical optimization problems, including as a subroutine for the solution of NP-hard combinatorial optimization problems that can be expressed as linear programs with integer variables.

Since the early days of Dantzig and Khachiyan, the solution of ever larger instances of optimization problems has witnessed tremendous development, not just for instances of Linear Programming (for which 15 years of progress in both hardware and algorithms were sufficient to achieve a speedup of six orders of magnitude [7]), but also for solving large instances of NP-hard optimization problems. However, such gains remain elusive for many important problems, reflecting the asymptotic worst-case behavior even at moderate instance sizes.

In recent years, the prospect of real-world quantum computing (based on exploiting fundamentally different computing paradigms) has raised the hope of applicable progress for such difficult optimization problems, fueling an increasing amount of theoretical work for the development of algorithmic methods. A key aspect has been the analysis of asymptotic complexity, often with improvements in theoretical worst-case runtime. At this time, running benchmark experiments does not yet provide a realistic alternative, as existing hardware platforms are still in their infancy. Developing them to the point of practical usefulness will involve tremendous effort and expenses, so estimating their future performance ahead of time is highly desirable.

How can one gauge the performance of a hardware platform that has not yet been realized? In this paper, we employ *hybrid benchmarking*, a fundamental alternative to asymptotic worst-case analysis, whereby the practical performance of a quantum algorithm is estimated on the basis of generous analytic estimates on the gate complexity of standard quantum algorithms.

This is similar in spirit to recent work by Cade et al. [14, 13]. Here we use hybrid benchmarking to achieve an analysis of a quantum method for Linear Programming, for which a recent paper by Nannicini [42] has provided an asymptotic speedup through quantum subroutines for the Simplex method.

### Our Results

- We describe an approach for gauging the practical performance of a fully fault tolerant quantum device for solving real-world instances of optimization problems.
- We provide a specific demonstration of this technique by analyzing a quantum method for linear programming.
- We perform a concrete study by evaluating the performance of the quantum Simplex algorithm for an established library of benchmark instances.
- We show that a practical quantum advantage for realistic problem sizes would require quantum gate operation times that are considerably below current physical limitations.

This main part of our paper focuses on the algorithmic analysis; our overall approach combines methods from classical mathematical programming and quantum computing, so we provide involved scientific details in Appendix B (for algorithmic and mathematical subroutines). Further details of the underlying quantum subroutines and the ensuing mathematical analysis form a separate paper from the realm of theoretical physics, which is enclosed as Appendix C.

**Related Work** Cade et al. [14, 13] presented an approach for computing bounds on the expected and worst-case number of oracle calls in quantum subroutines. Their technique was applied to synthetic benchmarks of MAX- $k$ -SAT to estimate the resources required for quantum unstructured search and maximum finding which replace classical subroutines. This should be contrasted with the techniques of, e.g., Tacla et al. [45], which consider the real-world performance of distinct quantum hardware against basic gate sets. Unlike hardware-based benchmarking techniques, our hybrid benchmarking assumes access to fully fault-tolerant hardware and computes a lower bound on the expected gate complexity. Further details are elaborated in Section 3.

Many quantum algorithms rely on quantum subroutines like QSearch [8, 14], quantum amplitude estimation QAE [8], quantum phase estimation QPE [19], quantum linear solvers QLS such as HHL [28] or QLSA [18] and quantum minimum finding QMin [22, 14] to

achieve better worst-case scalings than their classical counterparts. Quantum algorithms for semidefinite programming such as [1, 10, 47] can be applied to linear system problems. Quantum interior point methods (qIPM) [16, 20] have also been proposed. Casares et al. [16] embeds Grover and a QLS as subroutines of an otherwise classical algorithm to obtain an asymptotic speedup, while Dalzell et al. [20] analyze the qIPM of earlier work [32, 33] for small randomly selected portfolio optimization problems, aiming at a thorough estimation of the leading order resources required to run the quantum routine on real-world instances. For other recent related work, see [15, 2]. Quantum subroutines for the primal Simplex algorithm have been proposed by Nannicini [42], who proves an asymptotic speedup over the classical primal Simplex method. Importantly, Nannicini’s method works for classical and quantum inputs, and thus is well suited for an examination from a practical point of view. With current hardware designs, the proposed algorithm would be vulnerable to a latency problem as well as to other challenges, such as preparing oracles to encode (classical) data on the circuit, decoherence and gate error [31]. Presuming that future technologies will overcome the many challenges to creating fully fault tolerant quantum devices, we apply the hybrid benchmarking technique to Nannicini’s quantum subroutine and compare it to classical Simplex solvers, which have made tremendous progress in practical performance over many years [7].

The fastest isolated quantum gate operation to date is taking  $6.5 \cdot 10^{-9}$ s for two physically realized qubits [17]. Because any quantum computer requires classical control hardware by arbitrary waveform generators, there is a practical limit supplied by the bandwidth of these devices, with a current best resolution in the 1 – 100GHz regime. Thus, it is reasonable to expect gate times limited for the foreseeable future to above the  $10^{-10}$ s timescale.

## 2 Preliminaries

**2.1 The Simplex Algorithm** We briefly recall the simplex algorithm to fix notation and improve cross-community readability. The simplex algorithm solves a linear optimization problem of the form  $\min c^T x$  with constraints  $Ax = b, x \geq 0$ , where  $A \in \mathbb{R}^{m \times n}$ ,  $c \in \mathbb{R}^n$ ,  $b \in \mathbb{R}^m$ . A subset of  $m$  linearly independent columns of  $A$  is called a *basis*  $B \subset \{1, \dots, n\}$ . The set  $N = \{1, \dots, n\} \setminus B$  is called the set of *nonbasic* variables. We denote by  $A_B \in \mathbb{R}^{m \times m}$  an invertible submatrix of  $A$  with columns  $B$ , and by  $A_N$  the remaining submatrix. The term *basis* may refer to the set of column indices  $B$  or to the submatrix  $A_B$ , depending on context. The maximum number of nonzero entries

in any column or row of  $A$  is given by  $d_c$  and  $d_r$ , respectively. We also denote  $d = \max\{d_c, d_r\}$ . Based on  $\|A_B\|_p = \max_{\|x\|_p=1} \|A_B x\|_p$  the condition number of  $A_B$  is  $\kappa = \|A_B\|_2 \cdot \|A_B^{-1}\|_2$ . We assume  $\kappa$  to be a constant for one iteration, and a function  $\kappa : \mathbb{R}^{n \times n} \rightarrow \mathbb{R}_{\geq 1}$  in Section 5.4.

We sketch the simplex algorithm below, introducing some important terms along the way.

1. Choose any basic feasible solution and compute the current basis  $B$ , the nonbasic variables  $N$  and the current solution  $x = A_B^{-1}b$ .
2. Compute the *reduced costs*  $\bar{c}_N^\top = c_N^\top - c_B^\top A_B^{-1} A_N$ . If  $\bar{c}_N \geq 0$ , stop the algorithm and return the optimal solution. Otherwise choose the pivot column  $k$  with  $\bar{c}_k < 0$ .
3. Compute the *basis direction*  $u := A_B^{-1} A_k$ . If  $u \leq 0$ , stop the algorithm and return that the problem is unbounded.
4. Perform the *ratio test* by computing  $\theta^*$  as  $\theta^* = \min_{i:u_i>0} \frac{x_{B_i}}{u_i} =: \frac{x_{B_\ell}}{u_\ell}$  with the pivot row  $\ell \in [m]$ .
5. Replace  $B(\ell)$  by  $k$  in the basis. The new solution is  $y_{B_i} := x_{B_i} - \theta^* u_i$ . Go to step 2.

Several different pivoting rules such as *Dantzig’s* and *steepest edge* have been proposed. In Dantzig’s rule one chooses the column  $k$  with the most negative  $\bar{c}_k$  [21]. Goldfarb et al. [23] later introduced the computationally more expensive *steepest edge* pivoting rule that computes the basis direction  $u$  for every nonbasic variable with negative reduced cost and chooses  $k$  with the most negative reduced cost per additional unit ( $\frac{\bar{c}_k}{\|u_k\|} = \max_i \frac{\bar{c}_i}{\|u_i\|}$ ).

## 2.2 Quantum Computing and Gate Complexity

In this paper, we only consider the *quantum circuit model* of quantum computation. In this model, a quantum algorithm consists of three phases, which are briefly elaborated below: (i) state preparation, (ii) unitary evolution, and (iii) measurement; refer to [43] for more details.

A quantum computer operates on a  $2^n$ -dimensional complex Hilbert space, given by the tensor product of  $n$  2-dimensional complex Hilbert spaces, which we call *qubits*. We assume the ability to efficiently prepare qubits in two states,

$$(2.1) \quad |0\rangle = \begin{pmatrix} 1 \\ 0 \end{pmatrix}, \quad |1\rangle = \begin{pmatrix} 0 \\ 1 \end{pmatrix},$$

which form an orthonormal basis for the qubit Hilbert space. We call this the *computational basis*.<sup>1</sup> More generally, a qubit can be in a linear combination  $|\psi\rangle = \psi_0|0\rangle + \psi_1|1\rangle$ , which we call a *superposition*. Physical states have unit norm, i.e. for qubits, we require  $|\psi_0|^2 + |\psi_1|^2 = 1$ . We call the components  $\psi_0, \psi_1$  of the vector the *amplitudes*.

The first phase in a quantum algorithm is the preparation of  $n$  qubits in a desired computational basis state,  $|x_1\rangle \otimes |x_2\rangle \otimes \dots \otimes |x_n\rangle$ , with  $x_i \in \{0, 1\}$ . This state is typically  $|0\rangle \otimes |0\rangle \otimes \dots \otimes |0\rangle$ .

In the second phase, the quantum computer manipulates the state through a series of elementary operations, called *quantum gates*; these are unitary matrices acting non-trivially only on one or two qubits. The gates transform the state of the quantum computer from the initial computational basis element into a superposition of different computational basis states.

For the third phase, we assume that the quantum computer is able to efficiently measure the state in the computational basis. Consider an example with  $n = 2$  qubits, and let the final state of the quantum computation be  $|\psi\rangle = \psi_{00}|0\rangle \otimes |0\rangle + \psi_{01}|0\rangle \otimes |1\rangle + \psi_{10}|1\rangle \otimes |0\rangle + \psi_{11}|1\rangle \otimes |1\rangle$ . Then the measurement outcome is one of 00, 01, 10, or 11, with probability given by the corresponding component of  $|\psi\rangle$  squared. For example, we measure 00 with probability  $|\psi_{00}|^2$ . After the measurement, the system is left in the measured computational basis state; all information concerning the original superposition is lost.

We quantify the cost of a quantum algorithm by counting the number of quantum gates required to implement it, which we call *gate complexity*. This number depends on a choice of an “basic” gate set that we decompose quantum gates into. In general, this can be the set of gates native to a particular quantum hardware design, or can be chosen to be a theoretically convenient model.

### 3 Hybrid Benchmarking

In analogy to classical runtime analysis, we are benchmarking the expected computational effort in the standard model for asymptotic quantum algorithm analysis. Thus we are not benchmarking the performance of some assumed quantum device. Instead, we focus on quantifying or estimating (under a very generous set of assumptions) the runtime of a quantum algorithm by counting the minimum expected number of elementary gates required to run it. This allows us to compare

quantum performance and classical empirical runtime; the outcomes are benevolent estimates for the required clock frequency of practical quantum hardware to allow competitive performance.

The goal is to derive statements on the possible performance of quantum computers, making no strong assumptions on the quantum hardware in use. To this end, we use a relatively coarse (and benevolent) model of gate complexity: we count *any* 1-qubit and 2-qubit gates and assume that no errors occur in the circuit. This extends the techniques of Cade et al. [14] beyond simple query counts which we apply to real-world, non-synthetic benchmarks.

Given a classical algorithm,  $\mathcal{A}_c$ , composed of several subroutines  $\Sigma_j^c$ , for  $j = 0, 1, \dots$ , hybrid benchmarking can be applied to evaluate the required resources for a quantum algorithm built from  $\mathcal{A}_c$  by replacing some  $\Sigma_j^c$  with quantum subroutines,  $\Sigma_j^c \rightarrow \Sigma_j^q$ . The structure of  $\mathcal{A}_c$  is otherwise untouched; in particular, we require the quantum subroutines to have classical inputs and outputs  $(i_j, o_j)$ . Without this assumption, the exponential size of the Hilbert space needed for quantum simulations would prevent us from classically computing the inputs and outputs of the subroutines. In hybrid benchmarking, we find functions  $b_j(i_j)$  that provide lower bounds on the gate complexity of each  $\Sigma_j^q$  with input  $i_j$ . We then select a set of practical benchmarks of interest and solve them with  $\mathcal{A}_c$ , logging the  $i_j$ 's and the classical runtime of each instance. Finally, we use the logged inputs  $i_j$  in  $b_j(i_j)$  to compute the bounds for specific instances and compare them to each classical runtime, allowing us to set estimates for the required clock frequency of quantum hardware required to provide a speedup.

Moreover, the functions  $b_j(i_j)$  provide lower bounds on the gate complexity of the specific quantum subroutines  $\Sigma_j^q$  used to implement the algorithm. We emphasize that our goal is not to estimate the best achievable performance *in theory*, a notoriously hard problem, but possible performances *in practice*, for quantum subroutines currently standard to quantum computing literature. Thus, our overall strategy is to identify how the quantum algorithm would perform under ‘the best of all possible worlds’ assumptions, and identify ranges in which the quantum algorithm has a chance to be useful compared to its classical counterpart.

The subroutines considered in this work have been chosen because they are accepted as the standard in the literature. However, is entirely possible that other subroutines, possibly yet to be discovered, might be more efficient. Because the bounds on gate count we have used are extremely generous and alternative subroutines have comparable scaling to our selections, it is in our

<sup>1</sup>Notice that in Equation (2.1) we have used Dirac notation, as it is standard in quantum mechanics:  $|\cdot\rangle$  denotes a column vector, and  $\langle\cdot|$  its adjoint  $\langle\cdot| = (|\cdot\rangle)^\dagger$ .

opinion extremely unlikely that the qualitative results of this paper would change by simply swapping some quantum subroutine. We also note that one can use our methods to investigate the relative performance of competing quantum subroutines for real-world benchmarks without rerunning the classical experiments, by changing some of the functions  $b_j(i_j)$ .

The main advantage of the hybrid benchmarking technique is that it allows a large class of quantum algorithms to be benchmarked *without* access to a fully fault-tolerant quantum computer. This class includes algorithms for semi-definite programming [46, 10, 9], machine learning [35, 49, 36], the triangle problem [37], and Monte Carlo methods [38].

Furthermore, the quantum subroutines we use can have interesting applications in their own right, such as the quantum linear systems algorithm of [18].

#### 4 Fast Quantum Subroutines for the Simplex Method

To demonstrate and evaluate the usefulness of hybrid benchmarking, we consider the quantum Simplex iteration of Nannicini [42], which provides an asymptotic quantum speedup over the classical Simplex algorithm. This quantum algorithm replaces each Simplex iteration with a quantum subroutine that has the same inputs/outputs as the classical algorithm, allowing a meaningful benchmarking with the proposed technique.

**4.1 Algorithmic Details** In the classical Simplex method, an LU-factorization of the basis  $A_B$  is computed at every iteration.<sup>2</sup> This accounts for a total worst-case runtime of  $O(d_c^{0.7}m^{1.9} + m^{2+\sigma(1)} + d_cn)$  [42] when using the fast sparse matrix multiplication algorithm of Yuster and Zwick [50]. However, as long as one is able to identify the entering and leaving variables and if the current basis is optimal or unbounded, explicit knowledge about the solution vector or about any factorization of the basis matrix is not required. Based on that, Nannicini proposes to replace the pivoting step at each Simplex iteration by a quantum algorithm that never computes any explicit representation of  $A_B^{-1}$ ,  $A_B^{-1}b$  or  $A_B^{-1}A_N$ , thus circumventing the issue of managing a factorization. The variable update is then done classically.

Algorithm 4.1 takes as input the matrix  $A$ , the basis variables  $B$ , the cost vector  $c$ , and precisions  $\varepsilon$  and  $\delta$ . It outputs the indices of the pivot element. The quantum subroutines `IsOptimal` and `IsUnbounded` check if the current solution is optimal or unbounded,

<sup>2</sup>For tuning practical performance, the factorization may *not* be computed at every iteration.

---

#### Algorithm 4.1 SimplexIter

---

**function** SIMPLEXITER(Constraint Matrix  $A$ , basis  $B$ , cost  $c$ , precision  $\varepsilon > 0$ ,  $\delta > 0$ )

Normalize  $c$  and  $A$ , s. t.  $\|c_B\| = 1$  resp.  $\|A_B\| \leq 1$

Apply `IsOptimal`( $A$ ,  $B$ ,  $\varepsilon$ ). Output: 1, if current basis is optimal

Apply `FindColumn`( $A$ ,  $B$ ,  $\varepsilon$ ). Output: index  $k$  of a column with negative reduced cost

Apply `IsUnbounded`( $A_B$ ,  $A_k$ ,  $\delta$ ). Output: 1, if the problem is unbounded

Apply `FindRow`( $A_B$ ,  $A_k$ ,  $b$ ,  $\delta$ ). Output: index  $l$  of the row minimising the ratio test **return** ( $k, l$ )

**end function**

---

see Appendix B for details. The explicit computation of the solution vector  $A_B^{-1}b$  for an optimal basis  $B^*$  is only necessary in the last iteration.

**THEOREM 4.1.** ([42]: RUNTIME OF ALGORITHM 4.1) *There exist quantum subroutines<sup>3</sup> to identify if a basis is optimal, or determine a column with negative reduced cost, with runtime<sup>4</sup>*

$$\mathcal{C}(\text{SimplexIter}) = \tilde{O}\left(\frac{\sqrt{n}}{\varepsilon}(d_cn + dm)\right) + \tilde{O}\left(\frac{\eta}{\varepsilon}d^2\kappa^2m^{1.5}\right) + \tilde{O}\left(\frac{\eta}{\delta}d^2\kappa^2m^{1.5}\right),$$

where  $\eta$  is the maximum norm of a column of  $A$  or  $b$ .

The runtime of one quantum Simplex iteration scales better than the one of a classical Simplex iteration, with increasing system size. This indicates a possible quantum advantage for large instances. Classically, an efficient pivoting routine is crucial for the performance of the algorithm. As the original Simplex `FindColumn`-subroutine implements the *random pivoting rule*, i.e., an update to a random basis that improves the objective function, we replace it by `FindColumn - QStER`, equivalent to a quantum version of the *steepest edge rule*. `SimplexIter` is comprised of four subroutines, each of which in turn is comprised of different subroutines that can be broken down to basic quantum algorithms i.e., quantum search `QSearch` [8, 14], quantum amplitude estimation (QAE) [8], quantum phase estimation (QPE) [19], the quantum linear solver algorithm, `QLSA Fourier`

<sup>3</sup>We give a different asymptotic runtime than that originally given in [42]. This is traceable to a difference in subroutines in the `QLS`.

<sup>4</sup>The notation  $\tilde{O}$  is used to suppress polylogarithmic factors in the input parameters, i.e.,

$$\tilde{O}(f(x)) = O(f(x)\text{poly}(\log n, \log m, \log \frac{1}{\varepsilon}, \log \kappa, \log d, \log L)).$$

[18], and quantum minimum finding (QMin) [22, 14]. A detailed review of algorithms and complexities can be found in Appendix C.

**4.2 Expected Gate Complexity** The precise gate complexity of a quantum algorithm depends on the selected hardware and on the way the problem instance is specified. In the following, we provide lower bounds on the gate complexity (Lemmas 4.2 and 4.3) and the *expected* gate complexity (Lemmas 4.1 and 4.4–4.6) for each subroutine of SimplexIter. To obtain a general non-asymptotic analysis, we make a number of very benevolent assumptions towards the quantum hardware and use generous lower bound estimates. As a consequence, the overall estimates are already quite biased in favor of the quantum algorithms; if anything, practical performance would be even worse than displayed in the following Section 5.

We emphasize some of these simplifying assumptions. Firstly, it was beyond the scope of our analysis to compute the gate complexity of preparing every unitary used, and so we have dropped (potentially practically relevant) terms in order to bound the gate complexity. Furthermore, while we can straightforwardly lower bound the gate complexity of some quantum subroutines, for others it is more meaningful to compute an expected gate complexity. The Simplex routines incorporate subroutines of each type, and so we combine lower bound and expected gate complexities in a naive manner. We interpret this as a lower bound on the expected gate complexity of the routine. In taking a measure of gate complexity that incorporates both expected gate complexity and lower-bound gate complexity, we sacrifice adherence to a strict definition of either. In return, we obtain a measure that represents the lowest expected gate complexity one would need to allocate to run a quantum algorithm. Given the resource scarcity of current quantum hardware, this is a reasonable heuristic for filtering out when a quantum algorithm has any potential to be implemented.

Each subroutine of SimplexIter is built on two basic quantum algorithms: For QSearch we can compute an expected gate complexity, and for QLSA – Fourier, we can then provide a bound on the fewest number of quantum gates required. Subsequently, we state the lower bounds on the expected number of gates for Nannicini’s subroutines IsOptimal, FindColumn – QStER, IsUnbounded and FindRow.

The details of each subroutine and the proofs of the lemmas can be found in Appendix B and Appendix C.

**4.3 Quantum Subroutine Bounds** QSearch is an algorithm that performs an unstructured search among

a list of items; this is done by repeatedly acting with an operator  $Q$ . The expected number of calls to  $Q$  needed to find a marked element is given by Lemma 4.1. A QLS algorithm prepares a quantum state whose amplitude is equal to the solution of a linear system of equations. Here, we consider the algorithm QLSA – Fourier from [18]; its bounded expected gate complexity is given in Lemma 4.2.

**LEMMA 4.1. (ITERATIONS FOR QSearch)** *Let  $X$  be a list of length  $|X|$ , with  $t$  marked items. The expected number  $n_Q(|X|, t)$  of iterations that QSearch needs to find a marked item is*

$$n_Q(|X|, t) = \sum_{k=1}^{k_{max}} \frac{m_k}{2} \left[ \prod_{l=1}^{k-1} \frac{1}{2} + \frac{\sin(4(m_l + 1)\theta)}{4(m_l + 1)\sin(2\theta)} \right],$$

$$k_{max} = \left\lceil \log_{\lambda} \frac{|X|}{2\sqrt{|X|-1}} \right\rceil + 4,$$

with  $\sin^2 \theta = t/|X|$ ,  $m_k = \lfloor \min(\lambda^k, \sqrt{|X|}) \rfloor$ ,  $\lambda = 6/5$ .

**LEMMA 4.2. (QLSA – Fourier)** *The gate complexity of QLSA – Fourier that solves the linear equation  $Ax = b$  to precision  $\varepsilon$  has a lower bound of*

$$\mathcal{C}[\text{QLS}(A, b, \varepsilon)] \geq 10tw \left( \frac{\pi}{2 \arcsin(\alpha^{-1})} + 1 \right) \cdot$$

$$\left( \|A\|_1 - d^2\gamma \right) \left( \left\lceil \log \left( \frac{\|A\|_1}{\gamma} - d^2 \right) \right\rceil - 1 \right),$$

with the smallest integer  $w$  satisfying  $\frac{e^w}{w^w} \leq \frac{\varepsilon_{seg}^2}{2}$  and  $\alpha, \gamma, \Delta_z, K, t, \varepsilon_{seg}$  defined as

$$\alpha = 2\sqrt{\pi} \frac{\kappa}{\kappa + 1} \sum_{k=-K}^K |k| \Delta_z e^{-\frac{(k\Delta_z)^2}{2}}, \quad t = 2\sqrt{2}\kappa \log \left( 1 + \frac{8\kappa}{\varepsilon} \right),$$

$$\Delta_z = \frac{2\pi}{\kappa + 1} \left[ \log \left( 1 + \frac{8\kappa}{\varepsilon} \right) \right]^{-1/2}, \quad \varepsilon_{seg} = \frac{\varepsilon}{90\gamma t d^2 \left\lceil \frac{\|A\|_{max}}{\gamma} \right\rceil},$$

$$K = \left\lceil \frac{\kappa + 1}{\pi} \log \left( 1 + \frac{8\kappa}{\varepsilon} \right) \right\rceil, \quad \gamma = \frac{\varepsilon}{\sqrt{2}d^3 t}.$$

Here  $\|A\|_{max} := \max_{i,j} |A_{ij}|$  is the largest element of  $A$  in absolute value.

**4.4 Nannicini Subroutines** With these lemmas, we can now lower bound the expected gate complexity for each subroutine of SimplexIter. The gate complexity of IsOptimal can be bounded by Lemma 4.3.

**LEMMA 4.3. (IsOptimal)** *The gate complexity of IsOptimal has a lower bound of*

$$(4.2) \quad \mathcal{C}[\text{IsOptimal}(A, B, c, \varepsilon)] \geq (24\sqrt{n-m} - 1) \cdot$$

$$\left( \frac{450\sqrt{6}\pi}{11\varepsilon} - 1 \right) \mathcal{C} \left[ \text{QLS} \left( A_B, A_k, \frac{0.1\varepsilon}{\sqrt{2}} \right) \right].$$

*Proof.* To determine the optimality of the current basis, `IsOptimal` leverages quantum amplitude estimation. This procedure estimates the amplitude, denoted as  $\tilde{\phi}$ , corresponding to the scenario where the function `CanEnterNFP` yields an outcome of 1. Specifically, the function `CanEnterNFP` yields a value of 1 when a designated column satisfies the criterion to potentially enter the basis. Ultimately, the decision reached by `IsOptimal` hinges upon whether the estimated amplitude  $\tilde{\phi}$  is close to 1 or 0. See Appendices B.2.1 and B.2.2 for further implementation details.

The gate complexity of `IsOptimal` involves applying quantum amplitude estimation (QAE) to `CanEnterNFP` and verifying  $\tilde{\phi} \in [0, \varepsilon_{\text{QAE}}] \cup (1 - \varepsilon_{\text{QAE}}, 1]$  with precision parameters  $\varepsilon_{\text{QAE}} = \frac{1}{4\sqrt{n-m}}$  and  $\delta_{\text{QAE}} = \frac{1}{4}$ . We lower bound the gate complexity of `IsOptimal` by only considering the gate complexity of QAE. QAE and how to bound its gate complexity are explained in Appendix C.6. The gate complexity of QAE can be lower bounded by

$$\mathcal{C}[\text{QAE}(\mathcal{A}, \chi_l, \varepsilon_{\text{QAE}}, \delta_{\text{QAE}})] \geq (2^{n_c+1} - 1)\mathcal{C}[\mathcal{A}],$$

by combining Lemmas C.3 and C.4 with  $\mathcal{A} = \text{CanEnterNFP}$ , and

$$n_c = \left\lceil \log_2 \frac{1}{\varepsilon_{\text{QAE}}} + \log_2 \left( 1 + \frac{1}{2\delta_{\text{QAE}}} \right) \right\rceil.$$

A lower bound for the gate complexity of `CanEnterNFP` is given by Lemma B.6. Combining the bounds for `CanEnterNFP` and QAE concludes the proof.  $\square$

Bounds for choosing a pivot column based on the steepest edge pivoting rule can be found in Lemma 4.4. Results for other pivoting rules are given in Appendix B.3.2. In Lemma 4.5 we state a lower bound on the expected gate complexity for the routine that decides if the given linear program is unbounded. A bound for choosing a pivot row is given in Lemma 4.6. The proofs of Lemmas 4.4–4.6 are omitted due to space constraints and can be found in Appendix B.

**LEMMA 4.4. (FindColumn – QStER)** *The expected gate complexity of FindColumn – QStER has a lower bound of*

$$\begin{aligned} \mathcal{C}[\text{FindColumn} - \text{QStER}(A, B, c, \varepsilon)] &\geq 3 \left\lceil \log_3 \frac{1}{\varepsilon} \right\rceil \cdot \\ &\left( \frac{40\sqrt{3}\pi c_{\max}}{\varepsilon} - 1 \right) \sum_{t=1}^{n-m-1} \frac{n_Q(n-m, t)}{t+1} \cdot \\ &\mathcal{C} \left[ \text{QLS} \left( A_B, A_k, \frac{\varepsilon}{10c_{\max}\sqrt{2}} \right) \right], \end{aligned}$$

where  $c_{\max}$  is the (absolute) maximum component in the cost vector  $c$ .

**LEMMA 4.5. (IsUnbounded)** *The expected gate complexity of IsUnbounded has a lower bound of*

$$\begin{aligned} \mathcal{C}[\text{IsUnbounded}(A_B, A_k, \delta)] &\geq n_Q(m, t) \cdot \\ &\left( \frac{50\sqrt{3}\pi}{18\delta} - 1 \right) \mathcal{C} \left[ \text{QLS} \left( A_B, A_k, \frac{\delta}{10} \right) \right], \end{aligned}$$

where  $t$  is the number of positive components in  $u = A_B^{-1}A_k$ .

**LEMMA 4.6. (FindRow)** *The expected gate complexity of FindRow has a lower bound of*

$$\begin{aligned} \mathcal{C}[\text{FindRow}(A_B, A_k, b, \delta)] &\geq n_Q(m, 0) \cdot \\ &\left( \frac{\sqrt{3}\pi \|A_B^{-1}A_k\|}{2\delta} - 1 \right) \mathcal{C} \left[ \text{QLS} \left( A_B, b, \frac{\delta}{2} \right) \right]. \end{aligned}$$

## 5 Benchmarks and Evaluation

In the previous section we derived lower bounds on the expected number of quantum gates required for the subroutines of Nannicini’s Simplex algorithm. In this section we explicitly compute these bounds for various instances of linear programs using the steepest-edge pivoting rule on both the classical and quantum side. For each of these instances, we track the classical runtime of a Simplex iteration and compare these to the bounds for a quantum computer performing Nannicini’s algorithm, see Sections 3 and 4.2 for details. From this comparison we answer the following three questions.

- RQ1 Could Algorithm 4.1 provide a speedup over the classical Simplex algorithm when quantum hardware is ready?
- RQ2 What quantum gate operation times are required for Algorithm 4.1 to provide a speedup over the classical primal Simplex algorithm?
- RQ3 Can we find LP instances that are easier to solve on quantum hardware?

**5.1 Linear Programming Solvers** In order to apply the hybrid benchmarking technique, the classical runtime of each Simplex iteration and information regarding the iteration itself (e.g., the condition number) need to be logged; see Section 3. Choosing the proper LP solver is crucial for a fair comparison: On one hand, the solver must be widely accepted; and, on the other, it must implement a primal Simplex algorithm with the steepest edge rule. To ensure transparent and straightforward evaluation, we require the solver to be open source and easily extendable. The

survey by Gearhart et al. [26] compares the performance of open-source LP solvers against the commercial solver *CPLEX*. The survey included *COIN-OR Linear Programming* (CLP), GNU Linear Programming Kit (GLPK), *lp\_solve* and *Modular In-core Nonlinear Optimization System* (MINOS), with no open-source solver outperforming CPLEX, meaning that classical performance may be even better with commercial solvers. Among the open-source solutions, CLP and GLPK were found to be top performing. More recently, *Sequential object-oriented simplex* (SoPlex) was made open source as part of the *SCIP* software package [24] and can compete with commercial solvers like Gurobi or CPLEX. However, SoPlex does not implement a primal Simplex but only a composite Simplex. We ultimately chose GNU Linear Programming Kit (GLPK) for our experiments.

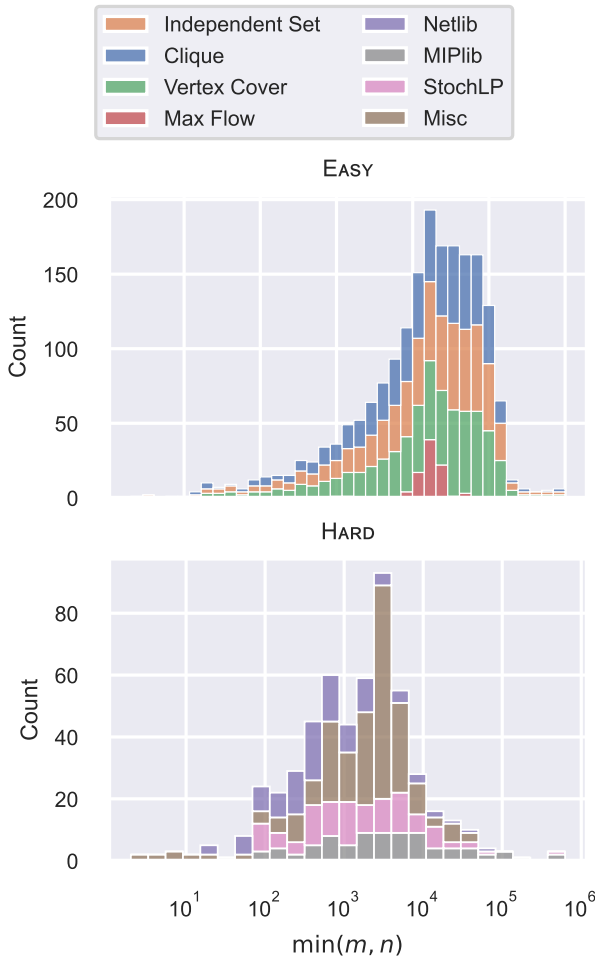


Figure 1: Size distribution of the used EASY (top) and HARD (bottom) instances.

Benchmark	group	# Instances	Source
Random Graphs <sup>5</sup>	EASY	1,711	self generated
DIMACS Graphs <sup>5</sup>	EASY	101	[30]
Maximum Flow	EASY	88	[48] via [29]
NETLIB	HARD	109	[25]
MIPLIB	HARD	84	[27]
STOCHLP	HARD	108	[40]
MISC	HARD	231	[39]

Table 1: Overview of the used benchmarking instances. Full overview can be found in Table 2.

<sup>5</sup>Instances are LP relaxations of Min Vertex Cover, Max Independent Set and Max Clique.

## 5.2 Instances from Existing Benchmark Libraries

We applied the hybrid benchmarking technique to a wide range of test instances. The HARD instance set consists of 532 instances from standard benchmark sets NETLIB [25], STOCHLP [40], MISC [39] for LP solvers, as well as LP-relaxations from the MIPLIB [27] benchmark set. The EASY instance set consists of self-generated LP formulations that are well-suited for the quantum subroutine. See Table 1 and Figure 1 for more details. The EASY instance set was generated in an attempt to answer RQ3. Many instances in HARD are not sparse nor well-conditioned. By Theorem 4.1, Algorithm 4.1 scales quadratically with the number of nonzero elements in the matrix  $A$  and the condition number  $\kappa$ . Therefore, we constructed instances for sparse and well-conditioned problems, giving the quantum algorithm an additional asymptotic benefit. These are *Maximum Flow*, *Minimum Vertex Cover*, and *Maximum Independent Set*. The Maximum Flow formulations were generated from the Max-Flow-Min-Cut benchmark set [29] and the graphs for the other problems were either (i) taken from the second DIMACS implementation challenge [30] or (ii) generated random Erdős-Rényi graphs with up to 1,000 vertices; see [3] for details.

## 5.3 Instance from Combinatorial Optimization

Nannicini [42] notes that his approach is most likely to be valuable for sparse instances with a low condition number. As this is rarely the case for the instances from the benchmark libraries, we also use well-known LP relaxations of graph problems, which ensure a low condition number.

- **Maximum Flow:** Given a directed weighted graph  $(V, A)$  with a source vertex  $s$ , a target vertex  $t$  and a capacity function  $c$ , the Maximum Flow Problem deals with finding the maximum amount of flow that can be sent through the edges while



not exceeding the maximum capacity of each edge. As relaxed linear formulation we use the following.

$$\begin{aligned} \max \quad & \sum_{(u,t) \in A} x_{u,t} - \sum_{(t,u) \in A} x_{t,u} \\ \text{s.t.} \quad & \sum_{(u,v) \in A} x_{u,v} - \sum_{(v,u) \in A} x_{v,u} = 0, \quad \forall u \in V \\ & x_{u,v} \leq c(u,v), \quad \forall (u,v) \in A \end{aligned}$$

- **Minimum Vertex Cover:** Given an undirected graph with a set of vertices  $V$  and a set of edges  $E$ , a Minimum Vertex Cover is a smallest set of vertices that contains at least one vertex of every edge. As linear relaxation, we use the following.

$$\begin{aligned} \text{minimize} \quad & \sum_{v \in V} x_v \\ \text{subject to} \quad & x_u + x_v \geq 1, \quad \forall \{u,v\} \in E \\ & 0 \leq x_v \leq 1, \quad \forall v \in V \end{aligned}$$

- **Maximum Independent Set:** A maximum independent set of an undirected graph  $(V, E)$  is a largest set of vertices that contains at most one vertex of every edge. This yields the following linear programming relaxation.

$$\begin{aligned} \text{maximize} \quad & \sum_{v \in V} x_v \\ \text{subject to} \quad & x_u + x_v \leq 1, \quad \forall \{u,v\} \in E \\ & 0 \leq x_v \leq 1, \quad \forall v \in V \end{aligned}$$

- **Maximum Clique:** A maximum clique of an undirected graph  $(V, E)$  is a largest set of vertices that contains an edge between any two vertices. A linear programming relaxation is the following.

$$\begin{aligned} \text{maximize} \quad & \sum_{v \in V} x_v \\ \text{subject to} \quad & x_u + x_v \leq 1, \quad \forall \{u,v\} \notin E \\ & 0 \leq x_v \leq 1, \quad \forall v \in V \end{aligned}$$

**5.4 Experimental Design** As the primal Simplex runs single-threaded, all experiments were executed on a single CPU core of an Intel Core i7 6700K or Intel Core i7 4770K with 16 GB DDR4 RAM and Ubuntu 22.04.2 LTS. We adapted the standard GLPK implementation compiled by gcc (v11.3.0) for our requirements and introduced callbacks into the primal Simplex routine to log all important data. The callbacks were written in Python 3.10 with native C elements using ctypes. The source code is available on GitHub<sup>6</sup>.

<sup>6</sup>URL not shown for double-blinding and available on authorized request.

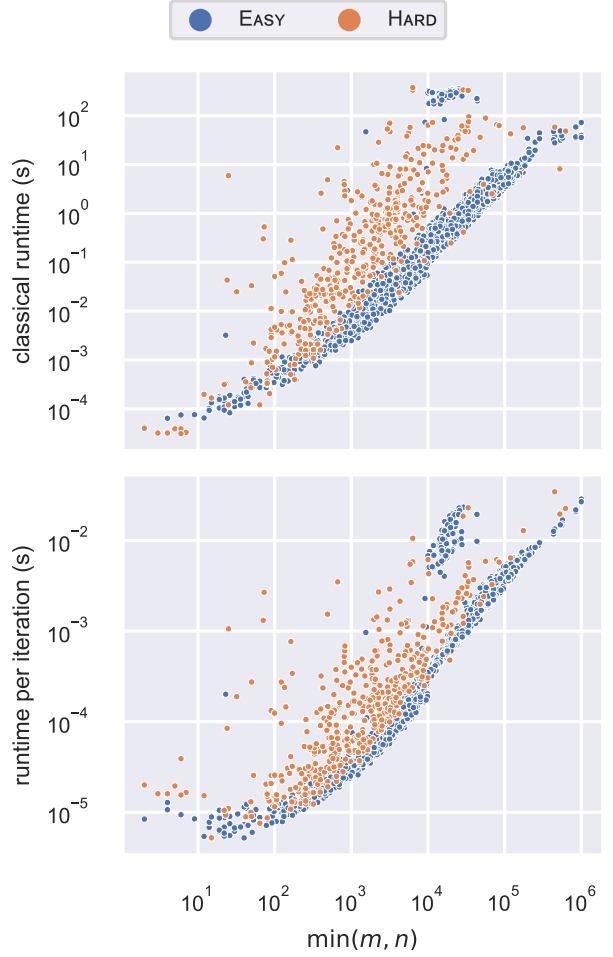


Figure 2: Pure runtime without logging, using GLPK. (Top) Total runtime. (Bottom) Average runtime per iteration.

We distinguish between *iteration-related* and *instance-related* measures; the latter include variable number  $n$ , constraint number  $m$ , the number of nonzero elements  $d_n$ , and the maximum weight  $c_i$  of the objective function.

In each iteration, we save the total number of nonzeros in the basis  $A_B$ , the maximum number of nonzeros in its columns, its maximum absolute value, and the norms  $\|A_B\|_1$ ,  $\|A_B\|_1^{-1}$ , as well as the condition number  $\kappa(A_B)$ . To compute the bound in Lemma 4.4, we log the number of columns that would improve the objective function, i.e., with reduced costs  $< 0$  for a minimization problem, as well as the absolute maximum reduced cost value. Additionally, Lemmas 4.5 and 4.6 require the number of positive components in  $u = A_B^{-1}A_k$  as well as  $\|u\|_2$ . Finally, we measure the time per iteration excluding the time for computing the above values. Computing the exact value of the condition

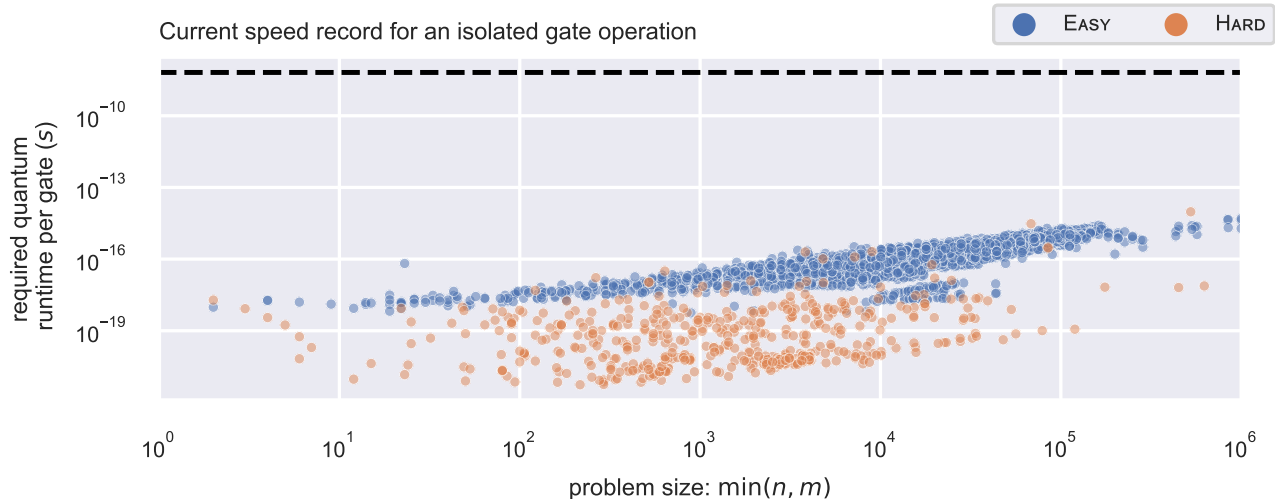


Figure 3: Minimum required gate evaluation time to outperform a classical iteration. Values are the average over all ratios between the (classical) iteration runtime and the iteration’s expected gate complexity bound, and are subject to a number of additional benevolent assumptions for the quantum algorithm. The dashed line at  $6.5 \times 10^{-9}$  is the best time achieved for an isolated gate operation [17]. While the gap to the dashed line slowly narrows with increasing  $\min(m, n)$ , the qualitative picture does not change for problem sizes that can realistically be treated.

number  $\kappa(A_B)$  in each iteration comes with major drawbacks in efficiency. Internally, GLPK computes the condition number  $\kappa_1(A_B) = \|A_B\|_1 \cdot \|A_B^{-1}\|_1$  to print out a user warning when an ill-conditioned basis matrix is encountered. Therefore, instead of calculating  $\kappa(A_B)$  explicitly, we only save the value of  $\kappa_1(A_B)$ . Given  $\kappa(A_B) \geq 1$  and  $\|A_B\|_2 \geq \frac{\|A_B\|_1}{\sqrt{m}}$ , we can establish  $\kappa(A_B) \geq \max\left(1, \frac{\kappa_1(A_B)}{m}\right)$  as a lower bound for  $\kappa(A_B)$ . This data is used to compute the lower bound for the expected number of gates per iteration. Therefore, we sum the individual costs of each subroutine of SimplexIter (stated in Lemmas 4.3–4.6). All plots were generated with the classical steepest edge pivoting rule as well as the quantum steepest edge bound, see Lemma 4.4. As Algorithm 4.1 operates on a normalized matrix  $\hat{A} = \frac{A}{\|A\|_2}$ , we lower bound the norms from Lemma 4.2 with  $\|\hat{A}_B\|_1 \geq \frac{\|A_B\|_1}{d\|A_B\|_{max}}$  and  $\|\hat{A}_B\|_{max} \geq \frac{1}{d}$ . For all calculations we used precision parameters  $\varepsilon = \delta = 10^{-3}$ ; as the performance of the quantum solver is linearly dependent on  $\varepsilon$  and  $\delta$ , a choice of  $\varepsilon = \delta = 10^{-6}$  (a default value for many classical solvers like CPLEX or Gurobi) would further diminish the performance of the quantum solver by a factor of  $10^{-3}$ .

**5.5 Evaluation** We ran the experiments on all instances from Table 1 with a maximum time limit of

1,800s. Evaluations for other pivoting rules that Nannicini [42] mentioned can be found in Appendix A. Figure 2 shows the runtime distribution of the two classes. It is clear that most of the instances from HARD needed more time, both in total and within each iteration. On the empirical basis of this study, we can answer the proposed research questions.

**RQ1: Could Algorithm 4.1 provide a speedup over the classical Simplex algorithm when quantum hardware is ready?**

Each dot in Figure 3 shows the average ratio between the classical runtime and the lower bound of the expected gate complexity in that iteration. Thus, the y-values give the time in which a quantum algorithm has to evaluate a single gate to get an overall improvement over the classical Simplex iteration. The black dotted line represents the fastest quantum gate that has currently been realized; the timescale are nanoseconds, based on the  $6.5 \cdot 10^{-9}$ s from [17]. As described in Section 1, it is reasonable to expect that gate times will be limited for the foreseeable future to above the  $10^{-10}$ s timescale. This suggests that even with a very optimistic view of future hardware improvements, quantum computers are several orders of magnitude away from being useful in practice for this specific algorithm. This holds for both the EASY and HARD set of instances.

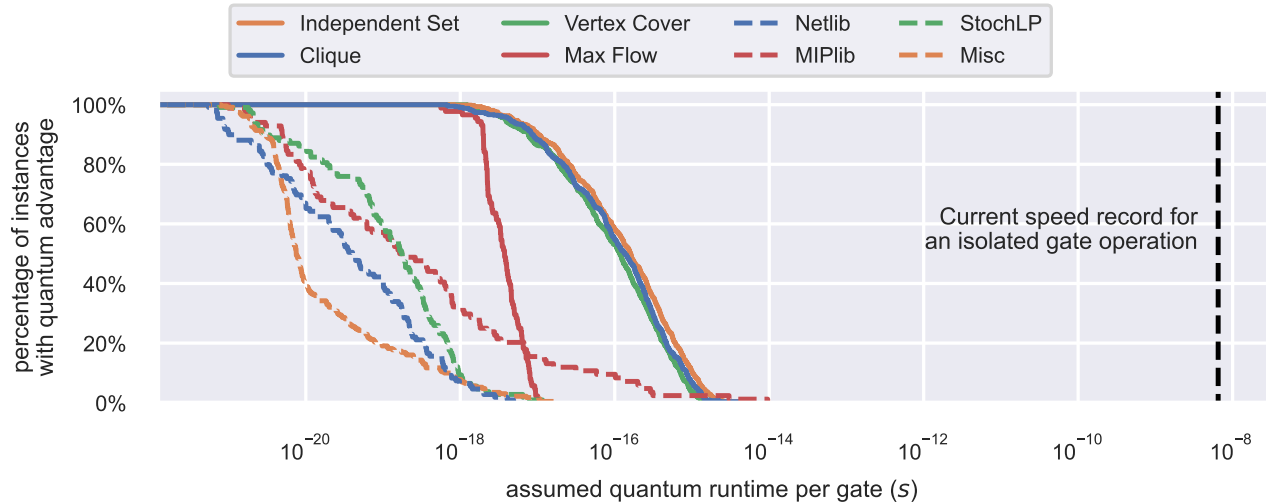


Figure 4: Percentage of instances (y-axis) that allow for a quantum advantage over the classical Simplex algorithm with the assumed given quantum gate evaluation time (x-axis). Despite the benevolent assumptions, none are even close to the realistic bound of  $6.5 \times 10^{-9}$  seconds.

**RQ2: What quantum gate operation times are required for Algorithm 4.1 to provide a speedup over the classical primal Simplex algorithm?**

Our framework allows an empirical answer. Figure 4 shows how many instances require a specific runtime per gate from a quantum computer to perform one Simplex iteration in the same runtime as a classical computer. To beat a classical computer on the EASY benchmark set, a quantum computer needs to evaluate one gate in about  $10^{-18}$  seconds. Further, a time of at most  $10^{-21}$  seconds per gate is needed to outperform the classical computer on every instance. In addition, recall that we estimated the number of gates by a lower bound. Thus, the true number of gates could be even larger, and the time left for one gate even lower.

**RQ3: Can we find LP instances that are easier to solve on quantum hardware?** Our EASY benchmark set aimed for instances that scale well with the asymptotic runtime from Theorem 4.1. Our instance set is well-conditioned (with a condition number of 1 in almost all iterations) and very sparse, see Figure 5. Figure 3 shows that the computed lower bounds, while being several orders of magnitude higher than for most of the HARD benchmark set, will still not allow for a quantum advantage over the classical methods.

**6 Conclusions**

We have presented an analysis for gauging the practical performance of quantum computers for solving large-scale, real-world instances of important optimization problems, resulting in estimates for the physical gate-

time requirements for future hardware to deliver real-world quantum speed up. We have evaluated the resulting hybrid benchmarking for solving linear optimization problems for Nannicini’s quantum version of the simplex method.

There are a number of important conclusions. Specifically, the asymptotic advantage of a quantum method like the one of Nannicini appears to be unlikely to play out in the practical dimensions that are relevant for realistic applications (reflected by the considered large-scale benchmark instances): Even under very benevolent assumptions (e.g., ignoring error correction and other physical aspects of quantum computers) and for purposefully constructed sparse and well-conditioned linear programs that are better suited for such a quantum algorithm, the required gate efficiency seems beyond what is physically possible. This will not fundamentally change for even larger instances of practical dimensions.

More generally, our methods offer a way to provide meaningful estimates for the practical performance of algorithms on future quantum devices. Many quantum subroutines are built from a fixed pool of algorithms like unstructured quantum search or QLS. Deriving such runtime estimates can be used to analyze a variety of quantum algorithms beyond asymptotic complexity. This offers a pathway for realistic perspectives of future progress, instead of just asymptotic worst-case runtime, which may lead to unrealistic expectations on possible benefits.

## References

- [1] Brandon Augustino, Giacomo Nannicini, Tamás Terlaky, and Luis F. Zuluaga. Quantum interior point methods for semidefinite optimization, 2022. [arXiv:2112.06025](#), doi:10.48550/arXiv.2112.06025.
- [2] Ryan Babbush, Jarrod R McClean, Michael Newman, Craig Gidney, Sergio Boixo, and Hartmut Neven. Focus beyond quadratic speedups for error-corrected quantum advantage. *PRX Quantum*, 2(1):010103, 2021.
- [3] Vladimir Batagelj and Ulrik Brandes. Efficient generation of large random networks. *Phys. Rev. E*, 71:036113, Mar 2005. doi:10.1103/PhysRevE.71.036113.
- [4] Dominic W. Berry, Andrew M. Childs, Richard Cleve, Robin Kothari, and Rolando D. Somma. Exponential improvement in precision for simulating sparse hamiltonians. In *Proceedings of the forty-sixth annual ACM symposium on Theory of computing*. ACM, may 2014. doi:10.1145/2591796.2591854.
- [5] Dominic W. Berry, Andrew M. Childs, Richard Cleve, Robin Kothari, and Rolando D. Somma. Simulating hamiltonian dynamics with a truncated Taylor series. *Physical Review Letters*, 114(9), mar 2015. doi:10.1103/physrevlett.114.090502.
- [6] Dominic W. Berry, Andrew M. Childs, and Robin Kothari. Hamiltonian simulation with nearly optimal dependence on all parameters. In *2015 (IEEE) 56th Annual Symposium on Foundations of Computer Science*. IEEE, oct 2015. doi:10.1109/focs.2015.54.
- [7] Robert E Bixby. Solving real-world linear programs: A decade and more of progress. *Operations Research*, 50(1):3–15, 2002. doi:10.1287/opre.50.1.3.17780.
- [8] Michel Boyer, Gilles Brassard, Peter Høyer, and Alain Tapp. Tight bounds on quantum searching. *Fortschritte der Physik: Progress of Physics*, 46(4-5):493–505, 1998. doi:10.1002/(SICI)1521-3978(199806)46:4/5<493::AID-PROP493>3.0.CO;2-P.
- [9] Fernando G. S. L. Brandão, Amir Kalev, Tongyang Li, Cedric Yen-Yu Lin, Krysta M. Svore, and Xiaodi Wu. Quantum SDP solvers: Large speed-ups, optimality, and applications to quantum learning, 2019. [arXiv:1710.02581](#), doi:10.48550/arXiv.1710.02581.
- [10] Fernando G. S. L. Brandão and Krysta Svore. Quantum speed-ups for semidefinite programming, 2017. [arXiv:1609.05537](#), doi:10.48550/arXiv.1609.05537.
- [11] Gilles Brassard, Peter Høyer, Michele Mosca, and Alain Tapp. Quantum amplitude amplification and estimation. *Contemporary Mathematics*, pages 53–74, 2002. URL: <https://doi.org/10.1090%2Fconn%2F305%2F05215>, doi:10.1090/conn/305/05215.
- [12] Chris Cade, Marten Folkertsma, Ido Niesen, and Jordi Weggemans. Quantifying Grover speed-ups beyond asymptotic analysis, 2022. doi:10.48550/arXiv.2203.04975.
- [13] Chris Cade, Marten Folkertsma, Ido Niesen, and Jordi Weggemans. Quantum algorithms for community detection and their empirical run-times, 2022. doi:10.48550/arXiv.2203.06208.
- [14] Chris Cade, Marten Folkertsma, Ido Niesen, and Jordi Weggemans. Quantifying Grover speed-ups beyond asymptotic analysis. *Quantum*, 7:1133, 2023.
- [15] Earl Campbell, Ankur Khurana, and Ashley Montanaro. Applying quantum algorithms to constraint satisfaction problems. *Quantum*, 3:167, 2019.
- [16] Pablo AM Casares and Miguel Angel Martin-Delgado. A quantum interior-point predictor–corrector algorithm for linear programming. *Journal of Physics A: Mathematical and Theoretical*, 53(44):445305, 2020. doi:10.1088/1751-8121/abb439.
- [17] Yeelai Chew, Takafumi Tomita, Tirumalasetty Panduranga Mahesh, Seiji Sugawa, Sylvain de Léséleuc, and Kenji Ohmori. Ultrafast energy exchange between two single Rydberg atoms on a nanosecond timescale. *Nature Photonics*, 16(10):724–729, 2022. doi:10.1038/s41566-022-01047-2.
- [18] Andrew M Childs, Robin Kothari, and Rolando D Somma. Quantum algorithm for systems of linear equations with exponentially improved dependence on precision. *SIAM Journal on Computing*, 46(6):1920–1950, 2017. doi:10.1137/16M1087072.
- [19] Richard Cleve, Artur Ekert, Chiara Macchiavello, and Michele Mosca. Quantum algorithms revisited. *Proceedings of the Royal Society of London. Series A: Mathematical, Physical and Engineering Sciences*, 454(1969):339–354, 1998. doi:10.1098/rspa.1998.0164.
- [20] Alexander M. Dalzell, B. David Clader, Grant Salton, Mario Berta, Cedric Yen-Yu Lin, David A. Bader, Nikitas Stamatopoulos, Martin J. A. Schuetz, Fernando G. S. L. Brandão, Helmut G. Katzgraber, and William J. Zeng. End-to-end resource analysis for quantum interior point methods and portfolio optimization, 2022. [arXiv:2211.12489](#), doi:10.48550/arXiv.2211.12489.
- [21] Geroge B. Dantzig. Linear programming in problems for the numerical analysis of the future. In *Proceedings of the Symposium on Modern Calculating Machinery and Numerical Methods*, UCLA, July, pages 29–31, 1948.
- [22] Christoph Dürr and Peter Hoyer. A quantum algorithm for finding the minimum. *arXiv preprint quant-ph/9607014*, 1999. [arXiv:quant-ph/9607014](#), doi:10.48550/arXiv.quant-ph/9607014.
- [23] John J Forrest and Donald Goldfarb. Steepest-edge simplex algorithms for linear programming. *Mathematical programming*, 57(1-3):341–374, 1992. doi:10.1007/BF01581089.
- [24] Gerald Gamrath, Tobias Fischer, Tristan Gally, Ambros Gleixner, Gregor Hendel, Thorsten Koch, Stephen J Maher, Matthias Miltenberger, Benjamin Müller, Marc Pfetsch, et al. The SCIP optimization suite 3.2, 2016.

- [25] David M. Gay. netlib/lp/data. URL: <https://netlib.org/lp/data/>.
- [26] Jared Lee Gearhart, Kristin Lynn Adair, Justin David Durfee, Katherine A Jones, Nathaniel Martin, and Richard Joseph Detry. Comparison of open-source linear programming solvers. Technical report, Sandia National Lab.(SNL-NM), Albuquerque, NM (United States), 2013. doi:10.2172/1104761.
- [27] Ambros Gleixner, Gregor Hendel, Gerald Gamrath, Tobias Achterberg, Michael Bastubbe, Timo Berthold, Philipp M. Christophel, Kati Jarck, Thorsten Koch, Jeff Linderoth, Marco Lübbecke, Hans D. Mittelmann, Derya Ozyurt, Ted K. Ralphs, Domenico Salvagnin, and Yuji Shinano. Miplib 2017: Data-driven compilation of the 6th mixed-integer programming library. *Mathematical Programming Computation*, 2021. doi:10.1007/s12532-020-00194-3.
- [28] Aram W Harrow, Avinatan Hassidim, and Seth Lloyd. Quantum algorithm for linear systems of equations. *Physical review letters*, 103(15):150502, 2009. doi:10.1103/PhysRevLett.103.150502.
- [29] Patrick Møller Jensen, Niels Jeppesen, Anders Bjorholm Dahl, and Vedrana Andersen Dahl. Min-cut/max-flow problem instances for benchmarking, 3 2022. URL: [https://data.dtu.dk/articles/dataset/Min-Cut\\_Max-Flow\\_Problem\\_Instances\\_for\\_Benchmarking/17091101](https://data.dtu.dk/articles/dataset/Min-Cut_Max-Flow_Problem_Instances_for_Benchmarking/17091101), doi:10.11583/DTU.17091101.v1.
- [30] David S Johnson and Michael A Trick. *Cliques, coloring, and satisfiability: second DIMACS implementation challenge, October 11-13, 1993*, volume 26. American Mathematical Soc., 1996.
- [31] Adeline Jordon, Prashanti Priya Angara, and Saasha Joshi. Implementing the simplex method with Grover’s search. In *2021 IEEE International Conference on Quantum Computing and Engineering (QCE)*, pages 435–436. IEEE, 2021. doi:10.1109/QCE52317.2021.00066.
- [32] Iordanis Kerenidis and Anupam Prakash. A quantum interior point method for LPs and SDPs. *ACM Transactions on Quantum Computing*, 1(1), oct 2020. doi:10.1145/3406306.
- [33] Iordanis Kerenidis, Anupam Prakash, and Dániel Szilágyi. Quantum algorithms for second-order cone programming and support vector machines. *Quantum*, 5:427, apr 2021. doi:10.22331/q-2021-04-08-427.
- [34] Leonid Genrikhovich Khachiyan. A polynomial algorithm in linear programming. In *Doklady Akademii Nauk*, volume 244, pages 1093–1096. Russian Academy of Sciences, 1979.
- [35] Tongyang Li, Shouvanik Chakrabarti, and Xiaodi Wu. Sublinear quantum algorithms for training linear and kernel-based classifiers. In Kamalika Chaudhuri and Ruslan Salakhutdinov, editors, *Proceedings of the 36th International Conference on Machine Learning*, volume 97 of *Proceedings of Machine Learning Research*, pages 3815–3824. PMLR, 09–15 Jun 2019. URL: <https://proceedings.mlr.press/v97/li19b.html>.
- [36] Yunchao Liu, Srinivasan Arunachalam, and Kristan Temme. A rigorous and robust quantum speed-up in supervised machine learning. *Nature Physics*, 17(9):1013–1017, jul 2021. doi:10.1038/s41567-021-01287-z.
- [37] Frederic Magniez, Miklos Santha, and Mario Szegedy. Quantum algorithms for the triangle problem, 2005. arXiv:quant-ph/0310134, doi:10.1137/050643684.
- [38] Ashley Montanaro. Quantum speedup of monte carlo methods. *Proceedings of the Royal Society A: Mathematical, Physical and Engineering Sciences*, 471(2181):20150301, sep 2015. doi:10.1098/rspa.2015.0301.
- [39] Csaba Mészáros. Index of / meszaros/public\_ftp/lptestset/misc, 2004. URL: [http://old.sztaki.hu/~meszaros/public\\_ftp/lptestset/misc/](http://old.sztaki.hu/~meszaros/public_ftp/lptestset/misc/).
- [40] Csaba Mészáros. Index of / meszaros/public\_ftp/lptestset/stochlp, 2004. URL: [http://old.sztaki.hu/~meszaros/public\\_ftp/lptestset/stochlp/](http://old.sztaki.hu/~meszaros/public_ftp/lptestset/stochlp/).
- [41] Yunseong Nam, Yuan Su, and Dmitri Maslov. Approximate quantum Fourier transform with  $O(n \log(n))T$  gates. *npj Quantum Information*, 6(1), mar 2020. URL: <https://doi.org/10.1038/2Fs41534-020-0257-5>, doi:10.1038/s41534-020-0257-5.
- [42] Giacomo Nannicini. Fast quantum subroutines for the simplex method. *Operations Research*, 2022. doi:10.1287/opre.2022.2341.
- [43] Michael A Nielsen and Isaac Chuang. Quantum computation and quantum information, 2002.
- [44] V.V. Shende, S.S. Bullock, and I.L. Markov. Synthesis of quantum-logic circuits. *IEEE Transactions on Computer-Aided Design of Integrated Circuits and Systems*, 25(6):1000–1010, jun 2006. doi:10.1109/tcad.2005.855930.
- [45] Alexandre B. Tacla, Nina Machado O’Neill, Gabriel G. Carlo, Fernando de Melo, and Raul O. Vallejos. Majorization-based benchmark of the complexity of quantum processors, 2023. arXiv:2304.04894, doi:10.48550/arXiv.2304.04894.
- [46] Joran van Apeldoorn and András Gilyén. Improvements in quantum SDP-solving with applications. In Christel Baier, Ioannis Chatzigiannakis, Paola Flocchini, and Stefano Leonardi, editors, *Colloquium on Automata, Languages, and Programming, ICALP*, volume 132, pages 99:1–99:15, 2019. doi:10.4230/LIPIcs.ICALP.2019.99.
- [47] Joran Van Apeldoorn, András Gilyén, Sander Gribling, and Ronald de Wolf. Quantum SDP-solvers: Better upper and lower bounds. *Quantum*, 4:230, 2020. doi:10.22331/q-2020-02-14-230.
- [48] Tanmay Verma and Dhruv Batra. Maxflow revisited: An empirical comparison of maxflow algorithms for dense vision problems. *BMVC 2012 - Electronic Proceedings of the British Machine Vision Conference 2012*, 01 2012. doi:10.5244/C.26.61.
- [49] Nathan Wiebe, Ashish Kapoor, and Krysta Svore. Quantum algorithms for nearest-neighbor methods for

supervised and unsupervised learning, 2014. [arXiv:1401.2142](https://arxiv.org/abs/1401.2142), [doi:10.48550/arXiv.1401.2142](https://doi.org/10.48550/arXiv.1401.2142).

- [50] Raphael Yuster and Uri Zwick. Fast sparse matrix multiplication. *ACM Transactions On Algorithms (TALG)*, 1(1):2–13, 2005. [doi:10.1145/1077464.1077466](https://doi.org/10.1145/1077464.1077466).

## A Additional Figures and Tables

Benchmark	group	# Instances	# Variables	# Constraints	Source
Random Graphs <sup>7</sup>	EASY	1,711	6 to 174,345	2 to 173,755	self generated
DIMACS Graphs <sup>7</sup>	EASY	101	912 to 1,001,836	702 to 999,836	[30]
Maximum Flow	EASY	88	13,792 to 1,112,772	890 to 44,032	[48] via [29]
NETLIB	HARD	109	49 to 243,209	24 to 78,862	[25]
MIPLIB	HARD	84	263 to 641,857	32 to 624,166	[27]
STOCHLP	HARD	108	178 to 1,298,168	80 to 450,047	[40]
MISC	HARD	231	5 to 1,124,162	2 to 34,078	[39]

Table 2: Full overview of the used benchmarking instances.

<sup>7</sup>Instances are LP relaxations of Min Vertex Cover, Max Independent Set and Max Clique.

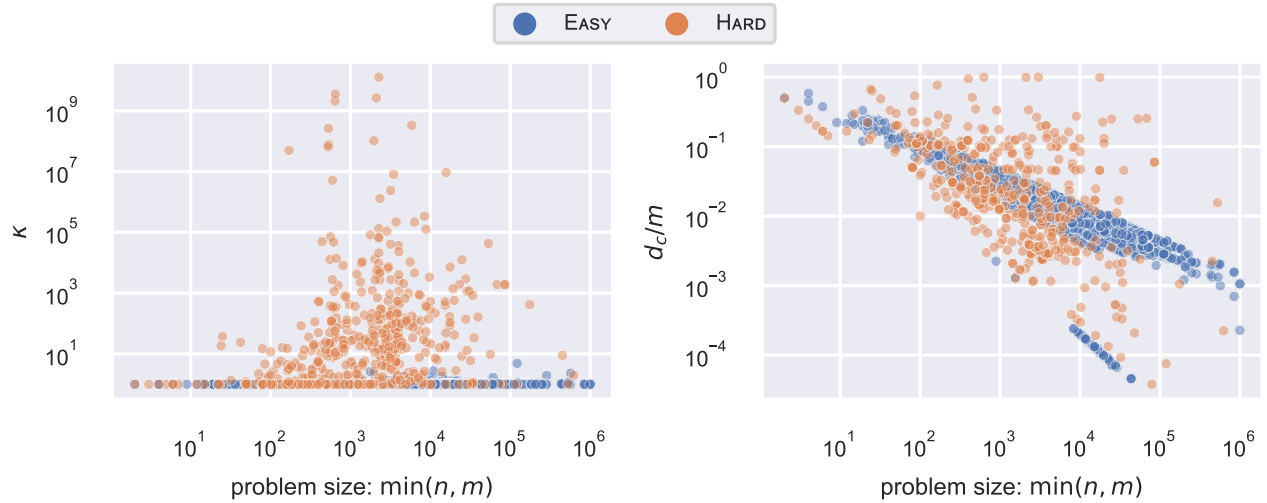


Figure 5: (Left) Average values for the condition number  $\kappa(A_B)$ . (Right) the average fraction of nonzeros  $d_c/m$  in the least sparse column of  $A_B$ .

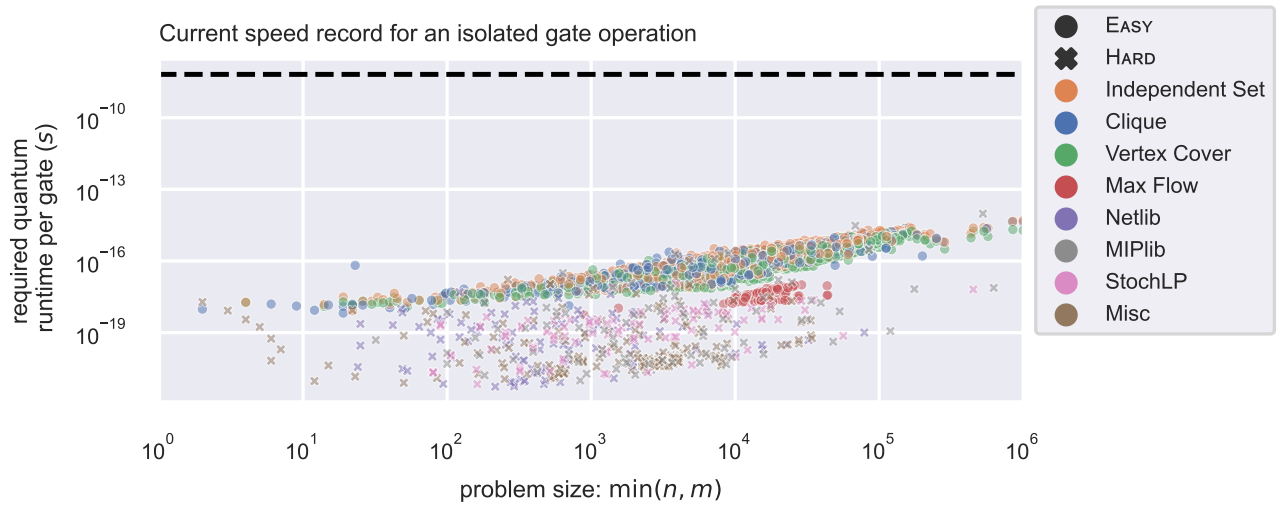


Figure 6: Extension of Figure 3. Minimum required gate evaluation time to outperform a classical iteration. Values are the average over all ratios between the (classical) iteration runtime and the iteration’s expected gate complexity bound, and are subject to a number of additional benevolent assumptions for the quantum algorithm. The black dotted line represents the fastest quantum gate that has currently been realized.

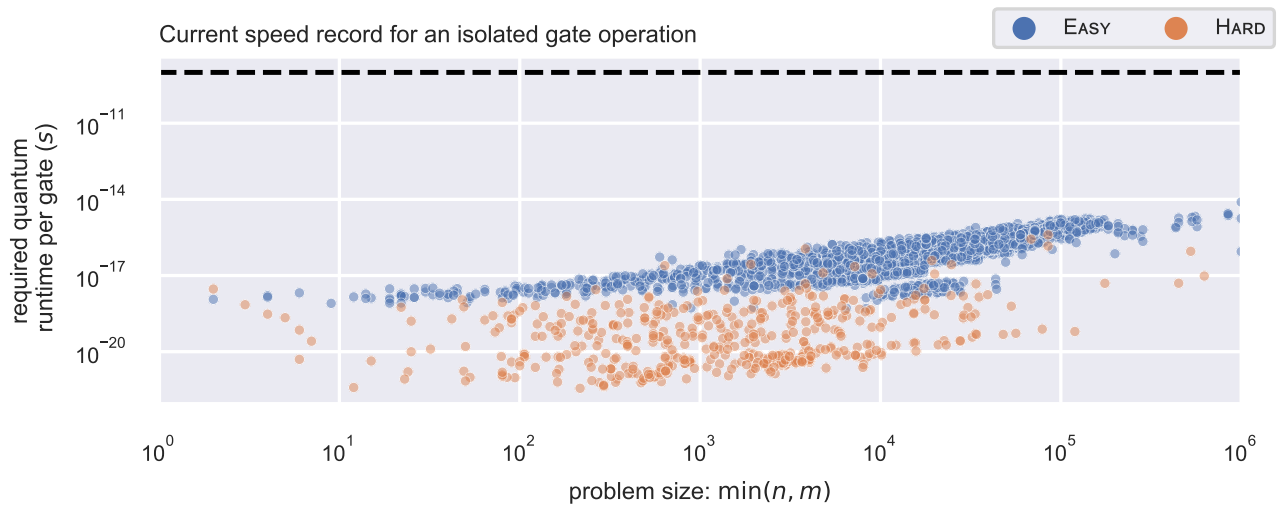


Figure 7: Analog to Figure 3 for the classical Dantzig pivoting rule and corresponding FindColumn – QDanR lower bounds from Lemma B.8. Minimum required gate evaluation time to outperform a classical iteration. Values are the average over all ratios between the (classical) iteration runtime and the iteration’s expected gate complexity bound, and are subject to a number of additional benevolent assumptions for the quantum algorithm. The black dotted line represents the fastest quantum gate that has currently been realized.



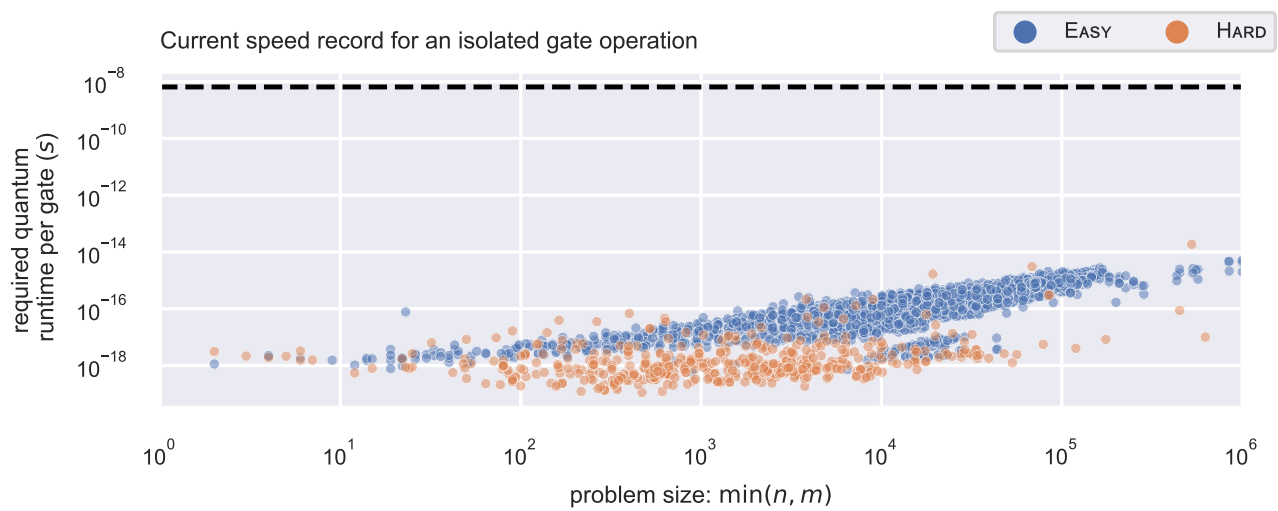


Figure 8: Analog to Figure 3 for the classical steepest edge pivoting rule and FindColumn – Random lower bounds from Lemma B.7. We compared against steepest edge, because a random pivoting rule is not available in GLPK. Minimum required gate evaluation time to outperform a classical iteration. Values are the average over all ratios between the (classical) iteration runtime and the iteration’s expected gate complexity bound, and are subject to a number of additional benevolent assumptions for the quantum algorithm. The black dotted line represents the fastest quantum gate that has currently been realized.

## B Fast Subroutines for the Simplex Method

In Appendix B.2 we provide more details about the subroutines used in Algorithm 4.1, in Appendix B.3 we give proofs for the lemmas presented in Section 4.

**B.1 Notation** In this section, we use the following conventions:

- Often we suppress Kronecker products when writing states, so that  $\otimes_{i=1}^n |x_i\rangle$  is denoted  $|x_1x_2\dots x_n\rangle$ .
- When denoting a quantum state whose amplitudes are given by a vector  $v$ , we write the quantum state as  $|v\rangle$ . For example,  $|\psi\rangle = |(0, 1)\rangle$  is a quantum state with  $\psi_0 = 0$  and  $\psi_1 = 1$ .
- To implement several subroutines, we need to prepare superpositions of states  $|A_k\rangle$  where  $A_k$  are the columns of matrix  $A$ . We assume access to a unitary  $U_{rhs}$  which can do this, namely  $U_{rhs}|k\rangle|0\rangle = |k\rangle|A_k\rangle$ .
- Some subroutines need to apply a QLS to a superposition of linear systems  $A_Bx = A_k$ , for different values of  $k$ . We can do this by using  $U_{rhs}$  as oracle  $\mathcal{P}_b$  in QLS as described in Appendix C.8. We write this as  $A_k = U_{rhs}(\cdot)$ .
- We always assume that the input matrix  $A$  and cost vector  $c$  are normalized, such that  $\|A_B\| \leq 1, \|c_B\| = 1$ .
- We denote by  $\text{ctrl}_n-U$  a controlled version of unitary  $U$ , controlled on  $n$  qubits, see Appendix C.2 for more details.

**B.2 Subroutines of SimplexIter** In the following, we explain in detail how the quantum subroutines used in Algorithm 4.1 are implemented. These are `IsOptimal`, `FindColumn`, `IsUnbounded`, and `FindRow`; they are built using a number of core subroutines, which we summarize in Appendix B.2.1, and several common quantum algorithms, which are explained in Appendix C.

**B.2.1 Core Subroutines** `IsOptimal`, `FindColumn`, `IsUnbounded`, and `FindRow` share some core subroutines, which we explain in further detail.

**RedCost** The first core subroutine is `RedCost`, which is used by `CanEnterNFN` and `CanEnterNFP`, `QStER`, `QDanR`. Given a basis  $A_B$ , a nonbasic column  $A_k$ , and a cost  $c$  as inputs, `RedCost` prepares a state  $|\psi\rangle$  with  $\psi_0 = \bar{c}_k$ . Here,  $\bar{c}_k$  is the reduced cost of the column  $k$ . We first encode the solution of

$$\begin{pmatrix} A_B & 0 \\ 0 & 1 \end{pmatrix} \begin{pmatrix} x \\ y \end{pmatrix} = \begin{pmatrix} A_k \\ c_k \end{pmatrix}$$

in a quantum state, using a quantum linear solver (QLS). For an explanation of QLS see Appendix C.8. At this point, the state is  $|\hat{x}\rangle = |(A_B^{-1}A_k, c_k)\rangle$ , tensored with the success/failure flag of the QLS. We then consider a unitary that acts on  $|0\rangle$  as  $U_c|0\rangle = |(-c_B, 1)\rangle$ . Acting with  $U_c^\dagger$  on  $|\hat{x}\rangle$ , we produce a state whose zeroth amplitude is given by  $c_k$ , as wanted. More precisely, we have

$$|\psi\rangle \equiv U_c^\dagger |\hat{x}\rangle = \frac{1}{\sqrt{2}} \begin{pmatrix} -c_B & 1 \\ \dots & \dots \end{pmatrix} \cdot \frac{1}{\|\hat{x}\|} \begin{pmatrix} A_B^{-1}A_k \\ c_k \end{pmatrix},$$

hence the zeroth amplitude of  $|\psi\rangle$  is

$$(B.1) \quad \psi_0 = \frac{1}{\sqrt{2}\|\hat{x}\|} \bar{c}_k.$$

The prefactors  $\sqrt{2}$  and  $\|\hat{x}\|$  are needed to maintain a proper normalization of the states. Moreover, `RedCost` also returns the success/failure flag of the QLS. This is used to ensure that the algorithm continues only if the former has been successful.

---

### Algorithm B.1 RedCost

---

**function** REDCOST(basis  $A_B$ , nonbasic column  $A_k$ , cost  $c$ , tolerance  $\varepsilon > 0$ )  
 $\hat{A}_B \leftarrow \text{diag}(A_B, 1)$ ,  $\hat{b} \leftarrow (A_k, c_k)^T$   
Apply QLS( $\hat{A}_B, \hat{b}, \varepsilon$ ), let  $|\hat{x}\rangle = |(A_B^{-1}A_k, c_k)\rangle$  be the solution  
Compute  $|\psi\rangle = U_c^\dagger |\hat{x}\rangle \quad \triangleright U_c|0\rangle = |(-c_B, 1)\rangle$ ,  
result:  $\psi_0 = \bar{c}_k$   
**return**  $|\psi\rangle$  and the QLS flag  
**end function**

---

**Interfere** The second core subroutine is `Interfere`. This is used by `SignEstNFN`, `SignEstNFP`, `QStER`, and `QDanR`. In order to understand how `Interfere` works, let  $U$  and  $V$  be two unitaries that act on  $|0\rangle$  as  $U|0\rangle = \sum \psi_j |j\rangle$  and  $V|0\rangle = \sum \beta_j |j\rangle$ . With the ancilla initialized to the state  $|0\rangle$ , `Interfere` subsequently prepares the state

$$|\phi\rangle = \frac{1}{2} |0\rangle_a \otimes \sum_j (\psi_j + \beta_j) |j\rangle - \frac{1}{2} |1\rangle_a \otimes \sum_j (\psi_j - \beta_j) |j\rangle$$

This can be done following the steps in Algorithm B.2.

**SignEstNFN and SignEstNFP** Given the similar structure of `SignEstNFN` and `SignEstNFP`, we address both subroutines simultaneously. `SignEstNFN` is used in `CanEnterNFN`, `QStER`, `QDanR`, `IsUnbounded`, and `FindRow`. `SignEstNFP` is used in `CanEnterNFP`. Both subroutines take as input a unitary  $U$ , an index  $l$ , and precision  $\varepsilon$ . Let  $|\psi\rangle$  be the state generated by  $U$

---

**Algorithm B.2** Interfere

---

**function** INTERFERE(unitaries  $U$ , unitary  $V$ )  
  Apply H on an auxiliary qubit prepared in state  $|0\rangle_a$   
  Act with  $(|0\rangle\langle 0| \otimes \mathbb{1} + |1\rangle\langle 1| \otimes U) \cdot (|0\rangle\langle 0| \otimes V + |1\rangle\langle 1| \otimes \mathbb{1})$   
  Apply H to the ancilla  
**end function**

---

acting on  $|0\rangle$ , the goal of SignEstNFN and SignEstNFP is to decide whether the  $l$ -th amplitude of  $|\psi\rangle$  is positive. More precisely, they should return 0 if  $\psi_l < -\varepsilon$ , and return 1 if  $\psi_l \geq -\varepsilon$ . Both subroutines have a bounded probability of failure. The difference between the two is that SignEstNFN returns false negatives with small probability, while SignEstNFP returns false positives with small probability. This affects only the last step of the algorithm, as we explain below.

The first steps and the overall strategy are the same. To implement SignEstNFN and SignEstNFP, we first add an ancilla and use Interfere, see Algorithm B.2. The inputs of Interfere are the unitary  $U$ , same as the input of SignEst, and another unitary  $V$ , that acts on  $|0\rangle$  as  $V|0\rangle = |l\rangle$ . Interfere generates a state with  $(0, l)$ -th amplitude equal to  $(\psi_l + 1)/2$ . We then use quantum amplitude estimation (QAE) to estimate this amplitude. If the amplitude is smaller than  $1/2$ , then we can conclude that  $\psi_l$  is negative. The way quantum amplitude estimation works is explained in Appendix C.5. The two subroutines differ in the precision parameters used for QAE, and in manner in which amplitude comparison is performed in the last step.

For SignEstNFN, we use QAE with precision parameters

$$\varepsilon_{\text{QAE}} = \frac{\varepsilon}{\sqrt{3\pi}}, \quad \delta_{\text{QAE}} = \frac{1}{4}.$$

The output of QAE is a number  $\tilde{\phi} \in [0, 1]$ , with probability greater than  $3/4$ ,  $\varepsilon_{\text{QAE}}$ -close to

$$\phi = \frac{1}{\pi} \arcsin\left(\frac{1 + \psi_l}{2}\right).$$

From this expression, we notice that  $\psi_l < 0$  if  $\phi \in [0, 1/6] \cup [5/6, 1]$ . Since QAE works with finite precision, using this interval we would run the risk of having false positives and negatives. Therefore, SignEstNFN returns 1 if  $\phi \in [1/6 - 2\varepsilon_{\text{QAE}}, 5/6 + 2\varepsilon_{\text{QAE}}]$ . As shown in [42] (see App. A.3), this ensures that SignEstNFN returns 1 if  $\alpha \geq -\varepsilon$  with probability at least  $3/4$ . In other words, SignEstNFN returns "no false negative" with bounded probability.

---

**Algorithm B.3** SignEstNFN

---

**function** SIGNESTNFN(unitary  $U$ , binary string  $l$ , tolerance  $\varepsilon > 0$ )

$\mathcal{A} \leftarrow \text{Interfere}(U, V)$ ,  $\chi_l(x) \leftarrow \begin{cases} 1 & x = (0, l) \\ 0 & \text{otherwise} \end{cases}$   
   $\triangleright V|0\rangle = |l\rangle$   
   $\varepsilon_{\text{QAE}} \leftarrow \varepsilon/\sqrt{3\pi^2}$ ,  $\delta_{\text{QAE}} \leftarrow 1/4$   
  Run QAE( $\mathcal{A}$ ,  $\chi_l$ ,  $\delta_{\text{QAE}}$ ,  $\varepsilon_{\text{QAE}}$ ), let  $\tilde{\phi}$  be the estimate obtained  $\triangleright$   
   $\sin(\pi\tilde{\phi}) \approx (1 + \psi_l)/2$   
  **if**  $\phi \in [1/6 - 2\varepsilon_{\text{QAE}}, 5/6 + 2\varepsilon_{\text{QAE}}]$  **then return 1**  
  **else return 0**  
  **end if**  
**end function**

---

For SignEstNFP, we use QAE with precision parameters

$$\varepsilon_{\text{QAE}} = \frac{\varepsilon}{9\sqrt{3\pi}}, \quad \delta_{\text{QAE}} = \frac{1}{4}.$$

SignEstNFP returns 1 if  $\phi \in (1/6 - 2\varepsilon_{\text{QAE}}, 5/6 + 2\varepsilon_{\text{QAE}})$ . This makes sure that SignEstNFP returns 0 if  $\alpha \leq -\varepsilon$  with probability at least  $3/4$ , see App. A.3 in [42]. In other words, SignEstNFP returns "no false positive" with bounded probability.

---

**Algorithm B.4** SignEstNFP

---

**function** SIGNESTNFP(unitary  $U$ , binary string  $l$ , tolerance  $\varepsilon > 0$ )

$\mathcal{A} \leftarrow \text{Interfere}(U, V)$ ,  $\chi_l(x) \leftarrow \begin{cases} 1 & x = (0, l) \\ 0 & \text{otherwise} \end{cases}$   
   $\triangleright V|0\rangle = |l\rangle$   
   $\varepsilon_{\text{QAE}} \leftarrow \varepsilon/9\sqrt{3\pi^2}$ ,  $\delta_{\text{QAE}} \leftarrow 1/4$   
  Run QAE( $\mathcal{A}$ ,  $\chi_l$ ,  $\delta_{\text{QAE}}$ ,  $\varepsilon_{\text{QAE}}$ ), let  $\tilde{\phi}$  be the estimate obtained  $\triangleright$   
   $\sin(\pi\tilde{\phi}) \approx (1 + \psi_l)/2$   
  **if**  $\phi \in (1/6 - 2\varepsilon_{\text{QAE}}, 5/6 + 2\varepsilon_{\text{QAE}})$  **then return 1**  
  **else return 0**  
  **end if**  
**end function**

---

**CanEnterNFN and CanEnterNFP** Given their similar nature, we give an explanation of both CanEnterNFN and CanEnterNFP subroutines together. The sole difference between these two is that CanEnterNFN uses SignEstNFN, while CanEnterNFP uses SignEstNFP.

Given a basis  $A_B$ , nonbasic column  $A_k$ , cost  $c$ , and tolerance  $\varepsilon$ , CanEnterNFN and CanEnterNFP return 1 if  $\bar{c}_k < -\varepsilon\|\hat{x}\|$ , and 0 otherwise. Here,  $\hat{x} = (A_B^{-1}A_k, c_k)$ ,

see RedCost (Algorithm B.1) for details. Notice that this quantity changes in unpredictable ways during runtime. In particular, one might run into problems if  $\hat{x}$  becomes large sometime during the simplex run. Therefore, fixing the "tolerance" in the quantum algorithm is not as simple as in the classical algorithm. For the moment, we set aside this subtlety, and use the same value for  $\varepsilon$  as that used in the classical algorithm.

The oracle CanEnterNFP is implemented in two steps. First, we use RedCost, see Algorithm B.1, to calculate the reduced cost of a given column and store it into the zeroth amplitude of a quantum state. Second, we use SignEstNFP or SignEstNFP, see Algorithm B.3 and Algorithm B.4, to estimate the sign of this amplitude. We can then implement CanEnterNFP by applying SignEstNFP with inputs  $U = \text{RedCost}$  and  $j = 0$ .

---

**Algorithm B.5** CanEnterNFP

---

**function** CANENTERNFP(basis  $A_B$ , nonbasic column  $A_k$ , cost  $c$ , tolerance  $\varepsilon > 0$ )  
 $\varepsilon_{SE} \leftarrow \varepsilon \cdot 1.1/\sqrt{2}$ ,  $\varepsilon_{RC} \leftarrow \varepsilon \cdot 0.1/\sqrt{2}$   
 $U \leftarrow \text{RedCost}(A_B, A_k, c, \varepsilon_{RC})$ ,  $l \leftarrow 0$   
Apply SignEstNFP( $U, l, \varepsilon_{SE}$ )  
**if** SignEstNFP returned 0 and flag ‘success’ **then**  
**return** 1  
**else return** 0  
**end if**  
**end function**

---

Similarly, CanEnterNFP is implemented by applying SignEstNFP with inputs  $U = \text{RedCost}$  and  $j = 0$ .

---

**Algorithm B.6** CanEnterNFP

---

**function** CANENTERNFP(basis  $A_B$ , nonbasic column  $A_k$ , cost  $c$ , tolerance  $\varepsilon > 0$ )  
 $\varepsilon_{SE} \leftarrow \varepsilon \cdot 1.1/\sqrt{2}$ ,  $\varepsilon_{RC} \leftarrow \varepsilon \cdot 0.1/\sqrt{2}$   
 $U \leftarrow \text{RedCost}(A_B, A_k, c, \varepsilon_{RC})$ ,  $l \leftarrow 0$   
Apply SignEstNFP( $U, l, \varepsilon_{SE}$ )  
**if** SignEstNFP returned 0 and flag ‘success’ **then**  
**return** 1  
**else return** 0  
**end if**  
**end function**

---

**B.2.2 IsOptimal** Given the matrix  $A$ , the basis  $B$ , the cost  $c$  and some precision  $\varepsilon$  as inputs, IsOptimal determines if the current basis is optimal. To implement IsOptimal, we use an oracle CanEnterNFP, see Algorithm B.6, which determines if an input column  $k$  has negative reduced cost. Here NFP stands for "no false positive", because the oracle is built such that with bounded probability it returns no false positive. We

act with CanEnterNFP on a superposition of all nonbasic columns, which we prepare by acting with  $U_{rhs}$  on  $|\psi_N\rangle \equiv 1/\sqrt{|N|} \sum_{k \in N} |k\rangle$ . Here  $N$  is the set of nonbasic columns and  $|N| = n - m$ . We then use quantum amplitude estimation (QAE) to estimate the amplitude with which CanEnterNFP returns 1. If this amplitude is zero, we can conclude that no nonbasic column has negative reduced cost and the solution is optimal. QAE is explained in Appendix C.5. Let  $\varepsilon_{QAE}$  and  $\delta_{QAE}$  be the precision parameters of QAE, and  $\psi_1$  be the amplitude we want to estimate. QAE outputs an estimate  $\tilde{\phi}$  that with probability at least  $1 - \delta_{QAE}$  is  $\varepsilon_{QAE}$ -close to  $\phi \equiv 1/\pi \arcsin \psi_1$ , i.e.  $|\tilde{\phi} - \phi| \leq \varepsilon_{QAE}$ . In the case of IsOptimal, we need to choose  $\varepsilon_{QAE}$  in a such a way that we are able to decide if no column has negative reduced cost. When only one column has negative reduced cost,  $\psi_1 = 1/\sqrt{|N|}$ ; therefore, we need to choose  $\varepsilon_{QAE} \sim 1/\sqrt{|N|}$ . We choose precision parameters  $\varepsilon_{QAE} = 1/(4\sqrt{|N|})$  and  $\delta = 1/4$ . Our choice of  $\varepsilon_{QAE}$  guarantees that if  $\tilde{\phi} \in [0, \varepsilon_{QAE}) \cup (1 - \varepsilon_{QAE}, 1]$ , then  $\psi_1 < 1/\sqrt{|N|}$ , and we can conclude that the solution is optimal.

---

**Algorithm B.7** IsOptimal

---

**function** ISOPTIMAL(matrix  $A$ , basis  $B$ , cost  $c$ , tolerance  $\varepsilon > 0$ )  
 $|\psi_N\rangle \leftarrow \frac{1}{\sqrt{|N|}} \sum_{k \in N} |k\rangle$  ▷ Prepare superposition nonbasic columns  
 $\mathcal{A} \leftarrow \text{CanEnterNFP}(A_B, A_k = U_{rhs}(\psi_N), c, \varepsilon)$ ,  
 $\chi \leftarrow \mathbb{1}_2$  ▷  $U_{rhs} |k\rangle |0\rangle = |k\rangle |A_k\rangle$   
 $\delta_{QAE} \leftarrow 1/4$ ,  $\varepsilon_{QAE} \leftarrow 1/(4\sqrt{|N|})$   
Run QAE( $\mathcal{A}, \chi, \varepsilon_{QAE}, \delta_{QAE}$ ), let  $\tilde{\phi}$  be the result  
**if**  $\tilde{\phi} \in [0, \varepsilon_{QAE}) \cup (1 - \varepsilon_{QAE}, 1]$  **then return** 1  
**else return** 0  
**end if**  
**end function**

---

**B.2.3 FindColumn: Random, QStER and QDanR** In the following we list three algorithms that can be used for determining the pivot column: Random – corresponding to the random pivot rule, QStER – corresponding to a quantum steepest edge rule and QDanR – corresponding to the quantum version of Dantzig’s rule. We first explain how FindColumn – Random is implemented.

**FindColumn - Random** Given a basis  $B$ , a cost  $c$ , and a tolerance  $\varepsilon > 0$  as inputs, FindColumn – Random outputs the index  $k$  of a column with negative reduced cost. This is done in two steps. First, we implement an oracle, CanEnterNFP, that takes as input the index of a column  $k$ , and re-

turns 1 if the reduced cost of the column is negative and 0 otherwise. Here NFN stands for "no false negative", because the oracle is built in such a way that it returns no false negative with bounded probability. Once we obtain this oracle, we can run QSearch (see Appendix C.3) on it to find a column with negative reduced cost.

---

**Algorithm B.8** FindColumn – Random

---

**function** FindColumn – Random(matrix  $A$ , basis  $B$ , cost  $c$ , tolerance  $\varepsilon > 0$ )  
 $\chi \leftarrow \text{CanEnter}(A_B, A_k = U_{rhs}(\cdot), c, \varepsilon)$  ▷  
 $U_{rhs} |k\rangle |0\rangle = |k\rangle |A_k\rangle$   
 Run QSearch( $\chi, \varepsilon$ )  
**end function**

---

**FindColumn - QStER** We explain how to implement the quantum steepest edge rule and afterwards the quantum version of Dantzig's rule. Both routines apply the *quantum minimum finding algorithm* to a subroutine that compares the reduced costs of two columns.

The algorithm FindColumn – QStER takes as input the simplex tableau  $A$ , the cost vector  $c$  and a precision parameter  $\varepsilon$  and applies QMin to a subroutine QStEC that returns 1 if

$$\frac{\bar{c}_k}{\|A_B^{-1}A_k\|} \leq (1 - \varepsilon) \frac{\bar{c}_j}{\|A_B^{-1}A_j\|} - \varepsilon,$$

where  $j$  is the reference index as determined by QMin, and 0 else. Here we interpret QStEC as an oracle function  $\chi_j(i) : c \rightarrow \{0, 1\}$  with

$$\chi_j(i) = \begin{cases} 1, & \text{if } \text{QStEC}(A_B, A_j, A_k, c, \varepsilon) = 1 \\ 0, & \text{else.} \end{cases}$$

**Remark:** It should be noted that we have employed a different precision parameter than Nannicini in [42]. In order to argue our choice, we reconstruct the relevant part of the proof of Theorem 10 in [42] in the following. For simplicity, we abbreviate the tilde above the  $\tilde{c}_j$  and  $\tilde{d}_j$  symbols. We want to show that, if Equation (B.2) holds, then SignEstNFN returns 0. In other words, we want to prove that if

$$(B.2) \quad \frac{\bar{c}_k}{\|A_B^{-1}A_k\|} \leq (1 - \varepsilon) \frac{\bar{c}_j}{\|A_B^{-1}A_j\|} - \varepsilon,$$

holds, then the following has to be true

$$\frac{1}{2}(\beta'_0 - \alpha'_0) \leq -\frac{\varepsilon}{8c_{max}},$$

where  $\alpha'_0 = \alpha_0 \cdot d_j / e_j c_{max}$  and  $\beta'_0 = \beta_0 \cdot d_k / e_k c_{max}$  correspond to the amplitudes encoded by the unitaries

---

**Algorithm B.9** FindColumn – QStER

---

**function** FindColumn – QStER( $A, B, c, \varepsilon$ ) ▷  
 $\|A_B\| \leq 1, \|c_B\| = 1$   
 Apply QMin( $\chi, |c| = n - m$ ) to the cost vector  $c$  interpreted as list and the oracle  $\chi$ :  
**function** QStEC( $A_B, A_j, A_k, c, \varepsilon$ )  
 Compute an estimate of the norms  $\tilde{d}_j = \|(A_B^{-1}A_j, c_j)\|$ ,  $\tilde{d}_k = \|(A_B^{-1}A_k, c_k)\|$  with relative error  $\varepsilon/4$ .  
 Compute an estimate of the norms  $\tilde{e}_j = \|A_B^{-1}A_j\|$ ,  $\tilde{e}_k = \|A_B^{-1}A_k\|$  with relative error  $\varepsilon/4$ .  
 Let  $U$  be the unitary that implements  $\text{RedCost}(A_B, A_j, c, \varepsilon / \max_{l \in [N]} |c_l|)$  and then multiplies  $|0^{\lceil \log m \rceil}\rangle$  with  $\frac{\tilde{d}_j}{\tilde{e}_j \max_{l \in [N]} |c_l|}$ .  
 Let  $V$  be the unitary that implements  $\text{RedCost}(A_B, A_k, c, \varepsilon / \max_{l \in [N]} |c_l|)$  and then multiplies  $|0^{\lceil \log m \rceil}\rangle$  with  $\frac{\tilde{d}_k}{\tilde{e}_k \max_{l \in [N]} |c_l|}$ .  
 Let  $W$  be the unitary that implements  $\text{Interfere}(U, V)$ .  
 Apply  $\text{SignEstNFN}(W, 0^{\lceil \log m \rceil + 1}, \frac{\varepsilon}{8 \max_{l \in [N]} |c_l|})$ .  
**if**  $\text{SignEstNFN}(W, 0^{\lceil \log m \rceil + 1}, \frac{\varepsilon}{8 \max_{l \in [N]} |c_l|})$  returns 0 **then return** 1  
**else return** 0  
**end if**  
**end function**  
 Let  $\chi_k(j) = 0$  for all  $j \in [n - m]$  **return**  $k$   
**end function**

---

$U$  and  $V$ . According to the RedCost subroutine  $\alpha_0$  and  $\beta_0$  have to satisfy

$$(B.3) \quad \beta_0 \leq \frac{\bar{c}_k}{d_k} + \frac{\varepsilon}{10c_{max}} \quad \text{and} \quad \alpha_0 \leq \frac{\bar{c}_j}{d_j} + \frac{\varepsilon}{10c_{max}}.$$

Moreover, as the norms have relative error of  $\varepsilon/4$ , we know that

$$\begin{aligned} \left(1 - \frac{\varepsilon}{4}\right) \|A_B^{-1}A_j\| &\leq e_j \leq \left(1 + \frac{\varepsilon}{4}\right) \|A_B^{-1}A_j\| \\ \left(1 - \frac{\varepsilon}{4}\right) \|(A_B^{-1}A_j, c_j)\| &\leq d_j \leq \left(1 + \frac{\varepsilon}{4}\right) \|(A_B^{-1}A_j, c_j)\|. \end{aligned}$$

Putting everything together, we estimate  $\beta'_0$  as follows

$$\beta'_0 \leq \left(\frac{\bar{c}_k}{d_k} + \frac{\varepsilon}{10c_{max}}\right) \frac{d_k}{c_{max}e_k} \left(\frac{1 + \frac{\varepsilon}{4}}{1 - \frac{\varepsilon}{4}}\right)$$

which leads to

$$\beta'_0 \leq \frac{\bar{c}_k}{e_k c_{max}} \left(\frac{1 + \frac{\varepsilon}{4}}{1 - \frac{\varepsilon}{4}}\right) + \frac{\varepsilon}{10c_{max}} \frac{d_k}{c_{max}e_k} \left(\frac{1 + \frac{\varepsilon}{4}}{1 - \frac{\varepsilon}{4}}\right).$$

Since

$$\frac{1 + \frac{\epsilon}{4}}{1 - \frac{\epsilon}{4}} \leq 1 + \frac{\epsilon}{2} + \frac{\epsilon^2}{4}.$$

We conclude that

$$\beta'_0 \leq \frac{\bar{c}_k}{e_k c_{max}} \left(1 + \frac{\epsilon}{2} + \frac{\epsilon^2}{4}\right) + \frac{\epsilon}{10c_{max} c_{max} e_k} \left(1 + \frac{\epsilon}{2} + \frac{\epsilon^2}{4}\right).$$

Assuming that Equation (B.2) holds true, we find

$$\beta'_0 \leq \frac{\bar{c}_j}{c_{max} e_j} \left(1 + \frac{\epsilon}{2} + \frac{\epsilon^2}{4}\right) (1 - \epsilon) \epsilon \frac{d_k}{10(c_{max})^2 e_k} \cdot \left(1 + \frac{\epsilon}{2} + \frac{\epsilon^2}{4}\right) - \left(1 + \frac{\epsilon}{2} + \frac{\epsilon^2}{4}\right) \frac{\epsilon}{c_{max}}.$$

Knowing that

$$\frac{d_k}{e_k c_{max}} \leq 1 \quad \text{and} \quad \left(1 + \frac{\epsilon}{2} + \frac{\epsilon^2}{4}\right) (1 - \epsilon) \leq 1,$$

we obtain

$$\beta'_0 \leq \frac{\bar{c}_j}{c_{max} e_j} + \frac{\epsilon}{10c_{max}} \left(1 + \frac{\epsilon}{2} + \frac{\epsilon^2}{4}\right) - \frac{\epsilon}{c_{max}} \left(1 + \frac{\epsilon}{2} + \frac{\epsilon^2}{4}\right).$$

Now using

$$1 + \frac{\epsilon}{2} + \frac{\epsilon^2}{4} \leq 2 \quad \text{and} \quad -1 - \frac{\epsilon}{2} - \frac{\epsilon^2}{4} \leq -1$$

we obtain

$$\beta'_0 \leq \frac{\bar{c}_j}{c_{max} e_j} + \frac{\epsilon}{5c_{max}} - \frac{\epsilon}{c_{max}} \leq \alpha'_0 - \frac{\epsilon}{4c_{max}}$$

which is equivalent to

$$\frac{1}{2} (\beta'_0 - \alpha'_0) \leq -\frac{\epsilon}{8c_{max}}.$$

However, we obtained this result only by including an additional factor  $1/c_{max}$  in the precision of the amplitudes  $\alpha_0$  and  $\beta_0$  (i.e. in Equation (B.3)).

**FindColumn - QDanR** In a similar fashion one can design a quantum subroutine that implements Dantzig's rule by applying QMin to a quantum oracle that compares two reduced cost vectors. The algorithm FindColumn - QDanR takes as input the simplex tableau  $A$ , the cost vector  $c$  and a precision parameter  $\epsilon$  and applies QMin to a subroutine that returns 1 if

$$(B.4) \quad \bar{c}_k \leq (1 - \epsilon)\bar{c}_j - \epsilon,$$

---

### Algorithm B.10 FindColumn - QDanR

---

**function** FindColumn - QDanR( $A, B, c, \epsilon$ ) ▷  
 $\|A_B\| \leq 1, \|c_B\| = 1$   
 Apply QMin( $\chi, |c| = n - m$ ) to the cost vector  $c$  interpreted as list and the oracle  $\chi$ :  
**function** REDCOSTCOMPARE( $A_B, A_j, A_k, c, \epsilon$ )  
 Compute an estimate of the norms  $\tilde{d}_j = \|(A_B^{-1} A_j, c_j)\|$ ,  $\tilde{d}_k = \|(A_B^{-1} A_k, c_k)\|$  with relative precision  $\epsilon/4$ .  
 Let  $U$  be the unitary that implements RedCost( $A_B, A_j, c, \epsilon/\max_{l \in N} |c_l| \tilde{e}_j$ ) and then multiplies  $|0^{\lceil \log m \rceil}\rangle$  with  $\frac{\tilde{d}_j}{\tilde{e}_j \max_{l \in N} |c_l|}$ . ▷  
 $\tilde{e}_j = \|A_B^{-1} A_j\|$   
 Let  $V$  be the unitary that implements RedCost( $A_B, A_k, c, \epsilon/\max_{l \in N} |c_l| \tilde{e}_k$ ) and then multiplies  $|0^{\lceil \log m \rceil}\rangle$  with  $\frac{\tilde{d}_k}{\tilde{e}_k \max_{l \in N} |c_l|}$ . ▷  
 $\tilde{e}_k = \|A_B^{-1} A_k\|$   
 Let  $W$  be the unitary that implements Interfere( $U, V$ ).  
 Apply SignEstNFN( $W, 0^{\lceil \log m \rceil + 1}, \frac{\epsilon}{8 \max_{l \in N} |c_l|}$ ).  
**if** SignEstNFN( $W, 0^{\lceil \log m \rceil + 1}, \frac{\epsilon}{8 \max_{l \in N} |c_l|}$ ) returns 0 **then return** 1  
**else return** 0  
**end if**  
**end function**  
 Let  $\chi_k(j) = 0$  for all  $j \in [n - m]$  **return**  $k$   
**end function**

---

where  $j$  is the reference index as determined by QMin, and 0 else. We interpret the oracle  $\chi$  as a function  $\chi_j(i) : c \rightarrow \{0, 1\}$  with

$$\chi_j(i) = \begin{cases} 1, & \text{if RedCostCompare}(A_B, A_j, A_k, c, \epsilon) = 1 \\ 0, & \text{else.} \end{cases}$$

The complexity of this algorithm scales the same as FindColumn - QStER (neglecting the cost of norm estimation):

$$\mathcal{C}[\text{QDanR}] = \langle n_{\text{QMin}} \rangle \times \mathcal{C}[\text{RedCostCompare}],$$

where  $\langle n_{\text{QMin}} \rangle$  is the number of calls from the quantum minimum finding algorithm to the oracle  $\chi$ .

**B.2.4 IsUnbounded** An instance is found to be unbounded if and only if  $u := A_B^{-1} A_k < 0$ . Hence the quantum algorithm IsUnbounded is a Grover search for a positive amplitude of  $u$ . The Grover oracle  $Q := \text{SignEstNFN}^+(\text{QLS}(A_B, A_k, \delta/10))$  comprises the following two steps:

- Solve the linear system  $A_B x = A_k$  with precision  $\frac{\delta}{10}$  by applying the QLS unitary, obtain the solution state  $|x^*\rangle$ .
- Apply SignEstNFN with precision  $\frac{9\delta}{10}$  to determine whether a specified amplitude of  $|x^*\rangle$  is positive.

If no positive amplitude is found, the algorithm returns 1, otherwise, it returns 0.

---

**Algorithm B.11** IsUnbounded

---

**function** ISUNBOUNDED(normalized basis  $A_B$  ( $\|A_B\| \leq 1$ ), non-basic column  $A_k$  to enter the basis, precision  $\delta > 0$ )  
 $\chi \leftarrow \text{SignEstNFN}^+(\text{QLS}(A_B, A_k, \frac{\delta}{10}))$   
Run QSearch( $\chi, \frac{9\delta}{10}$ )  
**end function**

---



---

**Algorithm B.12** FindRow

---

**function** FINDROW(normalized basis  $A_B$  ( $\|A_B\| \leq 1$ ), non-basic column  $A_k$  to enter the basis, constraint vector  $b$ , precision  $\delta > 0$ )  
 $\varepsilon_Q \leftarrow -2 \frac{\delta}{\|A_B^{-1} A_k\|} + \frac{\delta}{2}$   
 $\varepsilon_S \leftarrow \frac{\delta}{\|A_B^{-1} A_k\|}$   
 $\chi_r \leftarrow \text{SignEstNFN}(\text{QLS}(A_B, b - r A_k, \varepsilon_Q), \varepsilon_S)$   
 $\mathcal{A}_r \leftarrow 1$  if QSearch( $\chi_r$ ) finds a marked element, 0 otherwise.  
Binary search for  $r^* > 0$  such that  $\mathcal{A}_{r^*}$  returns 1 and  $\mathcal{A}_{r^* - \frac{\delta}{2\kappa\|A_k\|}}$  returns 0 **return** the index  $j$  corresponding to the marked element  
**end function**

---

### B.2.5 FindRow

**Description of the Algorithm.** The heart of this algorithm is solving the linear system  $A_B x = b - r A_k$  for  $r \geq 0$ . The solution is

$$x_r^* = A_B^{-1} b - r A_B^{-1} A_k = x - r u.$$

For each basis index  $j$  which satisfies  $u_j > 0$ , we write  $r_j := \frac{x_B(j)}{u_j} \geq 0$ . Observe that  $(x_{r_j}^*)_j = x_{B(j)} - \frac{x_B(j)}{u_j} u_j = 0$ . The goal of the algorithm is to find the smallest  $r_j$  and we write  $r^* := \min_j r_j$ . This value is characterized by the fact that  $x_{r^* - \delta}^* > 0$  for all (especially small)  $\delta > 0$  but  $x_{r^*}^* \not> 0$ . The quantum version of the logic described above is a quantum algorithm  $\mathcal{A}_r$ , where  $r > 0$ , which

- uses a QLS algorithm to solve the linear system  $A_B x = b - r A_k$ , preparing a quantum state  $|x^*\rangle$  proportional to the solution vector  $x^* = A_B^{-1}(b - r A_k)$ ,

- then applies SignEstNFN (like in FindColumn) to find out if a specific amplitude of the QLS solution state  $|x^*\rangle$  is negative
- Applies the Grover search QSearch to the two preceding steps to determine if any amplitude of  $|x^*\rangle$  is negative. More concretely, the Grover oracle is given by  $Q_r := \text{SignEstNFN}(\text{QLS}(A_B, b - r A_k, \delta'))$ , where  $\delta'$  is the QLS precision which we expand on in the paragraph below.

FindRow then performs a binary search on  $r$  to find  $r^*$  such that  $\mathcal{A}_{r^*}$  returns 1 and  $\mathcal{A}_{r^* - \delta}$  returns 0 for a specific small choice of  $\delta$ , chosen to control the overall error.

**Error Analysis** We now briefly discuss how to choose the precision for the QLS and sign estimation subroutines. We denote these precision values by  $\varepsilon_Q$  and  $\varepsilon_S$ , respectively. The sign estimation subroutine is applied to the QLS unitary to determine if a specified component of the solution vector  $x_r^* = A_B^{-1} b - r A_B^{-1} A_k$  is  $< \delta/2$ . The QLS precision  $\varepsilon_Q$  determines that

$$|\alpha_k - x_{r,k}^*| < \varepsilon_Q,$$

where  $x_{r,k}^*$  is the  $k$ -th component of the solution vector  $x_r^*$  and  $\alpha_k$  is the corresponding amplitude of the quantum state prepared by the QLS algorithm. According to Prop 3 of [42] the sign estimation procedure applied to the  $k$ -th amplitude returns 0 with high probability if  $\alpha_k < -2\varepsilon_S$ . For SignEstNFN to still correctly indicate whether this the case, we therefore require that

$$(B.5) \quad -2\varepsilon_S = -\frac{\delta}{2} + \varepsilon_Q.$$

Nannicini suggests  $\varepsilon_S := \frac{\delta}{\|A_B^{-1} A_k\|}$ , which would in turn determine  $\varepsilon_Q = -2 \frac{\delta}{\|A_B^{-1} A_k\|} + \frac{\delta}{2}$  according to Equation (B.5).

### B.3 Proofs of Lemmas from Section 4

In this section, we collect the proofs of Lemmas 4.3–4.6, presented in Section 4 and additionally provide the results for FindColumn–Random and FindColumn–QDanR. Notice that the proofs of Lemma 4.1 and Lemma 4.2 are instead given in Appendix C. As explained in Appendix B.2, IsOptimal, FindColumn, IsUnbounded, and FindRow rely on a number of core subroutines, see Appendix B.2.1. So, we first prove lower bounds for these core subroutines in Appendix B.3.1.

#### B.3.1 Lower Bounds for Core Subroutines

We prove lower bounds for the cost of the core subroutines presented in Appendix B.2.1. These are used in the proofs of the other lemmas presented in this section.

LEMMA B.1. (COST OF REDCOST) *The cost of RedCost is lower bounded by*

$$\mathcal{C}[\text{RedCost}(A_B, A_k, c, \varepsilon)] \geq \mathcal{C}[\text{QLS}(A_B, A_k, \varepsilon)].$$

A lower bound for the cost of implementing a version of QLS is provided in Lemma 4.2.

*Proof.* We lower bound the cost of RedCost by only considering the second step in Algorithm B.1.

$$\mathcal{C}[\text{RedCost}(A_B, A_k, c, \varepsilon)] \geq \mathcal{C}[\text{QLS}(\hat{A}_B, \hat{b}, \varepsilon)],$$

where

$$\hat{A}_B = \begin{pmatrix} A_B & 0 \\ 0 & 1 \end{pmatrix}, \quad \hat{b} = \begin{pmatrix} A_k \\ c_k \end{pmatrix}.$$

For simplicity, we lower bound the cost of solving this system of equations with a simpler system of equations, where we use  $A_B$  instead of  $\hat{A}_B$  and  $A_k$  instead of  $\hat{b}$ . The difference between the two is a small overhead, which we neglect. We conclude that

$$(B.6) \quad \mathcal{C}[\text{RedCost}(A_B, A_k, c, \varepsilon)] \geq \mathcal{C}[\text{QLS}(A_B, A_k, \varepsilon)].$$

□

LEMMA B.2. (COST OF INTERFERE) *The cost of Interfere is lower bounded by*

$$\mathcal{C}[\text{Interfere}(U, V)] \geq \mathcal{C}[U] + \mathcal{C}[V],$$

where  $\mathcal{C}[U]$  and  $\mathcal{C}[V]$  are the cost of implementing the input unitaries,  $U$  and  $V$ .

*Proof.* The cost of Interfere is dominated by the controlled action of  $U$  and  $V$ ,

$$\mathcal{C}[\text{Interfere}(U, V)] \geq \mathcal{C}[\text{ctrl}_1-U] + \mathcal{C}[\text{ctrl}_1-V].$$

To deal with the control, we consider the simple lower bounds  $\mathcal{C}[\text{ctrl}_1-U] \geq \mathcal{C}[U]$  and  $\mathcal{C}[\text{ctrl}_1-V] \geq \mathcal{C}[V]$ , leading to

$$(B.7) \quad \mathcal{C}[\text{Interfere}(U, V)] \geq \mathcal{C}[U] + \mathcal{C}[V].$$

□

LEMMA B.3. (COST OF SIGNESTNFN) *The cost of SignEstNFN is lower bounded by*

$$\mathcal{C}[\text{SignEstNFN}(U, l, \varepsilon)] \geq \left( \frac{5\sqrt{3}\pi}{\varepsilon} - 1 \right) \mathcal{C}[U].$$

*Proof.* The cost of SignEstNFN( $U, l, \varepsilon$ ) is given by the cost of implementing QAE, and the cost of checking whether the result of QAE is in  $[1/6 - 2\varepsilon_{\text{QAE}}, 5/6 + 2\varepsilon_{\text{QAE}}]$ , see Algorithm B.3 We lower bound the cost

of SignEstNFN by only considering the first, i.e. the cost of QAE. Let  $\varepsilon_{\text{QAE}} = \varepsilon/\sqrt{3\pi^2}$ ,  $\delta_{\text{QAE}} = 1/4$ ,  $\mathcal{A} = \text{Interfere}(U, \mathbb{1})$ , and  $\chi_l$  a function that selects the  $(0, l)$ -th component of the vector, i.e.

$$\chi_l(x) = \begin{cases} 1 & x = (0, l) \\ 0 & \text{otherwise} \end{cases},$$

then

$$\mathcal{C}[\text{SignEstNFN}(U, l, \varepsilon_{\text{SE}})] \geq \mathcal{C}[\text{QAE}(\mathcal{A}, \chi_l, \varepsilon_{\text{QAE}}, \delta_{\text{QAE}})].$$

The cost of quantum amplitude estimation can be lower bounded by

$$(B.8) \quad \mathcal{C}[\text{QAE}(\mathcal{A}, \chi_l, \varepsilon_{\text{QAE}}, \delta_{\text{QAE}})] \geq (2^{n_c+1} - 1)\mathcal{C}[\mathcal{A}],$$

where

$$n_c = \log_2 \frac{1}{2\varepsilon_{\text{QAE}}} + \log_2 \left( 1 + \frac{1}{\delta_{\text{QAE}}} \right).$$

This can be shown combining Lemma C.3 and Lemma C.4, and using  $\mathcal{C}[Q] \geq 2\mathcal{C}[\mathcal{A}]$  ( $Q$  is the Grover operator). A lower bound for the cost of  $\mathcal{A} = \text{Interfere}(U, \mathbb{1})$  is given in Lemma B.2. In this case,  $V = \mathbb{1}$ , so we have

$$\mathcal{C}[\text{Interfere}(U, \mathbb{1})] \geq \mathcal{C}[U].$$

Plugging this into Equation (B.8), and using the definition of  $\varepsilon_{\text{QAE}}$  and  $\delta_{\text{QAE}}$ , we get

$$(B.9) \quad \mathcal{C}[\text{SignEstNFN}(U, l, \varepsilon)] \geq \left( \frac{5\sqrt{3}\pi}{\varepsilon} - 1 \right) \mathcal{C}[U].$$

□

LEMMA B.4. (COST OF SIGNESTNFP) *The cost of SignEstNFP is lower bounded by*

$$\mathcal{C}[\text{SignEstNFP}(U, l, \varepsilon)] \geq \left( \frac{45\sqrt{3}\pi}{\varepsilon} - 1 \right) \mathcal{C}[U].$$

*Proof.* The proof is identical to the one of SignEstNFN, see Lemma B.3. The only difference is that now  $\varepsilon_{\text{QAE}} = \varepsilon/9\sqrt{3\pi^2}$ , which leads to a different prefactor. □

LEMMA B.5. (COST OF CANENTERNFN) *The cost of CanEnterNFN is lower bounded by*

$$\mathcal{C}[\text{CanEnterNFN}(A_B, A_k, c, \varepsilon)] \geq \left( \frac{50\sqrt{6}\pi}{11\varepsilon} - 1 \right) \cdot \mathcal{C} \left[ \text{QLS} \left( A_B, A_k, \frac{0.1\varepsilon}{\sqrt{2}} \right) \right].$$

A lower bound for the cost of implementing a version of QLS is provided in Lemma 4.2.



*Proof.* The cost of running CanEnterNFN is given by the cost of SignEstNFN and the if statement, see Algorithm B.5. To lower bound the cost of CanEnterNFN, we only consider the first, i.e. the cost of SignEstNFN. The cost of SignEstNFN is given by Lemma B.3. Let  $U = \text{RedCost}(A_B, A_k, c, \varepsilon_{\text{RC}})$ , with  $\varepsilon_{\text{RC}} = \varepsilon \cdot 0.1/\sqrt{2}$ ,  $l = 0$ , and  $\varepsilon_{\text{SE}} = 1.1\varepsilon/\sqrt{2}$ , then

$$\mathcal{C}[\text{CanEnter}(A_B, A_k, c, \varepsilon)] \geq \mathcal{C}[\text{SignEstNFN}](U, l, \varepsilon_{\text{SE}}).$$

Combining the results of Lemma B.1 and Lemma B.3, we obtain

$$(B.10) \quad \mathcal{C}[\text{CanEnterNFN}(A_B, A_k, c, \varepsilon)] \geq \left( \frac{50\sqrt{6}\pi}{11\varepsilon} - 1 \right) \cdot \mathcal{C} \left[ \text{QLS} \left( A_B, A_k, \frac{0.1\varepsilon}{\sqrt{2}} \right) \right].$$

□

LEMMA B.6. (COST OF CANENTERNFP) *The cost of CanEnterNFP is lower bounded by*

$$\mathcal{C}[\text{CanEnterNFP}(A_B, A_k, c, \varepsilon)] \geq \left( \frac{450\sqrt{6}\pi}{11\varepsilon} - 1 \right) \cdot \mathcal{C}[\text{QLS}(A_B, A_k, 0.1\varepsilon/\sqrt{2})].$$

A lower bound for the cost of implementing a version of QLS is provided in Lemma 4.2.

*Proof.* The proof is identical to the one of CanEnterNFN, see Lemma B.5. The only difference is that now we use SignEstNFP, which leads to a different prefactor. □

### B.3.2 Proofs of FindColumn with Different Pivoting Rules

#### Cost of Quantum Random Pivoting Rule

LEMMA B.7. (COST OF FindColumn – Random) *The cost of FindColumn – Random is lower bounded by*

$$\mathcal{C}[\text{FindColumn – Random}(A, B, c, \varepsilon)] \geq n_Q(n-m, t) \cdot \left( \frac{50\sqrt{6}\pi}{11\varepsilon} - 1 \right) \mathcal{C} \left[ \text{QLS} \left( A_B, A_k, \frac{0.1\varepsilon}{\sqrt{2}} \right) \right].$$

*Proof.* Let  $\chi = \text{CanEnterNFN}(A_B, A_k = U_{rhs}(\cdot), c, \varepsilon)$ , with  $U_{rhs} |k\rangle |0\rangle = |k\rangle |A_k\rangle$ , then the cost of FindColumn – Random is given by the cost of running QSearch on  $\chi$ :

$$\mathcal{C}[\text{FindColumn – Random}(A, B, c, \varepsilon)] = \mathcal{C}[\text{QSearch}(\chi, \varepsilon)]$$

A lower bound for the cost of running QSearch is given by Lemma 4.1. In this case,  $|X| = n-m$ , i.e. the number

of nonbasic columns, and the number of marked items is the number of nonbasic columns with negative reduced price. Up to a small overhead that we here neglect, the cost of one application of  $Q$  is equal to one query to  $\chi$ . In this case,  $\chi = \text{CanEnterNFN}$ . A lower bound for the cost of CanEnterNFN is given by Lemma B.5. Combining the bounds for CanEnterNFN and QSearch, we arrive to the wanted result. □

#### Proof of Lemma 4.4 (QStER)

LEMMA 4.4. (FindColumn – QStER) *The expected gate complexity of FindColumn – QStER has a lower bound of*

$$(B.11) \quad \mathcal{C}[\text{FindColumn – QStER}(A, B, c, \varepsilon)] \geq 3 \left\lceil \log_3 \frac{1}{\varepsilon} \right\rceil \cdot \left( \frac{40\sqrt{3}\pi c_{\text{max}}}{\varepsilon} - 1 \right) \sum_{t=1}^{n-m-1} \frac{n_Q(n-m, t)}{t+1} \cdot \mathcal{C} \left[ \text{QLS} \left( A_B, A_k, \frac{\varepsilon}{10c_{\text{max}}\sqrt{2}} \right) \right],$$

where  $c_{\text{max}}$  is the (absolute) maximum component in the cost vector  $c$ .

*Proof.* The complexity of FindColumn – QStER is given by

$$\mathcal{C}[\text{FindColumn – QStER}] = \langle n_{\text{QMin}} \rangle \times \mathcal{C}[\text{QStEC}],$$

where  $\langle n_{\text{QMin}} \rangle$  denotes the expected number of oracle calls of the quantum minimum finding algorithm and  $\mathcal{C}[\text{QStEC}]$  denotes the cost of the SteepestEdgeCompare subroutine. The latter can be lower bounded by the cost of SignEstNFN( $W, 0, c, \frac{\varepsilon}{8c_{\text{max}}}$ ) which itself can be lower bounded by the cost for quantum amplitude estimation

$$\begin{aligned} \mathcal{C}[\text{QStEC}] &\geq \mathcal{C}[\text{SignEstNFN}(W, 0, c, \varepsilon/8c_{\text{max}})] \\ &\geq \mathcal{C}[\text{QAE}(W, \chi_0, \varepsilon/8c_{\text{max}}, \delta')]. \end{aligned}$$

The cost of quantum amplitude estimation can be divided into the cost of implementing the unitary  $W$  and the cost of quantum phase estimation as

$$\begin{aligned} \mathcal{C}[\text{QAE}(W, \chi_0, \varepsilon/8c_{\text{max}}, \delta')] &= \mathcal{C}[\text{Interfere}(U, V)] \\ &\quad + \mathcal{C}[\text{QPE}(Q, \delta', \varepsilon/8c_{\text{max}})]. \end{aligned}$$

Here  $Q$  is the Grover operator used by the QAE subroutine. The parameter  $\delta'$  bounds the success probability  $p$  via  $p \geq 1 - \delta'$ . Analogous to the derivation of a lower bound for QAE in the proof of Lemma B.3, we can now do the following estimation

$$\mathcal{C}[\text{QStEC}] \geq \left( 2^{n_{\varepsilon', \delta'+1}} - 1 \right) \mathcal{C}[\text{Interfere}(U, V)],$$

where

$$n_{\varepsilon', \delta'} = \log_2 \frac{1}{2\varepsilon'} + \log_2 \left(1 + \frac{1}{\delta'}\right)$$

and  $\varepsilon' = \varepsilon_{\text{QPE}}/8c_{\text{max}} = \varepsilon/8\sqrt{3}\pi c_{\text{max}}$ . The cost of  $\mathcal{C}[\text{Interfere}(U, V)]$  can be lower bounded by the cost of  $V_r$ , and the cost of  $U_r$  (see discussion on Algorithm B.2). Hence, we get the following estimation

$$\mathcal{C}[\text{QStEC}] \geq \left(2^{n_{\varepsilon', \delta'}+1} - 1\right) \cdot \left(\mathcal{C}[V_r] + \mathcal{C}[U_r]\right)$$

where

$$\begin{aligned} \mathcal{C}[V_r] &= \mathcal{C}[\text{RedCost}(A_B, A_k, \varepsilon/c_{\text{max}}10\sqrt{2})] \\ &\geq \mathcal{C}[\text{QLS}(A_B, A_k, \varepsilon/c_{\text{max}}10\sqrt{2})], \\ \mathcal{C}[U_r] &= \mathcal{C}[\text{RedCost}(A_B, A_j, \varepsilon/c_{\text{max}}10\sqrt{2})] \\ &\geq \mathcal{C}[\text{QLS}(A_B, A_j, \varepsilon/c_{\text{max}}10\sqrt{2})]. \end{aligned}$$

With that, we get the estimation

$$\begin{aligned} \mathcal{C}[\text{QStEC}] &\geq \left(2^{n_{\varepsilon', \delta'}+1} - 1\right) \cdot \\ &\quad \mathcal{C}[\text{QLS}(A_B, A_k, \varepsilon/c_{\text{max}}10\sqrt{2})]. \end{aligned}$$

From Lemma C.2, the expected number of calls from QMin with cutoff for a list of length  $n - m$  is given by

$$\langle n_{\text{QMin}_{\text{finite}}} \rangle = 3 \lceil s_{\text{max}} \rceil \sum_{s=0}^{n-m-1} \frac{n_Q(n-m, s)}{s+1},$$

where  $s = \sin^2(\theta)|n - m|$ ,  $n_Q(n - m, s)$  denotes the number of times we need to apply the Grover operator in QSearch and  $s_{\text{max}} = \log_3 1/\varepsilon$ . Putting everything into Equation (B.11), we finally obtain that

$$\begin{aligned} \mathcal{C}[\text{QStER}] &\geq \left(2^{n_{\varepsilon', \delta'}+1} - 1\right) 3 \lceil s_{\text{max}} \rceil \\ &\quad \sum_{s=0}^{n-m-1} \frac{n_Q(n-m, s)}{s+1} \\ &\quad \cdot \mathcal{C}[\text{QLS}(A_B, A_k, \varepsilon/c_{\text{max}}10\sqrt{2})]. \end{aligned}$$

Now setting  $\delta' = 1/4$  and  $\varepsilon' \rightarrow \varepsilon/8\sqrt{3}\pi c_{\text{max}}$  we obtain

$$\begin{aligned} \mathcal{C}[\text{QStER}] &\geq \left(\frac{40\sqrt{3}\pi c_{\text{max}}}{\varepsilon} - 1\right) 3 \lceil s_{\text{max}} \rceil \cdot \\ &\quad \sum_{s=0}^{n-m-1} \frac{n_Q(n-m, s)}{s+1} \cdot \\ &\quad \mathcal{C}[\text{QLS}(A_B, A_k, \varepsilon/c_{\text{max}}10\sqrt{2})], \end{aligned}$$

completing the proof.  $\square$

### Cost of Quantum Danzig's Pivoting Rule

LEMMA B.8. (COST OF FindColumn – QDanR) *A lower bound for the gate count of FindColumn – QDanR is given by*

$$(B.12) \quad \mathcal{C}[\text{FindColumn} - \text{QDanR}(A, c, \varepsilon)] \geq 3 \left(\frac{40\sqrt{3}\pi c_{\text{max}}}{\varepsilon} - 1\right) \lceil s_{\text{max}} \rceil \cdot \sum_{t=0}^{n-m-1} \frac{n_Q(n-m, t)}{t+1} \mathcal{C} \left[ \text{QLS} \left( A_B, A_k, \frac{\varepsilon}{\|A_B^{-1}A_k\|c_{\text{max}}10\sqrt{2}} \right) \right]$$

Here  $s_{\text{max}} = \log_3 1/\varepsilon$  and  $n_Q(|n - m|, t)$  denotes the number of times we need to apply the Grover operator in QMin.

*Proof.* The proof is analogous to the one for Lemma 4.4. Only the precision parameter in the cost for QLS has to be adjusted to  $\varepsilon_{\text{QLS}} \rightarrow \varepsilon/10\sqrt{2} \|A_B^{-1}A_k\|c_{\text{max}}$ .  $\square$

### B.3.3 Proof of Lemma 4.5 (IsUnbounded)

LEMMA 4.5. (IsUnbounded) *The expected gate complexity of IsUnbounded has a lower bound of*

$$\mathcal{C}[\text{IsUnbounded}(A_B, A_k, \delta)] \geq n_Q(m, t) \cdot \left(\frac{50\sqrt{3}\pi}{18\delta} - 1\right) \mathcal{C} \left[ \text{QLS} \left( A_B, A_k, \frac{\delta}{10} \right) \right],$$

where  $t$  is the number of positive components in  $u = A_B^{-1}A_k$ .

*Proof.* Recall that the subroutine IsUnbounded is a Grover search for a basic index  $l$  that  $(A_B^{-1}A_k)_l > 0$ , up to a precision  $\delta$ . In order to bound the cost of the Grover oracle

$$Q = \text{SignEstNFN}^+ \left( \text{QLS}(A_B, A_k, \frac{\delta}{10}), \frac{9\delta}{10} \right)$$

we follow the procedure starting at Lemma B.3. The precision required for the sign estimation routine is  $\frac{9\delta}{10}$ , which we plug into Lemma B.3 to receive the bound

$$\mathcal{C}(Q) \geq \left(\frac{50\sqrt{3}\pi}{18\delta} - 1\right) \mathcal{C}[\text{QLS}(A_B, A_k, \frac{\delta}{10})].$$

Putting this together with the QSearch cost bound from Lemma 4.1, we obtain the desired result.  $\square$

### B.3.4 Proof of Lemma 4.6 (FindRow)

LEMMA 4.6. (FindRow) *The expected gate complexity of FindRow has a lower bound of*

$$\mathcal{C}[\text{FindRow}(A_B, A_k, b, \delta)] \geq n_Q(m, 0) \cdot \left( \frac{\sqrt{3}\pi \|A_B^{-1} A_k\|}{2\delta} - 1 \right) \mathcal{C} \left[ \text{QLS} \left( A_B, b, \frac{\delta}{2} \right) \right].$$

*Proof.* The sub-algorithm FindRow is a binary search on the quantum oracle  $U_r$ , looking for a value approximating  $r^*$ , satisfying the ratio test. Hence, the cost of the algorithm splits up as

$$\mathcal{C}[\text{FindRow}(A_B, A_k, b, \delta)] = S \cdot \mathcal{C}(U_r),$$

where  $S$  is the expected number of steps in the binary search. Each step of the binary search is an application of QSearch, which is looking for a negative component of  $A_B^{-1}(b - rA_k)$ . At least one step in the binary search yields that the Grover search in  $U_r$  did not find any marked elements (this is the case for small values of  $r$ , especially 0). We get the bound

$$S \cdot \mathcal{C}(U_r) \geq \mathcal{C}(U_0).$$

The quantum oracle  $U_r$  solves the linear system  $A_B x = b - rA_k$  and proceeds to search for a negative amplitude using the sign estimation subroutine. Hence, its cost decomposes as

$$\mathcal{C}[U_r] = \mathcal{C}[\text{QSearch}(Q_r)] \leq n_Q(m, t_r) \mathcal{C}[Q_r]$$

where the Grover oracle is given by  $Q_r = \text{SignEstNFN}(\text{QLS}(A_B, b - rA_k, \delta))$  and  $t_r$  is the number of marked elements in the Grover search corresponding to  $r$ . In the case of  $r = 0$ , we have  $t_r = 0$ . To bound the cost of the combination of sign estimation and a QLS we follow the proof of Lemma B.3. The precision of the sign estimation required in  $U_0$  is given by  $\varepsilon_S = \frac{\delta}{\|A_B^{-1} A_k\|}$ . Plugging this into Lemma B.3 yields

$$\mathcal{C}(U_0) \geq \left( \frac{\sqrt{3}\pi \|A_B^{-1} A_k\|}{2\delta} - 1 \right) \mathcal{C}[\text{QLS}(A_B, b, \frac{\delta}{2})].$$

Here  $\frac{\delta}{2} \geq \frac{\delta}{2} - 2 \frac{\delta}{\|A_B^{-1} A_k\|} = \varepsilon_Q$  is an upper bound to the QLS precision derived in Equation (B.5).  $\square$

## C Quantum Subroutines

We provide further physics-based foundations by presenting common quantum subroutines with corresponding bounds on the lowest possible gate cost. Additionally, we provide concise explanations of each subroutine. For further technical details, we refer the reader to respective original papers.

**C.1 Notation** In this section, we use the following conventions:

- The cost of a 1-qubit, 2-qubit, Toffoli gate is respectively  $\mathcal{C}_1, \mathcal{C}_2, \mathcal{C}_T$ ,
- The cost of a unitary operation  $U$  is denoted  $\mathcal{C}[U]$ ,
- A unitary operation  $U$  controlled on  $n$  qubits is denoted  $\text{ctrl}_n-U$ ,
- A *state preparation oracle*  $\mathcal{P}_\psi$  is a unitary operation preparing some  $n$ -qubit state  $|\psi\rangle$ , i.e.  $\mathcal{P}_\psi|0^n\rangle = |\psi\rangle$ . We do not take into account the costs of implementing state preparation oracles, and instead set  $\mathcal{C}[\mathcal{P}_\psi] = 1$ .

**C.2 Controlling Unitaries** We always assume that  $U$  is applied when all the controlling qubits are in state  $|1\rangle$ . In equation,

$$\text{ctrl}_n-U = |N-1\rangle\langle N-1| \otimes U + \sum_{\tau=0}^{N-2} |\tau\rangle\langle\tau| \otimes \mathbf{1},$$

where  $N = 2^n$  and  $|N-1\rangle = |11\dots 1\rangle$ .

As explained in chapter 4 from [43], we can implement  $\text{ctrl}_n-U$  by first calculating the AND of all the controlling qubits in an ancilla qubit, and then act with  $\text{ctrl}_1-U$ . Computing the AND of the controlling qubits requires  $n-1$  ancilla qubits and  $2(n-1)$  Toffoli gates (the factor 2 is due to the uncomputation step). The cost of  $\text{ctrl}_1-U$  can be bounded by the cost of  $U$ . So finally we have

$$(C.13) \quad \mathcal{C}[\text{ctrl}_n-U] \geq 2(n-1)\mathcal{C}_T + \mathcal{C}[U].$$

**C.3 QSearch** Algorithm C.1 is a modified version of QSearch from [8], which is an extension of Grover algorithm. It can be used to identify a marked item within a list. Assume a set  $X$  and function  $\chi$ , where  $\chi$  splits  $X$  in a set of *good* solutions,  $G = \{x \in X | \chi(x) = 1\}$ , and *bad* solutions,  $B = \{x \in X | \chi(x) = 0\}$ . Often  $X = \{0, 1\}^n$ ; otherwise, we set

$$n = \lceil \log_2 |X| \rceil.$$

QSearch outputs a marked (good) item,  $x \in G$ , or "No marked item", with error probability upper bounded by  $\varepsilon$ .

---

## Algorithm C.1 QSearch

---

```

function QSEARCH(oracle  $\chi : X \rightarrow \{0, 1\}$ ,  $\varepsilon > 0$ )
   $\lambda \leftarrow 6/5$ ,  $m \leftarrow \lambda$ 
   $s_{max} \leftarrow \lceil \log_3 1/\varepsilon \rceil$ ,  $k_{max} \leftarrow k_* + 4$  ▷
   $k_* = \left\lceil \log_\lambda \frac{|X|}{2\sqrt{|X|-1}} \right\rceil$ 
   $k \leftarrow 1$ ,  $s \leftarrow 1$ 
  while  $s \leq s_{max}$  do
    while  $k \leq k_{max}$  do
      Prepare  $|\psi_0\rangle$  ▷  $|\psi_0\rangle \propto \sum_{x=0}^{|X|-1} |x\rangle$ 
      Choose  $j$  uniformly at random in  $[0, [m]]$ 
      Apply  $Q^j$  ▷  $Q$  is the Grover operator
      Measure the register, let  $x_*$  be the outcome
      if  $\chi(x_*) = 1$  then return  $x_*$ 
      else
         $k \leftarrow k + 1$ 
         $m \leftarrow \min(\lambda m, \sqrt{|X|})$ 
      end if
    end while
     $s \leftarrow s + 1$ 
  end while
return "No marked item"
end function

```

---

LEMMA 4.1. (ITERATIONS FOR QSearch) *Let  $X$  be a list of length  $|X|$ , with  $t$  marked items. The expected number  $n_Q(|X|, t)$  of iterations that QSearch needs to find a marked item is*

$$n_Q(|X|, t) = \sum_{k=1}^{k_{max}} \frac{m_k}{2} \left[ \prod_{l=1}^{k-1} \frac{1}{2} + \frac{\sin(4(m_l+1)\theta)}{4(m_l+1)\sin(2\theta)} \right],$$

$$k_{max} = \left\lceil \log_\lambda \frac{|X|}{2\sqrt{|X|-1}} \right\rceil + 4,$$

with  $\sin^2 \theta = t/|X|$ ,  $m_k = \lfloor \min(\lambda^k, \sqrt{|X|}) \rfloor$ ,  $\lambda = 6/5$ .

*Proof.* We follow closely the notation and reasoning of [12]. Let  $X$  be a list of size  $|X|$ , with  $t$  elements marked by function  $\chi : X \rightarrow \{0, 1\}$ . Let  $G \equiv \{x \in X | \chi(x) = 1\}$  and  $B \equiv \{x \in X | \chi(x) = 0\}$  be the spaces of marked (good) and non-marked (bad) elements in  $X$ . Our goal is to find a marked element. In Grover's algorithm, we first prepare a uniform superposition of all elements in the list,

$$|\psi_0\rangle = \frac{1}{\sqrt{|X|}} \sum_{x=0}^{|X|-1} |x\rangle.$$

We then rotate this initial guess to a state which is approximately a superposition only of marked items. This is done by repeatedly applying the operator  $Q = R_0 R_B$ , made out of two reflections: one around the state  $|\psi_0\rangle$ ,  $R_0 = 2|\psi_0\rangle\langle\psi_0| - \mathbf{1}$ , and the other around the space

of non-marked items,  $R_B = 2\Pi_B - \mathbb{1}$ . Here  $\Pi_B$  is the projector on the space of non-marked items.

The optimal number of times we should apply  $Q$  depends on the ratio between  $t$  and  $|X|$ , which is typically unknown. The algorithm of [8] sidesteps this problem by randomly guessing a value for  $t$  in a range which is gradually extended. Following [19], we denote this algorithm as  $\text{QSearch}_\infty$ . This algorithm always outputs a solution if  $t \geq 1$ . We set a limit to the number of times we increase  $m$  by a factor  $\lambda$  to stop the algorithm if a solution is not found,  $k_{max}$ , after this limit is reached, the algorithm returns 'no marked item'. This allows the algorithm to manage  $t = 0$  cases. There is a finite probability of outputting 'no marked item' even when  $t \geq 1$ , however this failure probability can be bounded.

Let

$$|\psi_G\rangle \equiv \frac{1}{\sqrt{t}} \sum_{x \in G} |x\rangle, \quad |\psi_B\rangle \equiv \frac{1}{\sqrt{|X| - t}} \sum_{x \in B} |x\rangle,$$

be the superpositions of good and bad states. Our initial guess can be expressed as

$$|\psi_0\rangle = \sin \theta |\psi_G\rangle + \cos \theta |\psi_B\rangle,$$

where  $\sin^2 \theta = t/|X|$ . The operator  $Q$  generates translations in  $\theta$ . Let  $|\psi_j\rangle = Q^j |\psi_0\rangle$ , then one can show that

$$|\psi_j\rangle = \sin[(2j+1)\theta] |\psi_G\rangle + \cos[(2j+1)\theta] |\psi_B\rangle.$$

From this follows that, after  $j$  applications of  $Q$ , the probability of finding a good state as the outcome of the measurement is

$$p_j = \sin^2[(2j+1)\theta].$$

The algorithm proceeds as follows. Let  $m_k = \lfloor \min(\lambda^k, \sqrt{|X|}) \rfloor$ . We pick a uniformly random number  $j_k \in [0, m_k]$ , and apply  $Q^{j_k}$ . If  $t = 0$ , all the  $p_j = 0$  and we correctly output "no marked item". If  $t \geq 1$ , we still have a finite probability of outputting "no marked item", which for  $t \geq 1$  is incorrect. Averaging over the randomly chosen  $j_k$ , we find that the probability of outputting "no marked item" is given by

$$(C.14) \quad \langle p_{fail} \rangle = \prod_{k=1}^{k_{max}} (1 - \langle p_{j_k} \rangle),$$

where

$$(C.15) \quad \begin{aligned} \langle p_{j_k} \rangle &= \frac{1}{m_k + 1} \sum_{j_k=0}^{m_k} p_{j_k} \\ &= \frac{1}{2} - \frac{\sin[4(m_k + 1)\theta]}{4(m_k + 1) \sin(2\theta)}. \end{aligned}$$

To upper bound  $\langle p_{fail} \rangle$ , we use lower bounds on  $\langle p_{j_k} \rangle$  from [8, 12]. The bound provided by [8] follows directly from Equation (C.15): we have that  $\langle p_{j_k} \rangle > 1/4$  if  $m_k + 1 \geq 1/\sin(2\theta)$ . For  $\theta \rightarrow \pi/2$ , this quantity diverges, and the bound becomes useless; we have to consider the cases  $\theta < \pi/6, \theta \geq \pi/6$  separately for technical reasons. For  $\theta < \pi/6$ , rewrite  $1/\sin(2\theta)$  as

$$\frac{1}{\sin(2\theta)} = \frac{1}{2} \sqrt{\frac{|X|}{t}} \left(1 - \frac{t}{|X|}\right)^{-1/2} \leq \sqrt{\frac{|X|}{2}}.$$

The inequality is obtained by using  $t \geq 1$ , and set  $|X| = 2$  in the parentheses. From this follows that there exists a critical  $k$  for which  $m_k + 1 \geq 1/\sin(2\theta)$  and the bound applies. A sufficient condition for this to happen is that  $k \geq k_c$ , where

$$(C.16) \quad k_c = \lceil -\log_\lambda \sin(2\theta) \rceil.$$

From [12], for  $\theta \in [\pi/6, \pi/2]$ ,  $\langle p_{j_k} \rangle > 1/4$  for every  $k$ . Since our  $\theta$  is not known, we must use the bounds resulting in the weakest upper bound to  $\langle p_{fail} \rangle$ , which turns out to be the  $\theta < \pi/6$  case discussed above. For the same reason, we use the worst-case value of  $k_c$ . This is found by setting  $t = 1$  in Equation (C.16),

$$k_c \leq \left\lceil \log_\lambda \frac{|X|}{2\sqrt{|X|-1}} \right\rceil \equiv k_*.$$

Putting everything together, we find that for  $t \geq 1$  and for any  $\theta$ ,

$$\langle p_{fail} \rangle \leq \left(\frac{3}{4}\right)^{k_{max} - k_*}.$$

The value  $k_{max} = k_* + 4$  is obtained by requiring that  $\langle p_{fail} \rangle \leq 1/3$ . We can boost this probability to  $\varepsilon > 0$  repeating the algorithm  $s_{max} = \log_3 1/\varepsilon$ . The final result is algorithm Algorithm C.1.

We use a slightly different time out from the one considered in [12], which tracks the number of times  $Q$  has been applied. We instead set a limit to the number of times we increase  $m$  by a factor  $\lambda$ , i.e. stop the algorithm when  $k$  reaches a certain value. As in [12], we set  $\lambda = 6/5$  to optimize the expected number of queries to  $G$ . In our version of  $\text{QSearch}$ , it is much easier to calculate the expectation value of  $\langle n_Q \rangle$ , which we need below to compute a bound on the expected gate cost of the algorithm. Ultimately we define this as a function of  $|X|, t$ .

For the moment, we neglect the outer while loop required to boost the failure probability to  $\varepsilon$ . We then split the average cost of  $\text{QSearch}$  as

$$\langle \mathcal{C}[\text{QSearch}] \rangle = \langle n_Q \rangle \mathcal{C}[Q] + \langle n_{iter} \rangle (\mathcal{C}[\psi_0] + \mathcal{C}[meas]).$$

Above,  $\langle n_Q \rangle$  is the average number of times we need to apply the operator  $Q$ ,  $\mathcal{C}[Q]$  is the cost of one application

of  $Q$ ,  $\langle n_{iter} \rangle$  is the average number of iterations (i.e. number of times we increase  $m$  by a factor  $\lambda$ ),  $\mathcal{C}[\psi_0]$  is the cost of preparing  $|\psi_0\rangle$ , and  $\mathcal{C}[meas]$  the cost of performing the measurement. Typically the first term is the dominant one.

To find an expression for the average number of times we need to apply  $Q$ , consider again the iteration over iterated sets of  $j$ 's. Let  $J_1 = (j_1, j_2, j_3, \dots, j_{k_{max}})$  be a random draw for the  $j$ 's, and  $J_2 = (j_2, j_3, \dots, j_{k_{max}})$ , the same draw with  $j_1$  dropped. The average number of applications of  $Q$  given a draw  $J_1$ , which we denote  $\langle n_Q \rangle_{J_1}$  can be found through

$$\langle n_Q \rangle_{J_1} = j_1 + (1 - p_{j_1}) \langle n_Q \rangle_{J_2}.$$

We can define  $J_3$  by dropping  $j_2$  from  $J_2$  and find a similar expression for  $\langle n_Q \rangle_{J_2}$ , ad so on. The resulting recursion relation can be expanded to

$$\langle n_Q \rangle_{J_1} = \sum_{k=1}^{k_{max}} \left[ j_k \prod_{l=1}^{k-1} (1 - p_{j_l}) \right].$$

We are interested in averaging this expression over  $J_1$ . The result is

$$(C.17) \quad n_Q(|X|, t) = \sum_{k=1}^{k_{max}} \left[ \langle j_k \rangle \prod_{l=1}^{k-1} (1 - \langle p_{j_l} \rangle) \right],$$

where

$$(C.18) \quad \langle j_k \rangle = \frac{1}{m_k + 1} \sum_{j_k=0}^{m_k} j_k = \frac{m_k}{2},$$

and  $\langle p_{j_l} \rangle$  is given by Equation (C.15). The expression for  $n_Q(|X|, t)$  is difficult to handle analytically, but can be easily estimated numerically for a given  $\theta$ . To decompose the costs applying  $Q$ , consider  $R_B$ ,  $R_0$  separately. For  $R_B$ , we assume that the function  $\chi$  can be implemented as a quantum oracle (also denoted by  $\chi$ ) with action  $\chi \cdot |x\rangle |a\rangle = |x\rangle |a \oplus \chi(x)\rangle$ . Here,  $a = 0, 1$ , and  $\oplus$  denotes addition mod 2. Then we can implement  $R_\chi$  with a phase query to  $\chi$ ,

$$\chi \cdot |x\rangle |-\rangle = (-1)^{\chi(x)} |x\rangle |-\rangle,$$

so after tracing out the ancilla, we are left with the same action as  $R_B$ , with cost

$$(C.19) \quad \mathcal{C}[R_B] = \mathcal{C}[\chi] + \mathcal{C}_1 + \mathcal{C}_2.$$

The reflection around  $|\psi_0\rangle$  is  $R_{\psi_0} = \mathcal{A}R_0\mathcal{A}$ , where  $R_0 = 2|0\rangle\langle 0| - \mathbb{1}$ , and  $\mathcal{A}$  is a unitary that prepares  $|\psi_0\rangle$ , i.e.  $\mathcal{A}|0\rangle = |\psi_0\rangle$ . For QSearch,  $\mathcal{A}$  is implemented by a layer of Hadamard gates such that  $\mathcal{C}[\mathcal{A}] = n\mathcal{C}_1$ . We

state  $\mathcal{C}[R_{\psi_0}]$  in this more general form in anticipation of later Grover-oracle based routines.

For  $R_0$ , we use the same strategy as before, now with an oracle mapping  $x = 0$  to 0 and all other  $x$ 's to 1. This can be implemented as a Toffoli gate controlled on  $x = 0$  and targeting the  $|a\rangle$ , then finally apply  $X$  on  $|a\rangle$ , at cost

$$(C.20) \quad \mathcal{C}[R_{\psi_0}] = 2\mathcal{C}[\mathcal{A}] + \mathcal{C}_1 + 2(n-1)\mathcal{C}_T.$$

Let  $n = \lceil \log_2 |X| \rceil$ , and we find that altogether

$$(C.21) \quad \mathcal{C}[Q] = \mathcal{C}[\chi] + 2(n+1)\mathcal{C}_1 + \mathcal{C}_2 + 2(n-1)\mathcal{C}_T.$$

Here,  $\mathcal{C}[\chi]$  is the cost of one query to  $\chi$ .

Beside acting with  $Q$ , at every iteration, we need to prepare the state  $|\psi_0\rangle$ , and check that the outcome of the measurement is a good solution. The first requires  $n$  Hadamard gates. For the second, we typically need to apply the classical oracle  $\chi$  to the outcome of the measurement, or, in some other cases, we might need to use the quantum oracle instead.<sup>8</sup> The average number of iterations is

$$\langle n_{iter} \rangle = \sum_{k=1}^{k_{max}} \prod_{l=1}^{k-1} (1 - \langle p_{j_l} \rangle).$$

We want to boost the average success probability  $1 - \langle p_{fail} \rangle$  by repeating the protocol for applying  $Q^j$  with a bounded while loop, as established above. However, to obtain a simple bound, we count the cost of one iteration.  $\square$

**C.4 Quantum Minimum Finding** The quantum minimum finding algorithm of Høyer and Dürr (see [22]) takes as input an unsorted list  $L$  of  $N$  elements each holding a value from an ordered set which is assigned via a function  $T : L \rightarrow \mathbb{R}$  and outputs the element associated to the minimum of this set. The algorithm's main subroutine uses a generalization of Grover search, namely the *quantum exponential searching algorithm*, which we replace by QSearch, an algorithm that is discussed in Appendix C.3. We denote the running time by  $t$  and assume that we have oracle access to the function  $\chi : L \rightarrow \{0, 1\}$  with:

$$\chi_i(j) = \begin{cases} 1, & \text{if } T(j) < T(i) \\ 0, & \text{else.} \end{cases}$$

<sup>8</sup>For example, in Nannicini's algorithm, the quantum oracle queried by Grover has not a direct classical counter part, since it uses a quantum linear solver.

---

**Algorithm C.2** Quantum Minimum Finding

---

**function** QMin( $L, \chi : L \rightarrow \{0, 1\}$ )  
  Choose threshold index  $y \in [N]$  uniformly at random.  
  **while** True **do**  
    Initialize the memory as:  $|\psi_0\rangle = \frac{1}{\sqrt{N}} \sum_{x=0}^{N-1} |x\rangle |y\rangle$ .  
    Mark every item  $x$  for which  $\chi_y(x) = 1$ .  
    Apply QSearch( $L, \chi$ ) on the first register of  $|\psi_0\rangle$ .  
    Measure the first register: let  $y'$  be the outcome. If  $\chi_y(y') = 1$ , set  $y = y'$ .  
  **end while**  
**return**  $y$ .  
**end function**

---

The gate complexity of this algorithm is comprised of the following:

$$\mathcal{C}[\text{QMin}] = \langle n_{\text{QMin}} \rangle (\mathcal{C}[Q] + \mathcal{C}[\psi_0] + \mathcal{C}[\text{meas}])$$

Here  $\langle n_{\text{QMin}} \rangle$  is the expected number of calls to the oracle  $O_{\chi_i}$  required for finding the minimum,  $\mathcal{C}[Q]$  denotes the cost of the Grover operator,  $\mathcal{C}[\psi_0]$  is the cost for preparing the state  $|\psi_0\rangle$  and  $\mathcal{C}[\text{meas}]$  is the cost for performing a measurement. Typically, the measurement process requires one call, whereas the initialization of the memory state can be achieved using  $n$  Hadamard gates. The cost of  $Q$  and the expected number of applications of  $Q$  per iteration can be retrieved from the discussion on QSearch. We follow the work of [12] for the following cost analysis:

LEMMA C.1. (COST OF QMin I) *Given a list  $L$  and an oracle  $\chi$ , the expected number of queries to  $\chi$  by QMin in order to find the minimum is given by:*

$$\langle n_{\text{QMin}} \rangle = \sum_{s=1}^{N-1} \frac{\langle n_Q \rangle(s)}{s+1},$$

where  $\langle n_{\text{QSearch}} \rangle$  is the expected number of oracle calls made by QSearch.

The detailed proof can be found in Lemma 6 from the appendix of [12]. Note that we consider calls to the quantum oracle rather than to the classical function  $\chi$ , which would include an extra factor. Introducing a timeout to make the algorithm a finite-time algorithm, the expected number of iterations needed to find the minimum changes.

LEMMA C.2. (COST OF QMin II) *Given a list  $L$  and an oracle  $\chi$ , the expected number of queries to  $\chi$  by*

QMin in order to find the minimum with probability of success at least  $1 - \varepsilon$  is given by

$$\langle n_{\text{QMin}_{finite}} \rangle = \lceil \log_3(1/\varepsilon) \rceil 3 \langle n_{\text{QMin}} \rangle,$$

with  $\langle n_{\text{QMin}} \rangle$  as in Lemma C.1.

**C.5 Quantum Amplitude Estimation** Algorithm C.3 returns an estimate for the probability of measuring a *good* subset of solutions after preparing a given quantum routine, herein we follow an explanation from [11]. Let  $\mathcal{A}$  be a quantum algorithm that prepares a superposition of  $|x\rangle$ 's,  $\mathcal{A}|0\rangle = \sum_{x \in X} a_x |x\rangle$ . Let  $\chi : X \rightarrow \{0, 1\}$  be a Boolean function, with  $X = \{0, 1\}^n$ , which splits  $X$  in a set of *good* solutions,  $G = \{x \in X | \chi(x) = 1\}$ , and *bad* solutions,  $B = \{x \in X | \chi(x) = 0\}$ . Let  $p = \sum_{x \in G} |a_x|^2$  be the probability of finding this state in  $G$ . Quantum amplitude estimation returns an estimate  $p'$  which, with probability at least  $1 - \delta$ , is  $\varepsilon$ -close to  $p$ .

---

**Algorithm C.3** Quantum Amplitude Estimation

---

**function** QAE(unitary  $\mathcal{A}$ , oracle  $\chi : X \rightarrow \{0, 1\}$ ,  $\delta > 0, \varepsilon > 0$ )  
  Prepare  $|\psi\rangle = \mathcal{A}|0\rangle$   
  Run QPE( $Q, \varepsilon, \delta$ )   ▷ QPE is quantum phase estimation,  $Q$  is the Grover operator  
  **return**  $\theta$ , such that  $p' = \sin^2 \theta$   
**end function**

---

LEMMA C.3. (COST OF QAE) *The cost of quantum amplitude estimation is given by*

$$(C.22) \quad \mathcal{C}[\text{QAE}(\mathcal{A}, \chi, \varepsilon, \delta)] = \mathcal{C}[\mathcal{A}] + \mathcal{C}[\text{QPE}(Q, \varepsilon, \delta)].$$

$\mathcal{C}[\text{QPE}(Q, \varepsilon, \delta)]$  is bounded in Equation (C.24), and the cost of an action of  $Q$  is

$$(C.23) \quad \mathcal{C}[Q] = \mathcal{C}[\chi] + 2\mathcal{C}[\mathcal{A}] + 2\mathcal{C}_1 + \mathcal{C}_2 + 2(n-1)\mathcal{C}_T.$$

*Proof.* Let  $\mathcal{A}$  be an algorithm that prepares a superposition of  $x$ 's,  $\mathcal{A}|0\rangle = \sum_{x \in X} a_x |x\rangle$ . Define  $\sin^2 \theta = p$ , where  $p$  is the (unknown) probability with which  $\mathcal{A}$  prepares a good solution,  $p = \sum_{x \in G} |a_x|^2$ . We can rewrite  $|\psi\rangle = \mathcal{A}|0\rangle$  as

$$|\psi\rangle = \sin \theta |\psi_G\rangle + \cos \theta |\psi_B\rangle,$$

where we have defined

$$|\psi_G\rangle = \frac{1}{\sin \theta} \sum_{x \in G} a_x |x\rangle, \quad |\psi_B\rangle = \frac{1}{\cos \theta} \sum_{x \in B} a_x |x\rangle.$$

Consider the operator  $Q = R_\psi R_B$  from QSearch in Algorithm C.1.  $Q$  acts on the states  $|\psi\rangle_{G,B}$  as

$$\begin{aligned} Q|\psi_G\rangle &= \cos 2\theta |\psi_G\rangle - \sin 2\theta |\psi_B\rangle, \\ Q|\psi_B\rangle &= \sin 2\theta |\psi_G\rangle + \cos 2\theta |\psi_B\rangle. \end{aligned}$$

In the plane formed by the real linear combinations of  $|\psi_G\rangle$  and  $|\psi_B\rangle$ , the oracle  $Q$  generates rotations around the origin. To see this, we diagonalize  $Q$ ,

$$Q|\psi_{\pm}\rangle = e^{\mp 2i\theta}|\psi_{\pm}\rangle, \quad |\psi_{\pm}\rangle = \frac{1}{\sqrt{2}}\left(|\psi_B\rangle \pm i|\psi_G\rangle\right).$$

From this follows that we can estimate  $\theta$  by applying quantum phase estimation (QPE) on the state  $|\psi\rangle$  and the operator  $Q$ .

The cost of quantum amplitude estimation is then given by

$$\mathcal{C}[\text{QAE}(\mathcal{A}, \chi, \varepsilon, \delta)] = \mathcal{C}[\mathcal{A}] + \mathcal{C}[\text{QPE}(Q, \varepsilon, \delta)].$$

The first term accounts for the cost of preparing the state  $|\psi\rangle$ , parameters  $\varepsilon$  and  $\delta$  set the precision of the estimate of  $\theta$  and the probability of success of the algorithm. Let  $\hat{\theta}$  be the estimate outputted by QAE, then with probability  $p \geq 1 - \delta$ , we have  $|\hat{\theta} - \theta| \leq \varepsilon$ .

The QPE routine and gate cost are given in Appendix C.6, see Lemma C.4. It remains to compute the cost of a call to the Grover operator  $Q$ , where  $R_B$  has cost given in Equation (C.19), and now  $\mathcal{A}$  used in Equation (C.20) to compute  $R_{\psi} = \mathcal{A}R_0\mathcal{A}$  is given as an argument. Altogether, we arrive to Equation (C.23).  $\square$

**C.6 Quantum Phase Estimation** Algorithm C.4 implements quantum phase estimation, a standard result we take from [19], computing an  $T$ -bit estimate of a phase  $\phi$ . Let  $U$  be a unitary acting on  $n$  qubits, and let  $|\psi\rangle$  be one of its eigenstates:  $U|\psi\rangle = e^{i2\pi\phi}|\psi\rangle$ . Quantum phase estimation returns an estimate  $\phi'$ , which with probability at least  $1 - \delta$  is  $\varepsilon$ -close to  $\phi$ .

---

**Algorithm C.4** Quantum Phase Estimation

---

**function** QPE(unitary  $U$ , eigenstate  $|\psi\rangle$ ,  $\delta > 0$ ,  $\varepsilon > 0$ )

    Prepare the clock register in state  $|\Omega\rangle$   $\triangleright$

$|\Omega\rangle \propto \sum_{\tau=0}^{2^{n_c}-1} |\tau\rangle$ ,  $n_c = \lceil \log_2 1/\varepsilon + \log_2(1 + 1/2\delta) \rceil$

    Apply controlled unitary  $\mathcal{U}$   $\triangleright$

$\mathcal{U} = \sum_{\tau=0}^{2^{n_c}-1} |\tau\rangle\langle\tau| \otimes U^{\tau}$

    Apply QFT $^{\dagger}$

    Measure the clock register

**return**  $\tilde{\phi}$

**end function**

---

LEMMA C.4. (COST OF QPE) *The cost of QPE is bounded by*

$$(C.24) \quad \mathcal{C}[\text{QPE}(U, \varepsilon, \delta)] \geq n_c \mathcal{C}_1 + (2^{n_c} - 1) \mathcal{C}[U].$$

where

$$n_c = \left\lceil \log_2 \frac{1}{\varepsilon} + \log_2 \left(1 + \frac{1}{2\delta}\right) \right\rceil.$$

*Proof.* Let be  $U$  a unitary acting on  $n$  qubits and  $|\psi\rangle$  one of its eigenstates,  $U|\psi\rangle = e^{i2\pi\phi}|\psi\rangle$ . Consider the unitary

$$\mathcal{U} = \sum_{\tau=0}^{T-1} |\tau\rangle\langle\tau| \otimes U^{\tau}.$$

Each power of  $U$  acts on an  $n$  qubit register and is controlled by a  $T$ -qubit register called the *clock*-register. Preparing the clock-register in uniform superposition,  $|\Omega\rangle = \frac{1}{\sqrt{T}} \sum_{\tau=0}^{T-1} |\tau\rangle$  and acting on  $|\Omega\rangle|\psi\rangle$  with  $\mathcal{U}$ , we obtain

$$\mathcal{U}|\Omega\rangle \otimes |\psi\rangle = \left( \frac{1}{\sqrt{T}} \sum_{\tau=0}^{T-1} e^{i2\pi\tau\phi} |\tau\rangle \right) \otimes |\psi\rangle.$$

The term in parentheses is the quantum Fourier transform of  $|M\rangle$ , where  $M \in \mathbb{Z}$ . Applying the inverse QFT to the clock register, we get

$$\text{QFT}^{\dagger} \cdot \frac{1}{\sqrt{T}} \sum_{\tau=0}^{T-1} e^{i2\pi\tau\phi} |\tau\rangle = \sum_{\tau=0}^{T-1} \left( \frac{1}{T} \sum_{\tau'=0}^{T-1} e^{i2\pi\tau'(\phi - \tau/T)} \right) |\tau\rangle.$$

Applying an inverse QFT to the clock register gives us  $M$ , and then our estimate for  $\phi$  is  $M/T$ . The maximal precision of our estimate is order  $O(1/T)$ . However there is a non-zero probability of finding an estimate far from  $\phi$ , which we need to take into account. Consider the probability of measuring the clock register in state  $\tau$

$$(C.25) \quad p_{\tau} = \frac{1}{T^2} \frac{1 - \cos[2\pi T(\phi - \tau/T)]}{1 - \cos[2\pi(\phi - \tau/T)]}.$$

The probability  $p_{\tau}$ , as a function of  $\phi$ , is periodic with period 1,  $p_{\tau}(\phi) = p_{\tau}(\phi + 1)$ , and even around  $\phi = \tau/T$ . Moreover, we have  $p_{\tau+1}(\phi) = p_{\tau}(\phi - 1/T)$ , such that the probabilities for different  $\tau$ 's are equivalent up to a shift in  $\phi$ .

Intuitively, we expect that selecting a sufficiently large  $T$  will ensure a precise estimate with high probability. Let  $\phi = M/T + \Delta\phi$ , for  $M \in \mathbb{Z}$ ,  $N \in \mathbb{N}$  and  $\Delta\phi \leq 1/(2T)$ , such that  $M/N$  is the best approximation for  $\phi$  given  $T$ . Given  $\varepsilon$  and  $\delta$ , we want to find  $T$  such that we find an estimate  $\tilde{\phi}$  with  $|\tilde{\phi} - \phi| < \varepsilon$  with probability  $p \geq 1 - \delta$ .

Following [19], we bound the probability of measuring a  $K$  with  $|K - M| > E$ , for some given  $E$ . This is the probability of having an estimate differing more than  $E/T$  from the optimal estimate,

$$(C.26) \quad p_{err} = \sum_{K=-(M+E-N+1)}^{K=M-E} p_K + \sum_{K=M+E-N+1} p_K.$$

Each probability  $p_K$  is given by Equation (C.25), which we upperbound using the expression  $1 - \cos x \leq 2$  for



the upper part, respectively  $1 - \cos x \geq 2x^2/\pi^2$  for the lower part of the ratio, obtaining

$$p_K \leq \frac{1}{4} \frac{1}{(M - K + T\Delta\phi)^2}.$$

Plugging this in the equation Equation (C.26) and changing the summation index to  $D = M - K$ , we find

$$p_{err} \leq \frac{1}{4} \sum_{D=-(T-1-E)}^{D=-E} \frac{1}{(D - T\Delta\phi)^2} + \frac{1}{4} \sum_{D=E}^{D=T-1-E} \frac{1}{(D - T\Delta\phi)^2}.$$

Finally, using  $2\Delta\phi < 1/T$  and upper bounding the sum with an integral we arrive at

$$p_{err} \leq \frac{1}{2E - 1}.$$

Let  $\tilde{\phi} = K/T$  be our estimate, then

$$|\tilde{\phi} - \phi| = \frac{1}{T} |M - K + \Delta\phi| \leq \frac{|M - K| + 1/2}{T}.$$

Thus we have showed that with probability  $p = 1 - p_{err}$ ,  $|K - M| < E$ . Setting  $p_{err} = \delta$  and  $(|M - K| + 1/2)/T = \varepsilon$ , we find

$$(C.27) \quad T \leq \frac{1}{\varepsilon} \left(1 + \frac{1}{2\delta}\right).$$

Now that we have a bound on  $T$ , it remains to bound the cost of preparing the clock state and implementing  $\mathcal{U}$ .

We specialize to the case where  $T = 2^{n_c}$  for some  $n_c \in \mathbb{N}$ , and then set

$$n_c = \lceil \log_2 \frac{1}{\varepsilon} + \log_2 \left(1 + \frac{1}{2\delta}\right) \rceil.$$

The state  $|\Omega\rangle$  can be prepared by acting with  $H^{\otimes n_c}$  on  $|0\rangle$ . The unitary  $\mathcal{U}$  can be implemented by acting with  $U^{2^k}$  on the target qubit controlled on the  $k$ -th qubit of the clock register,  $k = 0, 1, \dots, n_c - 1$ . In this case, we have

$$\mathcal{C}[\mathcal{U}] = \sum_{k=0}^{n_c-1} \mathcal{C}[\text{ctrl}_1 - U^{2^k}] \geq (2^{n_c} - 1) \mathcal{C}[\text{ctrl}_1 - U].$$

Where to obtain a lowest cost bound, we neglect the overhead required by the control, i.e. use  $\mathcal{C}[\text{ctrl}_1 - U] \geq \mathcal{C}[U]$ . We also neglect the cost of QFT - the inverse Fourier transform can be replaced with a series of Hadamard gates in the QAE context [11] and more generally can be cheaply approximated [41]. Putting everything together,

$$\mathcal{C}[\text{QPE}(U, \varepsilon, \delta)] \geq n_c \mathcal{C}_1 + (2^{n_c} - 1) \mathcal{C}[U].$$

□

**C.7 Linear Combination of Unitaries** Linear combination of unitaries (LCU) is an algorithm originally from [5, 6] which implements a linear combination of unitary operations on a quantum circuit. Algorithm C.5 is a version of LCU from [18], specialized to the quantum linear system problem. We state the result with a fixed success probability.

---

**Algorithm C.5** LCU for QLSA

---

**function** LCU(state  $|b\rangle$ , set of coefficients  $\{\alpha_i\}$ , corresponding set of unitaries  $\{U_i\}$ ,  $\varepsilon > 0$ ,  $\Delta$ )

$U \leftarrow \sum_{i=0}^{\Delta} |i\rangle\langle i| \otimes U_i$ ,

Apply  $\mathcal{P}_b$ , preparing  $|b\rangle$  on register  $|0^n\rangle$  ▷ Neglect step when LCU is run within QAA or a similar routine

Apply  $V$  to register  $|0^m\rangle$  ▷

$V|0\rangle = \frac{1}{\sqrt{\alpha}} \sum_i \sqrt{\alpha_i} |i\rangle$ ,  $\alpha = \sum_i \alpha_i$

Apply  $U$

Apply  $V^\dagger$

**return**  $\sum \alpha_i U_i |b\rangle$  prepared on the device

**end function**

---

LEMMA C.5. (LCU, [18]) *Let  $A$  be a Hermitian operator with eigenvalues in a domain  $\mathcal{D} \subseteq \mathbb{R}$ . Suppose function  $f : \mathcal{D} \rightarrow \mathbb{R}$  satisfies  $\|f(x)\| \geq 1$  for all  $x \in \mathcal{D}$  and is  $\varepsilon$ -close to  $\sum_i \alpha_i T_i$  indexed  $i = 0, \dots, \Delta$  on  $\mathcal{D}$  for some  $\varepsilon \in (0, 1/2)$ ,  $\alpha_i > 0$ , and  $T_i : \mathcal{D} \rightarrow \mathbb{C}$ . Let  $\{U_i\}$  be a set of unitaries such that*

$$U_i |0^t\rangle |\phi\rangle = |0^t\rangle T_i(A) |\phi\rangle + |\Psi_i^\perp\rangle$$

for all states  $|\phi\rangle$  where  $t \in \mathbb{Z}_+$  and  $|0^t\rangle \langle 0^t| \otimes \mathcal{I} |\Psi_i^\perp\rangle = 0$ . Given an algorithm  $\mathcal{P}_b$  for preparing state  $|b\rangle$ , there is a quantum algorithm that prepares a quantum state  $4\varepsilon$ -close to  $f(A) |b\rangle / \|f(A) |b\rangle\|$  with success probability  $\frac{1}{\alpha^2}$  and outputs a bit indicating whether it was successful or not. The cost is bounded by

$$(C.28) \quad \mathcal{C}[\text{LCU}(\{U_i\}, \{\alpha_i\})] \geq \mathcal{C}[U] = \sum_{i=0}^{\Delta} |i\rangle\langle i| \otimes U_i.$$

*Proof.* Given for coefficients  $\alpha_i > 0$ , unitary operations  $U_i$ , and index  $i = 0, \dots, \Delta$ , define operation

$$M = \sum_{i=0}^{\Delta} \alpha_i U_i,$$

Where here  $M$  is  $\varepsilon$ -close to  $f(A)$  by assumption. In general  $M$  is not a unitary, hence we can apply this transformation to state  $|0^m\rangle |b\rangle$  probabilistically. To this end, we define a unitary  $V$  acting on an ancillary register such that

$$V|0\rangle = \frac{1}{\sqrt{\alpha}} \sum_{i=0}^{\Delta} \sqrt{\alpha_i} |i\rangle,$$

where  $\alpha = \sum_i \alpha_i$ , and the controlled unitary

$$U = \sum_{i=0}^{\Delta} |i\rangle\langle i| \otimes U_i.$$

We show that:

$$V^\dagger UV \cdot (|0^t\rangle \otimes |0^m\rangle |b\rangle) = \frac{1}{\alpha} |0\rangle \otimes M |0^m\rangle |b\rangle + |\Psi^\perp\rangle,$$

where  $(|0\rangle\langle 0| \otimes \mathbb{1}) |\Psi^\perp\rangle = 0$ . The algorithm produces the wanted state  $f(A) |b\rangle / \|f(A) |b\rangle\|$  with probability  $1/\alpha^2$ . The control register remains in state  $|0^t\rangle$ , and hence we can use oblivious amplitude amplification (OAA) to boost the success probability to  $\mathcal{O}(1)$ . We defer the costs of raising the probability in our routine to algorithms that call LCU as a subroutine. We assume that the costs of preparing  $|b\rangle$  with  $\mathcal{P}_b$  are known. Likewise,  $\alpha$ , and  $\mathcal{C}[U]$  should have bounds specific to the given  $f$ .  $V$  is interpreted as a state preparation map [18] on  $m = \lceil \log(\Delta + 1) \rceil$  qubits (note that the indexing starts at 0) and [44] gives a procedure for computing this with  $(\Delta + 1) - 2$  2-qubit gates.

$$\mathcal{C}[V] \leq (\Delta - 1) \mathcal{C}_2.$$

Altogether, the cost of LCU is given by

$$\mathcal{C}[\text{LCU}(\{U_i\}, \{\alpha_i\})] = 2(\Delta - 1) \mathcal{C}_2 + \mathcal{C}[U] + \mathcal{C}\mathcal{P}_b.$$

We have not argued this is an optimal state preparation scheme for  $V$ , but instead given a reasonable heuristic allows us to include a cost estimate. This is in any case not expected to be the dominant term, so it can be dropped to obtain a lowest gate cost bound.  $\square$

**C.8 Quantum Linear Solver** A quantum linear solver (QLS) is a quantum algorithm that can prepare the solution of a system of linear equations as the amplitude of a quantum state, herein an algorithm originally presented in [18]. QLS is a crucial subroutine within this work, and hence we give an overview of the general strategy for quantum linear system algorithms. Then, we will state the algorithm used along with its lowest bounded cost. Consider a linear system of equations  $Ax = b$ , where  $A \in \mathbb{C}^{N \times N}$  is a  $N \times N$  invertible Hermitian matrix, with  $\|A\| = 1$ , and  $b \in \mathbb{C}^N$  a vector. Up to normalization, we can encode the vector  $b$  and the solution  $x = A^{-1}b$  in quantum states,

$$|b\rangle := \frac{\sum_i b_i |i\rangle}{\|\sum_i b_i |i\rangle\|}, \quad |x\rangle := \frac{\sum_i x_i |i\rangle}{\|\sum_i x_i |i\rangle\|}.$$

The goal of a quantum linear solver is to output a state  $|\tilde{x}\rangle$  such that  $\|\tilde{x}\rangle - |x\rangle\| \leq \varepsilon$ . We say that the matrix  $A$

is  $d$ -sparse if it has at most  $d$  nonzero entries in any row or column. We denote by  $\kappa$  be the condition number of the matrix, and we say that the matrix is well-conditioned if  $\kappa = \text{poly}(\log N)$ . For hermitian matrices, the condition number is the ratio between the largest and smallest eigenvalues of the matrix. We assume that we have access to an oracle,  $\mathcal{P}_b$ , which prepares the quantum state  $|b\rangle$ ,

$$\mathcal{P}_b |0\rangle = |b\rangle.$$

The authors of [18] provide two approximations: one based on a Fourier representation, the other on Chebyshev polynomials. The basic idea of each is to decompose  $A^{-1}$  as a sum of unitaries that can be efficiently implemented. We can then use LCU to apply this sum to the state  $|b\rangle$ , which we prepare invoking  $\mathcal{P}_b$ . Herein, we consider only the Fourier version, where  $A^{-1}$  is approximated with a sum of exponential terms  $e^{iAt}$  which can be efficiently implemented using Hamiltonian simulation.

---

#### Algorithm C.6 QlsaFourier

---

**function** QLSAFOURIER(matrix  $A$ , vector  $b$ , condition number  $\kappa$ ,  $\varepsilon > 0$ )

$$\Delta_y \leftarrow \frac{\varepsilon}{16} \left[ \log \left( 1 + \frac{8\kappa}{\varepsilon} \right) \right]^{-1/2}, \quad \Delta_z \leftarrow \frac{2\pi}{\kappa+1} \left[ \log \left( 1 + \frac{8\kappa}{\varepsilon} \right) \right]^{-1/2}$$

$$J \leftarrow \frac{16\sqrt{2}\kappa}{\varepsilon} \log \left( 1 + \frac{8\kappa}{\varepsilon} \right), \quad K \leftarrow \frac{\kappa+1}{\pi} \log \left( 1 + \frac{8\kappa}{\varepsilon} \right),$$

**for**  $i = 0, \dots, J - 1$  and  $k = -K, \dots, K$  **do**

$$U_{kj} \leftarrow e^{-iAt_{kj}}$$

$$\alpha_{jk} \leftarrow \frac{1}{\sqrt{2\pi}} \Delta_y \Delta_z |z_k| e^{-z_k^2/2} \triangleright t_{jk} = j \Delta_y \cdot k \Delta_z$$

**end for**

Prepare  $|b\rangle$  with  $\mathcal{P}_b$

Apply LCU( $\{U_{kj}\}, \{\alpha_{kj}\}, J(2K + 1)$ )

Apply OAA(LCU,  $\alpha$ ,  $\log_2(J(2K + 1))$ )

**return**  $|\psi\rangle$  prepared on device,  $\| |\psi\rangle - A^{-1} |b\rangle \| \leq \varepsilon$

**end function**

---

LEMMA 4.2. (**QLSA – Fourier**) *The gate complexity of QLSA – Fourier that solves the linear equation  $Ax = b$  to precision  $\varepsilon$  has a lower bound of*

$$\mathcal{C}[\text{QLS}(A, b, \varepsilon)] \geq 10tw \left( \frac{\pi}{2 \arcsin(\alpha^{-1})} + 1 \right) \cdot (\|A\|_1 - d^2\gamma) \left( \left[ \log \left( \frac{\|A\|_1}{\gamma} - d^2 \right) \right] - 1 \right),$$

with the smallest integer  $w$  satisfying  $\frac{e^w}{w^w} \leq \frac{\varepsilon_{seg}^2}{2}$  and  $\alpha, \gamma, \Delta_z, K, t, \varepsilon_{seg}$  defined as

$$\alpha = 2\sqrt{\pi} \frac{\kappa}{\kappa+1} \sum_{k=-K}^K |k| \Delta_z e^{-\frac{(k\Delta_z)^2}{2}}, \quad t = 2\sqrt{2}\kappa \log\left(1 + \frac{8\kappa}{\varepsilon}\right),$$

$$\Delta_z = \frac{2\pi}{\kappa+1} \left[ \log\left(1 + \frac{8\kappa}{\varepsilon}\right) \right]^{-1/2}, \quad \varepsilon_{seg} = \frac{\varepsilon}{90\gamma t d^2 \left\lceil \frac{\|A\|_{\max}}{\gamma} \right\rceil},$$

$$K = \left\lfloor \frac{\kappa+1}{\pi} \log\left(1 + \frac{8\kappa}{\varepsilon}\right) \right\rfloor, \quad \gamma = \frac{\varepsilon}{\sqrt{2}d^3 t}.$$

Here  $\|A\|_{\max} := \max_{i,j} |A_{ij}|$  is the largest element of  $A$  in absolute value.

*Proof.* We first find an approximate representation of  $1/x$  as a linear combination of phases,  $1/x \sim h(x) = \sum_n e^{i\omega_n x} h_n$ . Then we replace the implementation of  $h(A)$  using a LCU. The approximation of  $1/x$  needs to be accurate only in the domain  $\mathcal{D}_\kappa := [-1, -1/\kappa] \cup [1/\kappa, 1]$ , from [18] once such representation is (C.29)

$$h(x) := \frac{i}{\sqrt{2\pi}} \sum_{j=0}^{J-1} \Delta_y \sum_{k=-K}^K \Delta_z z_k e^{-z_k^2/2} e^{-ixy_j z_k},$$

where  $y_j := j\Delta_y$ , with  $\Delta_y = y_J/J$ , and  $z_k := k\Delta_z$ , with  $\Delta_z = z_K/K$ .  $h(x)$  is  $\varepsilon$ -close to  $1/x$ , for  $x \in \mathcal{D}_\kappa$ , provided we choose appropriate  $\Delta_y, \Delta_z, K, J$  values. We briefly summarize the main steps that lead to such choices; more details can be found in the original paper [18]. The goal is to approximate  $1/x$  by a Fourier series. Consider the identity

$$\frac{1}{x} = \frac{1}{\sqrt{2\pi}} \int_0^\infty dy \int_{-\infty}^\infty dz z e^{-z^2/2} e^{-ixyz}.$$

Truncating and discretizing the integrals, one arrives at Equation (C.29). The authors of [18] prove that  $h(x)$  is  $\varepsilon$ -close to  $1/x$  in steps. We interpolate between between  $1/x$  and  $h(x)$  using 3 functions defined as

$$h_3(x) := \frac{1}{\sqrt{2\pi}} \frac{1}{x} \sum_{k=-\infty}^{+\infty} \Delta_z e^{-z_k^2/2},$$

$$h_2(x) := \frac{1}{\sqrt{2\pi}} \frac{1}{x} \sum_{k=-\infty}^{+\infty} \Delta_z e^{-z_k^2/2} (1 - e^{-ixy_j z_k}),$$

$$h_1(x) := \frac{1}{\sqrt{2\pi}} \frac{1}{x} \sum_{k=-K}^K \Delta_z e^{-z_k^2/2} (1 - e^{-ixy_j z_k}),$$

such that

$$\left| \frac{1}{x} - h(x) \right| \leq \left| \frac{1}{x} - h_3(x) \right| + |h_3(x) - h_2(x)| + |h_2(x) - h_1(x)| + |h_1(x) - h(x)|.$$

To have the  $|1/x - h(x)| \leq \varepsilon$ , it is sufficient that each term on the r.h.s. is smaller than  $\varepsilon/4$ . The following

bounds for the terms on r.h.s. are proven in [18]

$$\left| \frac{1}{x} - h_3(x) \right| \leq 2\kappa \left( \frac{1}{1 - \exp(-2\pi^2/\Delta_z^2)} - 1 \right),$$

$$|h_3(x) - h_2(x)| \leq \kappa \exp\left(-\frac{(\kappa y_J)^2}{2}\right) + 2\kappa \left( \frac{1}{1 - \exp[-\frac{1}{2}(2\pi/\Delta_z - y_J)^2]} - 1 \right),$$

$$|h_2(x) - h_1(x)| \leq \frac{4\kappa}{\sqrt{2\pi}} \int_{z_K}^\infty dz e^{-z^2/2},$$

$$|h(x) - h_1(x)| \leq 2\sqrt{2}\Delta_y.$$

These bounds are valid provided  $|\Delta_y z_K/k| = O(\varepsilon)$ . Then to ensure that  $|1/x - h(x)| \leq \varepsilon$ , it is sufficient to take

$$\Delta_y = \frac{\varepsilon}{16} \left[ \log\left(1 + \frac{8\kappa}{\varepsilon}\right) \right]^{-1/2},$$

$$J = \left\lfloor \frac{16\sqrt{2}\kappa}{\varepsilon} \log\left(1 + \frac{8\kappa}{\varepsilon}\right) \right\rfloor,$$

$$\Delta_z = \frac{2\pi}{\kappa+1} \left[ \log\left(1 + \frac{8\kappa}{\varepsilon}\right) \right]^{-1/2},$$

$$K = \left\lfloor \frac{\kappa+1}{\pi} \log\left(1 + \frac{8\kappa}{\varepsilon}\right) \right\rfloor.$$

We can implement  $h(A)$  as an LCU,

$$h(A) = \sum_{j=0}^{J-1} \sum_{k=-K}^K \alpha_{jk} \cdot \text{sign}(k) e^{-iAt_{kj}},$$

where we have defined

$$\alpha_{jk} = \frac{1}{\sqrt{2\pi}} \Delta_y \Delta_z |z_k| e^{-z_k^2/2}, \quad t_{jk} = y_j z_k.$$

A short calculation leads to

$$\alpha = 2\sqrt{\pi} \frac{\kappa}{\kappa+1} \sum_{k=-K}^K |k| \Delta_z e^{-(k\Delta_z)^2/2}.$$

The last sum can be calculated numerically, provided we know  $\kappa$ ; it scales as  $O(\Delta_z^{-1})$ . Using this, we see that  $\alpha = O(\kappa \sqrt{\log(\kappa/\varepsilon)})$ .

To bring the probability of success from  $\frac{1}{\alpha^2}$  to  $\mathcal{O}(1)$ , we use quantum amplitude amplification (QAA), with costs given in Lemma C.6. Note that because the solution we care about is coupled to  $|00\dots 0\rangle$  on the ancillary register  $V$  is applied on, one can simplify the reflection operator by rotating only around this register. It contains  $\lceil \log_2(\Delta + 1) \rceil$  qubits (since  $i$  index runs  $t = 0, \dots, \Delta$ ), where  $\Delta = |\{\alpha_i\}| = J(2K + 1)$  is the number of terms used in the sum over  $i$ . Altogether,

$$\mathcal{C}[\text{QLS}] = 4l\mathcal{C}_1 + 2l\mathcal{C}_2 + (2 \log_2(J(2K + 1)) - 1)\mathcal{C}_T + (2l + 1)\mathcal{C}[\text{LCU}(\{U_i\}, \{\alpha_i\}, J(2K + 1))],$$

To lower bound the cost of QLSA, we consider only the last term. The cost of using the LCU is given in Equation (C.28), specifically

$$\mathcal{C}[\text{LCU}(\{U_i\}, \{\alpha_i\})] = 2(J(2K+1))\mathcal{C}_2 + \mathcal{C}[\{U_i\}] + \mathcal{C}\mathcal{P}_b,$$

The cost of LCU is dominated by the cost of implementing the controlled unitary  $\mathbf{U}$  which comprises all  $\{U_i\}$  steps,

$$\mathbf{U} = \sum_{kj} |kj\rangle\langle kj| \otimes e^{-iAt_{kj}},$$

We lower bound the cost of implementing  $\mathbf{U}$  with

$$\mathcal{C}[\mathbf{U}] \geq \mathcal{C}(e^{-iAy_J z_K}),$$

where

$$y_J \equiv J\Delta_y = \sqrt{2}\kappa \sqrt{\log\left(1 + \frac{8\kappa}{\varepsilon}\right)},$$

$$z_K \equiv K\Delta_z = 2\sqrt{\log\left(1 + \frac{8\kappa}{\varepsilon}\right)}.$$

The cost of QLSA can be lower bounded by the cost of Hamiltonian simulation for a time given by  $t = y_J z_K$ , and finally

$$(C.30) \quad \mathcal{C}[\mathbf{U}] \geq \mathcal{C}[e^{iAy_J z_K}]$$

For Hamiltonian simulation we use the bound given in Lemma C.8. With  $\gamma = \varepsilon/\sqrt{2}d^3t$  and  $w$  computed from Equation (C.39),

$$\mathcal{C}[e^{iAy_J z_K}] \geq 10t(\|A\|_1 - d^2\gamma)w \cdot \left(\lceil \log(\|A\|_1/\gamma - d^2) \rceil - 1\right)\mathcal{C}_T.$$

Finally a Toffoli gate can be decomposed in  $C_1, C_2$  gates at the expense of small linear factors, hence we set  $\mathcal{C}_T = 1$  as a coarse bound.  $\square$

**C.9 Quantum Amplitude Amplification** Given a quantum algorithm  $\mathcal{A}$  preparing a desired state with bound probability, Algorithm C.8 is used to increase the probability of preparing a desired state  $|\psi_G\rangle$  to  $\mathcal{O}(1)$  in a procedure using the Grover oracle. We mainly follow [11] herein.

**LEMMA C.6. (COST OF QAA)** *Assume an initial  $n$ -qubit state  $|\psi\rangle$  that can be prepared from some oracle  $\mathcal{P}_b$ , and consider unitary operation  $\mathcal{A}$  such that*

$$(C.31) \quad \mathcal{A}|\psi\rangle = \sin\theta|\psi_G\rangle + \cos\theta|\Psi_\perp\rangle.$$

---

**Algorithm C.7** Quantum Amplitude Amplification

---

**function** QAA(unitary  $\mathcal{A}$ , probability  $p$ ,  $\mu \in \mathbb{Z}_+$ )  
 Prepare  $|\psi\rangle$   $\triangleright$  Ignore step if QAA is a subroutine  
 Apply  $S^m(\mathcal{A}, \mu)$   $\triangleright$   
 $m = \lfloor \frac{\pi}{4\arcsin\sqrt{p}} \rfloor$  **return**  $|\psi_m\rangle = |\psi_G\rangle$  prepared on device with probability  $\mathcal{O}(1)$   
**end function**

---

where  $\theta \in (0, \pi/2)$  is determined by the known (or bounded) probability of finding this state in  $|0^\mu\rangle V|\psi\rangle$ ,  $p = \sin^2\theta$ . The cost of quantum amplitude amplification is given by

$$(C.32) \quad \mathcal{C}[QAA] = m\mathcal{C}[\chi] + (2m+1)\mathcal{C}[\mathcal{A}] + 2m\mathcal{C}_1 + m\mathcal{C}_2 + 2m(n-1)\mathcal{C}_T$$

where

$$m = \left\lfloor \frac{\pi}{4\theta} \right\rfloor,$$

*Proof.* Let  $\chi : X \rightarrow \{0, 1\}$ ,  $\mathcal{A}|\psi_G\rangle$ , and  $|\psi_B\rangle$  be defined as in Appendix C.3, consider state

$$|\psi\rangle = \mathcal{A}|0\rangle = \sin\theta|\psi_G\rangle + \cos\theta|\psi_B\rangle.$$

Using the operators  $R_\psi, R_B, Q$  defined in Appendix C.3, one can show  $Q$  generates translations in  $\theta$ . Let  $|\psi_j\rangle = Q^j|\psi\rangle$ , and then

$$|\psi_j\rangle = \sin[(2j+1)\theta]|\psi_G\rangle + \cos[(2j+1)\theta]|\psi_B\rangle.$$

So we can repeatedly apply  $Q$  to boost the probability with which we measure a good  $x$ .

Let  $m$  be the number of times we apply  $Q$ . We want to find the value such that  $|\psi_m\rangle$  is close as possible to  $|\psi_G\rangle$ . If there exists  $n \in \mathbb{N}$  such that  $(2n+1)\theta = \pi/2$ , then we can boost the success probability to 1 by choosing  $m = n = \pi/4\theta - 1/2$ . More generally, if we pick

$$m = \left\lfloor \frac{\pi}{4\theta} \right\rfloor,$$

we have that the probability of success is lower bounded by  $1-p$ . To see this consider the probability of failure  $p_{fail} = \cos^2[(2m+1)\theta]$ , and let  $\mu \in \mathbb{R}$  such that  $(2\mu+1)\theta = \pi/2$ , then

$$(C.33) \quad \begin{aligned} p_{fail} &= \cos^2[2(m-\mu)\theta + (2\mu+1)\theta] \\ &= \sin^2[2|m-\mu|\theta] \\ &\leq \sin^2\theta = p, \end{aligned}$$

where, in going to the last line, we have used  $|m-\mu| \leq 1/2$ . Notice that if  $p \geq 1/2$ ,  $m = 0$  and we don't apply  $Q$  at all. So the algorithm works with probability of success lower bounded by  $\max(1-p, p)$ .

The cost of the algorithm is given by

$$(C.34) \quad \mathcal{C}[QAA] = \mathcal{C}[A] + m\mathcal{C}[Q],$$

where the first terms accounts for the preparation of the initial state, and the second term for the repeated action of  $Q$ .

Putting everything together from Equation (C.19) and Equation (C.20), we find that

$$(C.35) \quad \mathcal{C}[Q] = \mathcal{C}[\chi] + 2\mathcal{C}[A] + 2\mathcal{C}_1 + \mathcal{C}_2 + 2(n-1)\mathcal{C}_T.$$

□

**C.10 Oblivious Amplitude Amplification** There are many variants of quantum amplitude amplification, here we consider oblivious quantum amplitude amplification (OAA) from [4] along with bound cost. To utilize OAA, we assume initial state  $|0^\mu\rangle|\psi\rangle$ , and consider a quantum routine  $\mathcal{A}$  that prepares

$$\mathcal{A} |0^\mu\rangle|\psi\rangle = \sin\theta |0^\mu\rangle V|\psi\rangle + \cos\theta |\Psi_\perp\rangle$$

where  $p = \sin^2\theta$  is the probability of finding this state in  $|0^\mu\rangle V|\psi\rangle$ . Oblivious amplitude amplification gives a good solution with probability greater than  $\max(1-p, p)$ .

---

**Algorithm C.8** Oblivious Amplitude Amplification

---

**function** OAA(unitary  $\mathcal{A}$ , probability  $p$ ,  $\mu \in \mathbb{Z}_+$ )  
 Prepare  $|\psi\rangle$  ▷ Ignore step if OAA is a subroutine  
 Apply  $S^m(\mathcal{A}, \mu)$  ▷  
 $m = \lfloor \frac{\pi}{4 \arcsin \sqrt{p}} \rfloor$  **return**  $|\psi_m\rangle = |0^\mu\rangle V|\psi\rangle$  prepared on device with probability  $\mathcal{O}(1)$   
**end function**

---

LEMMA C.7. (COST OF OAA) Assume an initial  $n$ -qubit state  $|\psi\rangle$  that can be prepared from some oracle  $\mathcal{P}_b$ , and consider unitary operations  $\mathcal{A}, V$  such that

$$(C.36) \quad \mathcal{A} |0^\mu\rangle|\psi\rangle = \sin\theta |0^\mu\rangle V|\psi\rangle + \cos\theta |\Psi_\perp\rangle.$$

where  $|\Psi_\perp\rangle$  satisfies  $(|0^\mu\rangle\langle 0^\mu| \otimes \mathbb{I}_n)|\Psi_\perp\rangle = 0$ ,  $V$  is a unitary operator on  $n$  qubit space of  $|\psi\rangle$ , and  $\theta \in (0, \pi/2)$  is determined by the known (or bounded) probability of finding this state in  $|0^\mu\rangle V|\psi\rangle$ ,  $p = \sin^2\theta$ . The cost of oblivious amplitude estimation is given by

$$(C.37) \quad \mathcal{C}[\text{OAA}] = 4m\mathcal{C}_1 + 2m\mathcal{C}_2 + (2\mu-1)\mathcal{C}_T + (2m+1)\mathcal{C}[A],$$

where

$$m = \left\lfloor \frac{\pi}{4\theta} \right\rfloor,$$

*Proof.* As in Lemma 3.6 of [4], define two operators

$$R = 2(|0^\mu\rangle\langle 0^\mu| \otimes \mathbb{I}_n) - \mathbb{I}_{\mu+n}$$

and

$$S = -\mathcal{A}R\mathcal{A}^\dagger R.$$

Then for any  $l \in \mathbb{Z}_+$ ,

$$S^l \mathcal{A} |0^\mu\rangle|\psi\rangle = \sin[(2l+1)\theta] |0^\mu\rangle V|\psi\rangle + \cos[(2l+1)\theta] |\Psi_\perp\rangle.$$

This result follows by demonstrating that  $S$  is a rotation in the subspace spanned by  $\{|\Psi\rangle, |\Psi_\perp\rangle\}$  when  $\Psi$  has the form  $|0^\mu\rangle V|\psi\rangle$ . The success probability is boosted by choosing  $m = \left\lfloor \frac{\pi}{4\theta} \right\rfloor$ . We introduce  $\nu \in \mathbb{R}$  such that  $(2\nu+1)\theta = \pi/2$ . The probability of failure is, following the same reasoning as in Equation (C.33),  $p_{fail} \leq \sin^2\theta = p$

Therefore, the algorithm works with probability of success lower bounded by  $\max(1-p, p)$ . The costs are adapted from Appendix C.9. We get

$$\mathcal{C}[R] = 2\mathcal{C}_1 + \mathcal{C}_2 + (2\mu-1)\mathcal{C}_T$$

leading to

$$\mathcal{C}[\text{OAA}] = 4m\mathcal{C}_1 + 2m\mathcal{C}_2 + (2\mu-1)\mathcal{C}_T + (2m+1)\mathcal{C}[A].$$

To put the result in a more standard convention where the algorithm begins in initial state  $|0^{\mu+n}\rangle$ , we need only to redefine  $\mathcal{A}' = \mathcal{A}\mathcal{P}_\psi$  and  $|\psi'\rangle = |0^n\rangle$ . □

**C.11 Hamiltonian Simulation** The objective of Hamiltonian simulation is to approximate the unitary evolution of a  $d$ -sparse matrix  $H$ , denoted by  $e^{-iHt}$ . Berry et al. [4] provide an algorithm to simulate the Hamiltonian efficiently by reducing it to the fractional-query model. We refer to reader to Lemma 3.5 in [4] for further details.

LEMMA C.8. Given a  $d$ -sparse hermitian matrix  $H$  and  $\varepsilon \geq 0$ , the algorithm from [4] simulates  $e^{-iHt}$  up to error  $\varepsilon$ , with cost lower bounded by

$$(C.38) \quad \mathcal{C}(e^{iHt}) \geq 5t(\|H\|_1 - d^2\gamma)w\mathcal{C}[Q],$$

where  $t$  is the simulation time and  $\gamma = \varepsilon/\sqrt{2}d^3t$ , and  $w$  is the smallest integer such that the following bound holds

$$(C.39) \quad \frac{e^w}{w^w} \leq \frac{\varepsilon_{seg}^2}{2}, \quad \varepsilon_{seg} = \frac{1}{3} \frac{1}{6d^2 \lceil \|H\|_{max}/\gamma \rceil} \frac{\varepsilon}{5\gamma t},$$

with norm  $\|H\|_{max} = \max_{ij} |H_{ij}|$ . Finally,  $Q$  is an oracle whose cost is lower bounded by

$$(C.40) \quad \mathcal{C}[Q] \geq 2\left(\lceil \log(\|H\|_1/\gamma - d^2) \rceil - 1\right)\mathcal{C}_T,$$

where  $\mathcal{C}_T$  is the cost of implementing one Toffoli gate.

*Proof.* The algorithm relies on reducing Hamiltonian evolution to the fractional-query model. We start by explaining how this linkage is established.

To begin with, it is necessary to decompose the Hamiltonian into a sum of 1-sparse Hamiltonians,  $H_j$ ,

$$H = \sum_{j=1}^{n_c} H_j.$$

To accomplish this, one solves an auxiliary edge-coloring problem, as explained in Lemma 4.4 from [4]. The number of 1-sparse Hamiltonians required, which corresponds to the number of necessary colors, is bounded as:  $d \leq n_c \leq d^2$ . The next step involves decomposing each  $H_j$  into 1-sparse Hamiltonians that have eigenvalues of 0 and  $\pi$ . We refer to these Hamiltonians as  $G_{jk}$

$$\sum_{j=1}^{n_c} H_j = \gamma \sum_{j=1}^{n_c} \sum_{k=1}^{\eta_j} G_{jk}.$$

The exact number  $\eta_j$  of matrices  $G_{jk}$  necessary to decompose matrix  $H_j$  is dependent on the details of the construction, which are outlined in Lemma 4.3 of [4].

In the following analysis, we provide a lower bound for the total number of matrices  $G_{jk}$ , denoted as  $\Omega \equiv \sum_j \eta_j$ . However, for the time being, we keep this expression in a general form.

The basic Lie product formula can then be applied to approximate the Hamiltonian evolution

$$e^{-iHt} \approx \left( \prod_{j,k} e^{-iG_{jk}\gamma t/r} \right)^r.$$

As shown in Theorem 4.1 from [4] this is equivalent to a fractional-query algorithm utilizing the oracle

$$(C.41) \quad Q = \sum_{j,k} |j, k\rangle \langle j, k| \otimes e^{iG_{jk}}.$$

The fractional-query cost of this algorithm is  $\gamma t \Omega$ . For a definition of fraction-query algorithm and cost, we refer the reader to Definition 1 in [4].

Lemma 3.5 from [4] proves that a fractional-query algorithm can be simulated up to an error  $\varepsilon_{seg}$  with fractional-query complexity less than  $1/5$  using  $w$  queries to the oracle  $Q$ .

In this context,  $w$  represents the smallest integer that satisfies the following inequality

$$\frac{e^w}{w^w} \leq \frac{\varepsilon_{seg}^2}{2}.$$

One can show that  $w$  is of order  $\mathcal{O}(\log 1/\varepsilon_{seg})$ .

In order to apply Lemma 3.5 to Hamiltonian simulation, it is necessary to divide the time evolution into

smaller segments, each with a fractional-query complexity of no more than  $1/5$ . This implies that  $5\gamma t \Omega$  segments must be simulated.

To implement the Hamiltonian simulation to a precision of  $\varepsilon$ , each segment must be approximated to a precision of

$$\varepsilon_{seg} = \frac{1}{3} \frac{1}{6d^2 \lceil \|H\|_{max}/\gamma \rceil} \frac{\varepsilon}{5\gamma t}.$$

Here, the factor of  $1/3$  is necessary due to the oblivious amplitude amplification step (see Algorithm C.8); and we have used  $\Omega \leq 6d^2 \lceil \|H\|_{max}/\gamma \rceil$ . See the proof of Lemma 4.3 in [4] for more details.

Hence, we deduce that the cost of implementing the unitary ( $e^{iHt}$ ) is lower bounded by

$$(C.42) \quad \mathcal{C}(e^{iHt}) \geq 5\gamma t \Omega w \mathcal{C}[Q].$$

The next step is to determine a lower bound for both the cost of one query to  $Q$  and the value of  $\Omega$ .

Following the reasoning of the proof of Lemma 4.3 in [4], each  $H_j$  is decomposed in at least

$$\eta_j \geq \frac{\|G_X\|_{max} + \|G_Y\|_{max} + \|G_Z\|_{max}}{\gamma} - 1.$$

Here  $G_X$ ,  $G_Y$ ,  $G_Z$  are matrices obtained selecting from  $H_j$  respectively the real off-diagonal entries, the imaginary off-diagonal entries, and the diagonal entries;  $\|M\|_{max}$  denotes the largest entry of  $M$  in absolute value; and  $\gamma$  is a precision parameter which needs to be set to  $\gamma = \varepsilon/\sqrt{2}d^3t$ . Clearly we have  $\|G_X\|_{max} + \|G_Y\|_{max} + \|G_Z\|_{max} \geq \|H_j\|_{max}$ . So we have the following bound

$$\Omega \geq \sum_j \left( \frac{\|H_j\|_{max}}{\gamma} \right) - n_c.$$

We can lower bound the term in the sum as follows. Every element of  $H$  that occupies the same column will be in distinct  $H_j$  matrices, hence we have

$$\sum_{j=1}^{n_c} \|H_j\|_{max} \geq \|H\|_1,$$

where the 1-norm is defined as the largest column-sum in the matrix,  $\|H\|_1 = \max_j \sum_i |H_{ij}|$ . The number of colors  $n_c$  is upper bounded by  $d^2$ . Finally, we obtain

$$\Omega \geq \frac{\|H\|_1}{\gamma} - d^2.$$

Plugging this in Equation (C.42), we get Equation (C.38).

The matrices  $G_{jk}$  are, up to signs, given by permutation matrices. Without carrying out the decomposition explicitly, the best we can do is lower bound their cost by one gate. To implement  $Q$ , we need to take into account the cost of implementing controlled versions of  $G_{jk}$ . The number of controlling qubits is given by  $\lceil \log \Omega \rceil$ . Following the discussion in Appendix C.2, we arrive to Equation (C.40).  $\square$